Review on carbonate-based systems for thermochemical energy storage for concentrating solar power applications: State-of-the-art and outlook

Journal:	*Energy & Fuels*
Manuscript ID	ef-2022-03853a.R1
Manuscript Type:	Review
Date Submitted by the Author:	n/a
Complete List of Authors:	Raganati, Federica; Consiglio Nazionale delle Ricerche, Istituto di Scienze e Tecnologie per l'Energia e la Mobilità Sostenibili (STEMS) Ammendola, Paola; Consiglio Nazionale delle Ricerche, Istituto di Scienze e Tecnologie per l'Energia e la Mobilità Sostenibili (STEMS)

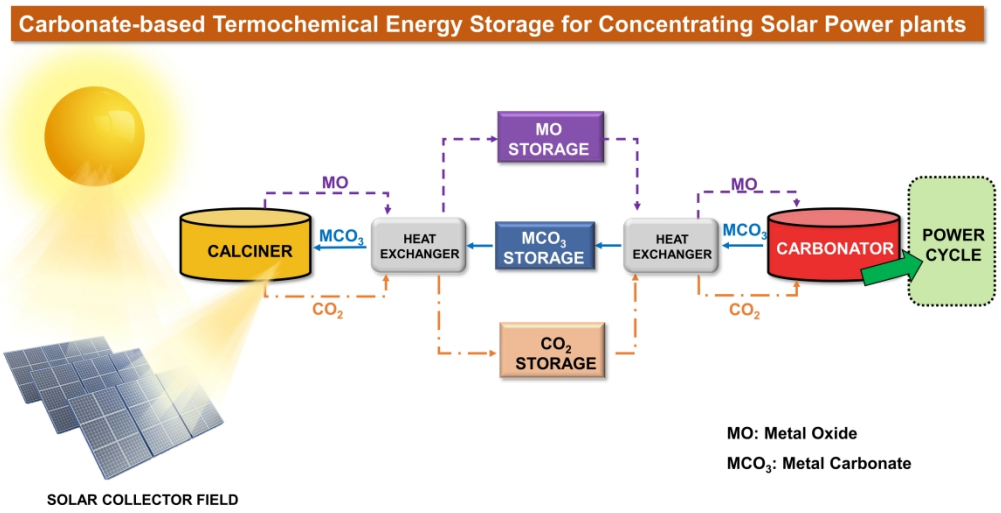

338x190mm (300 x 300 DPI)

Review on carbonate-based systems for thermochemical energy storage for concentrating solar power applications: State-of-the-art and outlook

*Federica Raganati, Paola Ammendola**

Istituto di Scienze e Tecnologie per l'Energia e la Mobilità Sostenibili (STEMS) - CNR, Piazzale Tecchio 80, 80125 Naples, Italy

*Corresponding author

Tel.:+39 0817682237; fax:+39 0815936936.

E-mail address: paola.ammendola@stems.cnr.it

ABSTRACT

Thermochemical energy storage (TCS) systems are receiving increasing research interest as a potential alternative to molten salts in concentrating solar power (CSP) plants. In this framework, alkaline-earth metal carbonates are very promising candidates since they can rely on: wide availability, low cost, high volumetric density (> 1 GJ m^{-3}), relatively high operating temperatures (> 800 ˚C), non-toxic and non-corrosive chemical nature, no occurrence of any side reactions involving the production of undesired by-products. Therefore, their reversible calcination/carbonation reaction with CO_2 can be used to store/release energy in CSP plants. However, in spite of these promising features, TCS research field is relatively new and most of it is still limited to the lab-scale. Therefore, great research efforts are needed to bridge the gap from fundamental research to real-scale application and implementation of TCS-CSP systems.

This manuscript reviews the state-of-the-art of carbonate-based systems for TCS in CSP plants. In particular, the literature has been in-depth analyzed, paying attention to: i) the materials development, with a focus on the solutions available to improve the durability of the materials (namely the ability to withstand repeated carbonation/calcination cycles); ii) the design of the reactor configuration for both the solar-driven endothermic calcination and the exothermic carbonation reaction, focusing on

the optimization of the reactor concept, based on the physicochemical properties and working temperatures of the reagents.

Keywords: Thermochemical energy storage (TCS); Concentrated solar powers (CSP); Carbonate looping; Carbonation; Calcination

1 Introduction

Aiming at addressing the depletion of fossil fuel resources and the environmental issues associated to their intensive utilization (especially CO_2 emitted by their combustion), the development and use of renewable energy resources (RES) has been increasingly encouraged.[1–3] Among the available RES, solar energy represents an infinite source; 173000 TW of solar energy impinges the earth continuously, which is 10000 times more than the total energy requirement of the world.[4,5] Despite being infinite, solar energy suffers from an intrinsic dilute and intermittent nature; indeed, solar insolation is seasonal and location-dependent, also varying significantly in the course of a single day at a particular site, which limits the period of electricity production to about 7-8 h per day.[6]

In this framework, a viable and promising solution is represented by concentrating solar power (CSP) plants combined with thermal energy storage (TES), whose main concept consists in solving the mismatch between the electricity demand and solar electricity production[7,8] A TES-CSP plant is basically composed of the following main parts: collector, receiver, thermal energy storage and electric power block (Fig. 1).[9] The solar radiation is concentrated in the collector and then transformed in thermal energy in the solar receiver, which is basically a heat exchanger, by heating up a fluid (heat transfer fluid, HTF). Then, through the HTF, the thermal energy is transferred from the receiver to the power block. Obviously, the HTF must be selected on the basis of the temperature range in which

the HTF is thermally stable, and on the basis of its physical properties (e.g. heat capacity, density, and thermal conductivity). In this framework, several HTFs can be used, such as molten salts, liquid metals (like sodium), water/steam, air, or even moving solid particle streams.[8,10,11] Regarding the power block, the thermal energy is first transformed into mechanical energy through a thermodynamic cycle and then converted into electricity by a generator. Among the available thermodynamic cycle, the most commonly implemented in commercial CSP plants are the Rankine cycle (working with steam) and the Brayton cycle (operating with gases, air).[12] Both these concepts may be improved using, for example, supercritical steam or supercritical CO_2 and combined cycles (Rankine−Brayton).[12] Finally, regarding the storage system, the working principle consists in collecting the solar energy in excess, thus storing the fraction that is not used for immediate electricity generation in order to use it subsequently when it is needed. More specifically, the excess thermal energy is stored during the on-sun hours (charging period), whereas, during off-sun hours (i.e. when the solar resource is not sufficient to produce enough electricity), it is retrieved for electricity production (discharging period).[13] Therefore, the CSP-TES integration would provide an excellent remedy for fixing the mismatch between energy supply and demand deriving from the intermittent nature of solar energy, i.e. enabling energy availability over a 24-hour cycle.[7] It is clear that CSP plants integrated with TES require a larger solar field, thus implying higher investment costs, but, at

the same time, they are also characterized by a higher solar-to-electricity efficiency, due to the larger (round-the-clock) electricity production.[14]

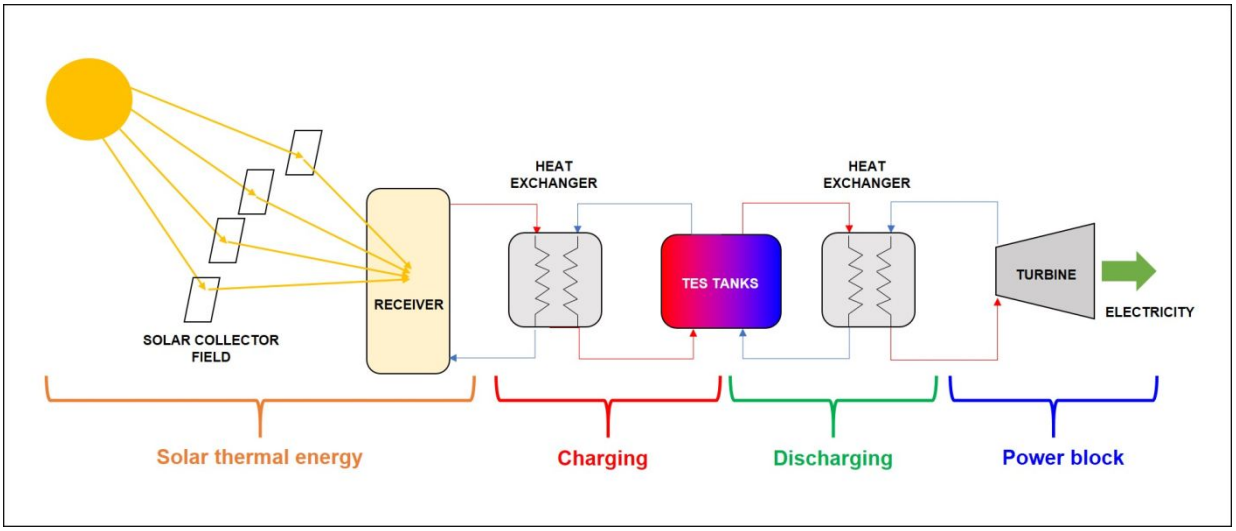

Figure 1. TES-CSP scheme.

Clearly, in this scenario, developing low-cost systems with high-energy storage density and stability is of utmost importance to limit the expenses of CSP plants deployment, since the thermal energy storage subsystem counts for about 18% of the total investment of a solar power plant;[15] hence, reducing TES costs will positively affect the minimization of the levelized cost of energy (LCOE).[15] It is also noteworthy that, besides storage energy density and costs, the temperature range in which the TES system is operated is crucially important because the storage media must keep its stability at temperatures compatible with the working conditions of the other sections of the CSP plants (receiver, HTF and heat engine).[12] More specifically, it must be considered that the exergy efficiency (depending on the ratio between the released and stored heat and the difference between HTF

temperatures in the TES charge stage) can be maximized, besides reducing heat losses, also using charging and discharging temperatures as much similar as possible.[8]

Depending on how the heat storage is accomplished, TES can be classified as:[4]

- sensible heat storage (SHS) – thermal energy is stored as sensible heat, i.e. by the temperature change experienced by a storage material;[4]
- latent heat storage (LHS) - thermal energy is stored as heat of fusion, i.e. by the phase change experienced by a storage media, known as phase change material (PCM), at constant temperature;[4]
- thermochemical heat storage (TCS) – thermal energy is stored as heat of reaction, i.e. by the energy absorbed (charging step - endothermic reaction) and released (discharging step - exothermic reaction) when molecular bonds are broken and reformed, respectively, in a reversible chemical reaction.[16]

The main characteristics of all the TES systems are summarized in Table 1.

To date, commercial CSP plants mainly employ SHS solutions using molten salts (mixture of nitrates like Solar Salt, $NaNO_3$–KNO_3, and nitrides and nitrates like commercial Hitec, $NaNO_3$–$NaNO_2$–KNO_3) as storage medium in a two-tank storage configuration; other commonly used liquids are water and oils (mineral, synthetic, silicone), whereas, typical solid media are

concrete, rocks, or sand.[12] Despite being deployed at industrial scale, several major concerns are associated with these systems, which end up in severely penalizing the CSP plant performances and reliability:

- poor storage capacity due to inferior energy density (~ 0.2 m^{-3}),[17] implying massive storage volume requirement;
- salt corrosiveness, requiring the use of expensive highly resistant materials for transport and storage [18];
- high material cost (~ 900$/tonne);[19]
- low power cycle efficiency caused by the limited maximum working temperature (about 550 - 600 ˚C to avoid salt degradation);[18]
- Very high risk of solidification due to relatively high freeze point (~240 ˚C), which implies severe O&M issues and the necessity of installing auxiliary heaters, i.e. additional energy consumption, for keeping the salts above their solidification temperature.[18]

Table 1. Characteristics of TES systems.[17]

Reaction	**SHS**	**LHS**	**TCS**
Power density	Small ~ 50 kWh m^{-3}	Medium ~ 100 kWh m^{-3}	High ~ 500 kWh m^{-3}

	~ 0.02 – 0.03 kWh kg^{-3}	~ 0.05 – 0.1 kWh kg^{-3}	~ 0.5 – 0.1 kWh kg^{-3}
Energy density	Small ~ 0.2 GJ m^{-3}	Medium ~ 0.3 – 0.6 GJ m^{-3}	High ~ 0.5 - 4 GJ m^{-3}
Storage temperature	Charging step T	Charging step T	Ambient T
Storage period	Limited (hour/days due to heat losses)	Limited (hour/days due to heat losses)	Unlimited
Transport	Small distance	Small distance	Unlimited
Complexity	Simple	Medium	Complex
Maturity	Commercial scale	Pilot scale	Lab scale

As regards LHS, they can rely on higher energy densities (~100 kWh m^{-3})[4] with respect to SHS systems and on the ability to operate at near-constant temperatures during both charging and discharging. The most investigated comprise metals (Zn, Al), metal alloys (Mg−Zn), salts (alkali nitrates, hydroxides, or chlorides), or salt mixtures (KNO_3− KCl).[12] However, PCMs also suffers from important shortcomings, such as: corrosion of metallic walls, chemical instability, phase segregation and uncertainty over long-term thermal behavior.[18] On the contrary, TCS can potentially overcome the above-mentioned issues due to several benefits including:

- high energy density (up to 4 GJ m^{-3}),[17] thus making possible to store a greater amount in the same volume in comparison to both SHS and LHS. This is particularly relevant in applications where there are space limitations;[19]

- non-toxic reactants which can be stored separately after the dissociation reaction also at ambient temperature. This make it possible to remarkably extend the storage time and to improve the system generation elasticity. Moreover, these storage conditions also considerably limit the heat losses, which still represent a crucial challenge in traditional storage systems, such as those based on molten salts;[19]

- high thermal stability and working temperatures (> 600 ˚C) leading to high power generation efficiency, according to the second law of thermodynamics and Carnot efficiency.[20] However, it is also important to point out that the working temperature range affects, besides the thermodynamic efficiency of the power block, also the solar collection cost, i.e. the required area of the solar mirror field, which represents about 60 % of the whole CSP plant costs.[21] In this framework, a distinction should be made between the temperature of the endothermic reaction, whose increase implies a larger area of solar mirror field (i.e. larger solar collection cost), and the temperature of the exothermic reaction, whose increase leads to an enhanced thermodynamic efficiency of the power cycle. This aspect has been carefully discussed by Peng at al.,[22] showing that for each reaction system, it is possible to evaluate an optimized working temperature range. In particular, the Authors showed that the collection cost is inversely proportional to both the receiver efficiency, which decreases with increasing the

temperature of the endothermic reaction (leading to greater radiation and convection losses), and turbine efficiency, which increases with increasing the temperature of the exothermic reaction. Therefore, as a general rule, the collection cost can be limited by reducing the endothermic reaction temperature and increasing the exothermic reaction temperature.

However, in spite of these promising features, TCS suffers from some issues that are still object of research investigation, such as: material degradation leading to material stability/durability issues, complexity of reactor design, poor heat and mass transfer performances. Therefore, great research efforts are still needed to bridge the gap from fundamental research to real-scale application and implementation of TCS-CSP systems. First of all, cost effective, abundant and affordable materials, characterized by high energy density, multicyclic stability and fast kinetics for heat storage and release, are needed. Besides the materials, further research and technological developments are required for the design and set-up of optimized reactor configurations and large-scale integration, thus maximizing the efficiency of the heat transfer between the storage medium and the high temperature solar receiver.

2 Thermochemical energy storage (TCS)

TCS systems rely on reversible chemical reactions (Eq. 1). In particular, during the endothermic reaction, serving as charging step, a reactant (A) is converted in the products (B and C) thanks to the

energy provided by the sun [23]. The obtained products are then stored and subsequently re-used in the reverse exothermic reaction, serving as discharging step, in which the stored energy is released.[24]

$$A + \Delta H_r \leftrightarrow B + C \quad (1)$$

Clearly, the heat (Q) storable in the material is proportional to the molar reaction enthalpy (ΔH_r), the moles of reactant A reacted (n_A^r) and the conversion degree (X) according to:

$$Q = n_A^r \cdot \Delta H_r \cdot X \quad (2)$$

As briefly discussed in the previous paragraph, the great interest in TCS systems is mainly due to their remarkable benefits with respect to SHS and LHS systems, i.e. higher energy storage densities (8–10 times higher than SHS, and two times higher than LHS),[25] which is potentially not affected by any loss during long-term storage when the products of the reaction (B and C) are stored separately.[26] Besides, TCS can rely on a great flexibility due to the huge number of viable reversible reactions, which makes it possible to select the most appropriate one for the desired working temperature range to be used at the solar receiver and power block.[26]

In this framework, the ideal heat storage media/reactions should be characterized by several distinctive features:[4,12,15]

- High energy storage density – it should be as high as possible in order to reduce the required weight/volume of the system and, consequently, the material requirement. Target values - >300 $kWh \cdot m^{-3}$ or >1000 $kJ \cdot kg^{-1}$.[12]
- High working temperatures - the higher the temperatures the higher the power generation efficiency (according to Carnot's theorem), up to certain limit established by radiative heat losses. Target values - for the charging step 700 ˚C < T < 1500 ˚C.[12]
- High cycling and chemical/thermal stability – since TCS materials and processes are meant to last long periods in a CSP plant, the use of reversible chemical reactions in a cyclic way is necessary and the material multi-cyclic stability must be carefully monitored in order to get a full understanding of the chemico-physical changes that can occur at the severe high-temperatures operating conditions of TCS reactions. In this framework, limited degradation/deactivation of the storage materials over prolonged cyclic operations delays its replacement and reduces maintenance costs. Target values - several years of continuous operation, i.e. >1000 cycles with no significant reduction of the performances.[12]
- Strong mechanical properties – the physical/mechanical integrity of the storage media must be ensured in the long term over prolonged cyclic operations.[12] As a matter of fact, solid materials are prone to undergo morphological degradations and/or structural transformations over repeated cyclic operations, thus affecting their total storage capacity. For example,

particle sintering and agglomeration phenomena can typically occur at high temperatures hindering the gas-solid contact efficiency and, consequently, resulting in slower reactions and eventually in loss of the multi-cyclic activity. Besides, limited thermal stresses, contained volume change and, in the case of fluidized beds, low attrition degradation is also required.

- Low-cost storage material - inexpensive and abundant (i.e. available at large-scale) materials are required to guarantee economic viability steady supply. Target values - 4.2$ MJ^{-1} (15 $ kWh^{-1}) DOE (2020).[12,27]
- Low toxicity, flammability, and corrosion - non-toxic, non-corrosive, non-flammable, and non-explosive materials, which can be easily and stably stored, are desirable to simplify handling and operation of the plant, and, eventually, safe disposal.
- Fast and stable kinetics of both the forward and reverse reactions – fast kinetics are required to facilitate the energy charging and discharging steps. Target values - it depends on the specific plant configuration, which determines the duration of the cycles.
- Favorable reaction thermodynamics - a decisive role when selecting the most appropriate reaction is played by thermodynamics, from which the working temperatures and the reaction enthalpy derive. Considering that the reaction enthalpy defines the amount of energy that the can be stored/exchanged in the TCS system, preliminary thermodynamic analyses are commonly required, once the specific power block is defined, to establish the merit and the

suitability of a certain reaction with respect to others (e.g. a TCS system envisaging the exothermic reaction to occur at a discharging temperature of 1000 ˚C cannot be integrated with a Rankine cycle but in an Air Brayton cycle).[12]

- High optical absorptivity and thermal conductivity – aiming at maximizing the amount of collected heat, the storage materials should be characterized great optical and thermal properties. As a matter of fact, materials with weak ability of collecting the solar energy either directly, via absorption of the solar radiation, or indirectly, via conduction, make it difficult to reach the high temperature needed to drive the endothermic calcination reaction.[28] Therefore, the improvement of the sorbent optical and thermal conduction properties represents one of the most crucial challenges in the framework of the CaL-TCS for CSP applications.[29]

Table 2 reports the storage properties of some of the most investigated and promising TCS reactions, whereas, Table 3 summarizes their advantages and drawbacks. High-temperature TCS reactions, applicable to CSP plants, can be classified according to the nature of the material involved in the reversible reactions: solid-gas, liquid-gas, and gas-gas systems. Among all the these, the solid-gas reaction pairs (including carbonates, hydroxides, metals oxides and metal hydrides) are considered to be one of the most promising solution since the main products of their reactions are solids that can be stored easily.[30] Therefore, the present review will be only focused on solid-gas

systems. Clearly, the nature of the reactants and the specific type of reaction have a great impact on the selection and design of both the storage and the reactor scheme.[31] For example, gas−solid TCS systems can be also classified into: i) open systems – the gaseous reactant/product (i.e. air) is released to the atmosphere (thus avoiding gas storage); ii) closed systems - the gaseous reactant/product (e.g. CO_2, H_2, etc.) is stored in a separate tank (condensable gases, such as H_2O, can be easily kept in simple reservoirs, whereas, non-condensable gases require pressurized tanks).[12]

Considering all the features that a storage material should have, and the unavoidable combination of pros and cons characterizing each system (Table 3), one of the most promising class of gas-solid systems for high-temperature TCS in CSP plants consists of those relying on the reversible decomposition of metal carbonates; indeed, they can rely on a great number positive features:[19] low material cost (e.g. ~10$/tonne for $CaCO_3$/CaO and ~600 $/tonne $SrCO_3$/SrO), great availability, non-toxicity, very high energy density (up to 4 GJ m^{-3}) and reaction enthalpy, very high operating temperatures (> 800 °C), no need of catalyst, reactions occurring without by-product formation, very wide experimental feedback coming from CCS applications and cement industry.

Table 2. Promising high-temperature TCS reactions.

REACTION	T (°C)	P (atm)	ΔH kJ mol^{-1}	Eg kJ kg^{-1}	Ev GJ m^{-3}	Ref.
SOLID-GAS						
Carbonates						
$CaCO_3 + \Delta H \leftrightarrow CaO + CO_2$	895-1273	1-10	178	1494	3-4	4,32,33
$SrCO_3 + \Delta H \leftrightarrow SrO + CO_2$	900-1200	1-2	234	926	4	34
$BaCO_3 + \Delta H \leftrightarrow BaO + CO_2$	1560	1	273	278	-	20,35
Hydroxide						
$CaO + H_2O \leftrightarrow Ca(OH)_2 + \Delta H$	400-600	0.1-10	104	2000	1.64	35–37
Metal Hydrides[1]						
$Ca + H_2 \leftrightarrow CaH_2 + \Delta H$	1100-1400	1-5	186	3857	7.37	38,39
$CaAl_2 + H_2 \leftrightarrow CaH_2 + 2Al + \Delta H$	~600	-	83	865	1.49	40
$Mg + H_2 \leftrightarrow MgH_2 + \Delta H$	300-480	1-63	75	2160	3.99	41
$2Mg + Fe + 3H_2 \leftrightarrow Mg_2FeH_6 + \Delta H$	300-500	0-60	77	2106	5.77	42
$Mg_2Ni + 2H_2 \leftrightarrow Mg_2NiH_4 + \Delta H$	253-523	1-20	65	1160	3.14	38,43
$2TiH + H_2 \leftrightarrow 2TiH_2 + \Delta H$	650-750	1-10	170	890	4.01	44
Metal Oxide						
$2Co_3O_4 + \Delta H \leftrightarrow 6CoO + O_2$	~900	~1	200	844	0.72	45,46
$6Mn_2O_3 + \Delta H \leftrightarrow 4Mn_3O_3 + O_2$	1000	1	32	204	0.23	47,48
$2BaO_2 + \Delta H \leftrightarrow 2BaO + O_2$	727-1027	0.11-1	77	468	2.90	49
$4CuO + \Delta H \leftrightarrow 2Cu_2O + O_2$	1030	~1	64	811	-	47,50
LIQUID-GAS						
$NH_4HSO_4 + \Delta H \leftrightarrow NH_3 + H_2O + SO_3$	417	1.5	336	-	3.01	32

GAS-GAS						
$2NH_3 + \Delta H \leftrightarrow N_2 + 3H_2$	400-700	100-300	67	3924	6.75E-4	[51]
$CH_4 + H_2O + \Delta H \leftrightarrow 3H_2 + CO$	1000-1500	20-150	250	-	2.81E-2	[52]
$CH_4 + CO_2 + \Delta H \leftrightarrow 2H_2 + 2CO$	1000-1500	3-4	247	3924	2.77E-2	[52]
$2SO_3 + \Delta H \leftrightarrow 2SO_2 + O_2$	1000-1500	1-5	198	-	2.33	[52,53]

T= operating temperature range; ΔH = Entalpy of reaction; E_g = gravimentric energy density; E_v = volumetric energy density

[1] ΔH [=] kJ $mol_{H_2}^{-1}$

Table 3. Advantages and disadvantages of potential high-temperature TCS systems.

Material	Advantages	Disadvantages	Technology status
Carbonates	• Low material cost • Abundant • Non-toxic • High volumetric energy density • High operating T (up to 1500 °C) • No catalyst needed • No by-product • Similarity to cement industry • Experimental feedback from CCS	• Limited reversibility • Limited cyclic stability • Sintering and agglomeration • CO_2 storage	Lab-scale and pilot-scale (CaL CCS)
Hydroxide	• Low material cost • Abundant • Non-toxic • Good reversibility • No by-product • Experimental feedback	• Agglomeration • Side reactions	Lab-scale and pilot-scale
Metal hydrides	• High volumetric energy density • High reversibility • No by-product	• H_2 storage • H_2 embrittlement • High material cost • High operating pressure	Pilot-scale

		• Catalyst needed • Slow reaction kinetics • Sintering	
Metal Oxides	• Good reversibility • No by-product • No catalyst needed	• Toxicity • High material cost • Scarcity of materials • O_2 storage • Medium energy density • Sintering	Lab-scale
Ammonia synthesis	• Easy to control • No side reactions • Vast industrial experience	• Low operating T • Toxicity • High cost of containment • Corrosiveness • H_2/N_2 storage • Catalyst needed • High operating pressure	Pilot-scale
Methane reforming	• High operating T (up to 1500 °C) • High gravimetric energy density • Industrial feedback	• Low volumetric energy density • Catalyst needed • High cost • Toxicity of CO • Low reversibility • Side reactions	Pilot-scale

$SO_3/O_2/SO_2$ system	• High operating T (up to 1500 °C) • Industrial feedback from production of sulfuric acid	• H_2 storage • High operating pressure • Low volumetric energy density • Toxicity • High corrosiveness • Catalyst needed	Lab-scale

Aiming at evidencing the increasing research interest in both TCS and carbonate-based TCS systems, a thorough bibliographic research has been carried. In particular, the statistics on the number and trend of published articles (TCS, number of published papers = 1454; Carbonate-based TCS, number of published papers = 333) has been analyzed, by means of the "search" and "analyze search results" tools provided by Scopus (Elsevier); the relative graphs are shown in Fig. 2. The result of literature survey, clearly evidences that the number of published papers in the last decade has experienced an exponential growth, thus proving the increasing relevance of the topic.

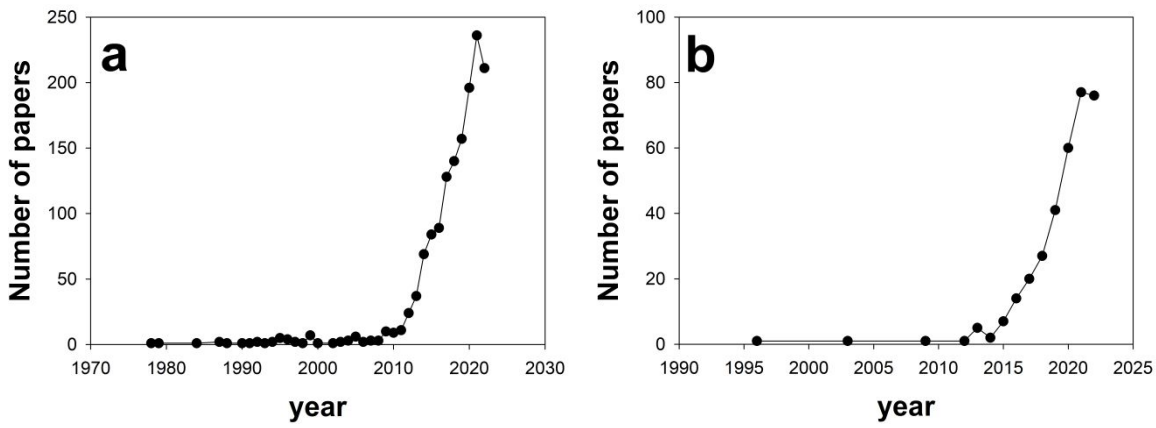

Figure 2. Time evolution of the number of papers published about TCS (a) and carbonate-based TCS (b) systems.

The bibliographic survey has been further analyzed refining the results obtained and limiting them only to the "review" type papers (TCS in general and TCS by means of carbonate-based systems). Table 4 reports the information of all the published review papers. Twenty-six review papers have

been published about TCS (starting from 2011 until 2022); among these, twenty-one papers are more generically focused on the different types of TCS systems and, therefore, only refer to carbonate systems as one of the possible alternatives. On the contrary, five papers (highlighted in Table 3) are more specifically focused on carbonate-based TCS systems, starting from 2019 until 2021.

Table 4. Review papers on TCS.

Source	Publication date	Review scope
Abedin[24]	2011	Presentation of TCS systems and critical comparison with other TES technologies o *TCS candidate materials and their properties tabled without further discussion*
Felderhoff[54]	2013	Brief review of TCS systems based on metal hydrides, metal hydroxide and metal carbonates o *Metal carbonates briefly presented in their most basic features*
Pardo et al.[32]	2014	Review of chemical reactions (gas-gas, gas-liquid and gas solid) for high temperature TCS o *Brief discussion on pros and cons of carbonate-based systems*
Aydin et al.[25]	2015	Review of TCS systems for chemical heat pumps and adsorption/absorption cycles o *No reference to carbonate-based systems*
Wu and Long[55]	2015	Overview of solar TCS systems in their basic principle and main components o *Metal carbonates briefly presented in their most basic features*
Yan et al.[35]	2015	Insight into the promising candidate reactions for TCS systems o *Metal carbonates briefly presented in their most basic features*
André et al.[56]	2016	Overview of high temperatures solid-gas TCS systems with screening of the most suitable materials and selection criteria o *Metal carbonates briefly presented in their most basic features*
Prieto et al.[57]	2016	Review of TCS systems based on redox reactions, sulfur-based cycles and metal oxide reduction–oxidation cycles o *$CaO/CaCO_3$ system discussed with a focus on the carbonator/calciner design*
Pan and Zhao[58]	2017	Overview of gas-solid reactors for TCS applications o *Metal carbonates briefly discussed with reference to the most suitable reactors*
André and Abanades[1]	2018	Review on redox reaction-based TCS systems o *Metal carbonates briefly described in their most basic features*
Chen et al.[9]	2018	Insight in the high temperature TCS systems based on hydride, metal oxide and organic materials o *$CaO/CaCO_3$ system discussed with reference to multicyclic stability issues and reactor design*

Liu et al.[59]	2018	Progress in thermochemical energy storage for concentrated… o *$CaO/CaCO_3$ system briefly described in its most basic features*
Yuan et al.[60]	2018	Review of TCS systems based on CaO-based materials o *$CaO/CaCO_3$ system briefly described with some insight in the possible process scheme*
Zsembinszki et al.[61]	2018	Review of the reactors with potential use in TCS applications o *No discussion provided on the materials*
Carrillo et al. [12]	2019	Review of TCS systems based on hydrides, hydroxides, or carbonates o *Carbonate-based system discussed with reference to multicyclic stability issues and possible solutions*
Fedunik-Hofman et al.[62]	2019	Review of solid-gas reaction kinetics o *Insight in the kinetic models applied for carbonate looping systems*
Khosa et al.[30]	2019	Review of CaL-based TCS systems o *$CaO/CaCO_3$ system discussed referring to reaction kinetics, multicyclic stability issues, reactor design, process integration*
Ortiz et al.[19]	2019	Review of CaL-based TCS systems o *$CaO/CaCO_3$ system discussed with reference to multicyclic stability issues and possible solution, process integration, economics*
Sunku et al.[4]	2019	Review of TCS systems on solid-gas and gas-gas reactions o *$CaO/CaCO_3$ system briefly discussed with reference to the process integration issues and pilot plant trials*
André and Abanades[16]	2020	Review of the recent advances in TCS systems based on hydroxides, carbonates, redox pairs and perovskites since 2016 o *Metal carbonates systems briefly discussed with reference to multicyclic stability issues and possible solutions*
Yan et al.[63]	2020	Review of high temperature TCS systems based on redox cycles o *$CaO/CaCO_3$ system discussed with reference to process concept, integration schemes, multicyclic stability and possible solutions*
Zhao et al.[64]	2020	Review LHS and TCS systems based on metals and metallic compounds with a focus on heat transfer, mutlicyclic stability, reactor/system design o *Metal carbonates briefly mentioned*
Yang et al.[29]	2021	Outlook on the TCS systems based on CaL o *$CaO/CaCO_3$ system discussed with reference to reactor design, integration schemes, multicyclic stability issues and solutions*
Ortiz et al.[65]	2021	Review the latest results from international projects on CaL for CCS and TCES with a focus on the challenges for the process scale o *$CaO/CaCO_3$ system discussed with reference to reactor design, power cycle, auxiliary equipment*

Alvare Rivero et al.[7]	2022	Review of solid–gas reactors for solar-driven reactions ○ *Identification of the relevant criteria for the selection of solar reactors with potential application for the $CaCO_3$ calcination*
Bellan et al.[66]	2022	Review of TCS systems and comparison with other TES technologies ○ *Metal carbonates briefly described in their most basic features*

More specifically, two reviews are focused on a very specific aspect of the process: Fedunik-Hofman et al.[62] reviewed the kinetics of solid-gas reactions and their application to carbonate looping systems for both CCS and TCS applications; likewise, Ortiz et al.[65], critically assessed the technology needed to scale up the Ca-Looping process for both CCS and TCS applications. Yang et al.[29], Khosa et al.[30] and Ortiz et al.,[19] on the contrary, addressed the process in a more systematic and extensive way, namely not focusing on only one aspect of the process; however, these three reviews are specific on the $CaCO_3$/CaCO couple, i.e. not considering other alternative carbonate systems.

The results of the above-discussed literature survey evidenced that providing a critical review of the state-of-the-art carbonate-based systems for TCS-CSP applications is indeed in need and timely. In particular, the literature has been in-depth analyzed, paying attention to the materials and reactor configurations, thus tracing the main paths currently pursued toward the development of suitable TCS-CSP systems.

3 Carbonate-based TCS systems

Alkaline-earth metal carbonates can be used in TCS applications through their reversible carbonation/calcination reaction with CO_2 (Eq. 3).[20]

$$MCO_3 + \Delta H \leftrightarrow MO + CO_2 \quad (1)$$

From the thermodynamic point of view, the system is strongly dependent on the CO_2 partial pressure (P_{CO2}) [34]. In particular, the CO_2 partial pressure at equilibrium ($P_{Co_2}^{eq}$) is equivalent to equilibrium constant and, hence, it can be calculated as:

$$P_{Co_2}^{eq} = exp\left(-\frac{\Delta G_{rxn}^{0}(T)}{RT}\right) \quad (2)$$

where R is the universal gas constant, T is the temperature and $\Delta G_{rxn}^{0}(T)$ is the standard state Gibbs free energy change for the reaction at temperature T.[67] It can be inferred that, at a fixed temperature, increasing values of $P_{Co_2}^{eq}$ shifts the thermodynamic equilibrium towards the carbonation reaction, thus resulting in a greater carbonation conversion [32]. Likewise, at a constant $P_{Co_2}^{eq}$, decreasing values of temperature also favors the carbonation reaction thermodynamically.

Alkaline-earth metal carbonates are very promising candidates since they can rely on: wide availability, low cost, high volumetric density (> 1 GJ m^{-3}), relatively high operating temperatures (> 800 ˚C), non-toxic and non-corrosive chemical nature, no occurrence of any side reactions involving the production of undesired by-products.[30] The relevant storage properties of some of the most investigated carbonates are reported in Table 2.

More specifically, the endothermic decomposition of the carbonate (MCO_3) in the metal oxide (MCO) and CO_2 is performed in the calcination reactor, at relatively low temperature (< 800 ˚C) and low partial pressure of CO_2 (P_{CO2}), thanks to the heat adsorbed at the solar receiver. Then, the

exothermic reaction between MO and CO_2, which can be stored separately, is carried in the carbonation reactor to release the heat previously stored. In particular, this reaction might be performed at the highest temperature (> 800 ˚C) and high CO_2 partial pressure in order to enhance the efficiency of the power cycle.

The following sections review the most promising carbonate-based systems to be applied for TCS-CSP applications.

3.1 $CaO/CaCO_3$ (Ca-Looping)

Among the possible MCO_3/MCO systems, the couple $CaCO_3$/CaO is one of the most investigated one in the so-called Calcium Looping (CaL) process.[60,68,69] In the recent years, CaL has been mainly studied for CO_2 capture and storage (CCS) applications,[65,70,71] namely aiming at reducing CO_2 emissions to the atmosphere, and it has been successfully demonstrated at pilot-scale level.[72] As regards the application of CaL in the framework of TCS for CSP plants, the first concepts were proposed in the late 1970s[73–75] and, most recently, several studies have been also published regarding Ca-based materials for TCS applications.[68,76–80] Besides, several international projects are focused on the CSP-CaL integration [19]. A scheme of the CaL-CSP process is reported in Fig. 3. The endothermic calcination reaction is carried in the calciner using the concentrated solar power, thus releasing CO_2 and CaO as products that are stored separately. When energy is needed, the stored products are sent

in the carbonator, wherein the exothermic carbonation reaction takes place, thus releasing the stored energy, which is used to run the power cycle.

As a matter of fact CaL can rely on a huge number of remarkable advantages: i) limestone, is indeed the second most abundant material on Earth after water and, therefore, it is rather cheap, which is essential for TCS systems to be massively and sustainably developed and deployed at large-scale; ii) the theoretical energy density of the $CaCO_3$/CaO (about 3-4 GJ m^{-3}) couple is one of the largest available among all the gas-solid candidates for TCS, thus allowing the maximization of the storage capacity;[19] iii) as shown in Table 2, the reversible carbonation/calcination reaction of CaO/$CaCO_3$ with CO_2 can provide an equilibrium temperature of 895 ˚C (at P_{CO_2} = 1 atm), which is suitable for operating high-efficiency power cycles, such as the supercritical CO_2-based Brayton cycle, ultra-supercritical H_2O-based Rankine cycle and dish Stirling cycle.[4]

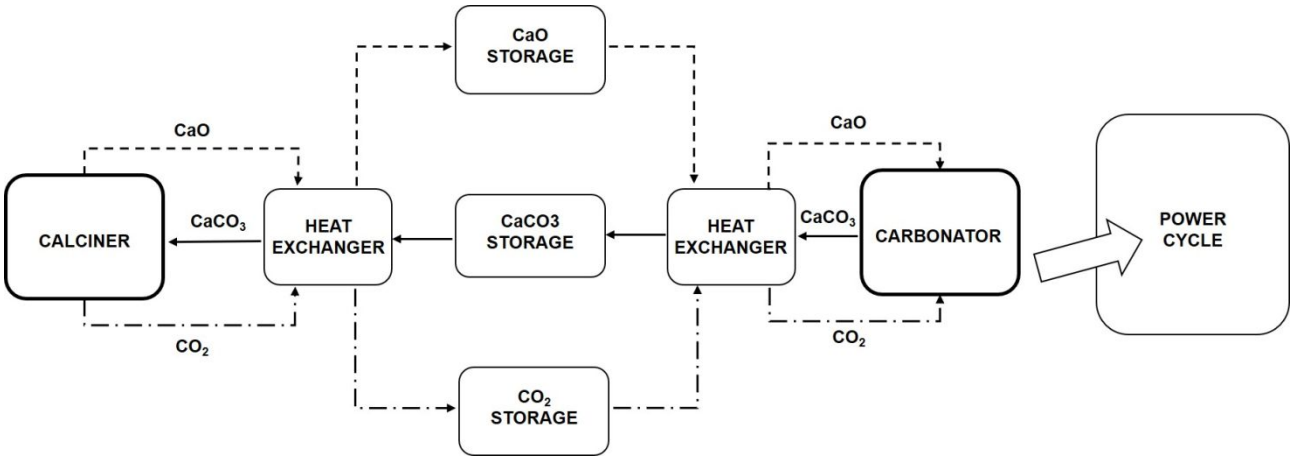

Figure 3. CaL-CSP scheme. [19]

However, in spite of these favorable features, the CaL process suffers from some important shortcomings mainly regarding the CaO multi-cyclic stability, which, as discussed in the previous sections, is one of the most important and distinctive parameters in assessing and selecting a storage media for TCS. More specifically, the decline in CaO reactivity implies the need to use large-sized equipment due to the huge presence of non-reacting solids in the system; this means that with increasing the CaO deactivation, the amount of inert solid, which must be conveyed, pre-heated, cooled and processed through the plant, also increases, thus leading to a loss of the overall plant efficiency.[19] In this context, it has been shown that the overall thermal-to-electric efficiency can be enhanced by more than 10% points and 2-3% points if the CaO residual conversion is increased from X = 0.007 to X = 0.5, in the case of ambient-temperature[81] and high-temperature[82] solids storage, respectively. Therefore, enhancing the CaO multicycle conversion is of utmost importance.

As a matter of fact, the actual deployment of the CaL process as a viable TCS system has been critically undermined by the multi-cyclic CaO deactivation, which has been largely reported in the literature concerning the use of CaL for CCS.[83] However, in this context, it must be considered that the CaO deactivation is strongly dependent on the operating conditions (i.e. temperature, pressure and gas composition).[84] Indeed, in the case of CCS, CaL operating conditions are strictly determined by the requirements associated with the CO_2 capture and storage stages. More specifically, the

calcination conditions are dictated by the necessity to extract from the calciner a high-concentrated CO_2 stream, which is then destined to the compression and sequestration stages. Hence, calcination is carried out at the highest possible temperature (~ 950 ˚C) under high CO_2 partial pressure. Likewise, the carbonation conditions are dictated by the CO_2 concentration in the combustion flue gas (10-20 %vol.) fed to the carbonator reactor; hence it is carried out under low P_{CO2} at the lowest possible temperature (~650 ˚C) dictated by the reaction thermodynamics.[77] On the contrary, in the case of TCS, the CO_2 capture/storage requirements are no longer an issue and, hence, the operating conditions are more flexible and can be purposefully tuned in order to minimize the CaO deactivation and, in turn, maximize the overall efficiency and electricity generation of the CSP plant. Therefore, the carbonation can be performed at the highest CO_2 partial pressures and temperatures (> 800 ˚C), thus maximizing the thermal to electricity conversion efficiency of the power cycle.[77] Likewise, the calcination can be performed at relatively low temperature (~750 ˚C) and CO_2 partial pressures, i.e. using a gas easily separable from CO_2 (e.g. superheated steam or helium), thus also limiting costs and allowing the use of already available solar receiver.[84] In this framework, a major point to be taken into account is the need to realize a process with no additional CO_2 emissions. This can be achieved integrating CaL with a closed Brayton cycle,[81] which means that the plant does not need to be continuously fed by any gas stream (this goes for both CO_2 and helium, which is a very expensive gas). According to these process scheme integration, the carbonator is fed with a pure CO_2 stream

using a molar rate well above that needed for the carbonation stoichiometry. Then, the excess CO_2, which leaves the carbonator unreacted, serves as HTF in the power cycle, i.e. it removes the heat released by carbonation, expands in a gas turbine for power production and, afterwards, it is compressed and stored for the subsequent cycles.

3.1.1 Multi-cyclic decline of CaO reactivity and technological solutions

It is well-known that, while the calcination reaction is complete, the carbonation reaction is incomplete [85]. In particular, the CaO carbonation takes place according to two different mechanisms, as clearly illustrated in Fig. 4:

- Fast kinetics-controlled stage - at the beginning, carbonation occurs relatively fast with CO_2 molecules getting adsorbed on the free surface of the CaO particles.[70,86] In this initial stage, the reaction is not only controlled by the reaction kinetics itself, but also by the mass and heat to the particles surface,[70] meaning that carbonation can be strongly hampered by poor gas/solids contact efficiency.[70]
- Slow diffusion-controlled stage – as the carbonation reaction proceeds, a thin $CaCO_3$ layer is formed on the CaCO surface, which make the reaction shifts to be controlled by the diffusion of CO_2 molecules through the limestone layers before reaching and continue to react with the sill available CaO surface (beneath the product layer)[87] (Fig.5).

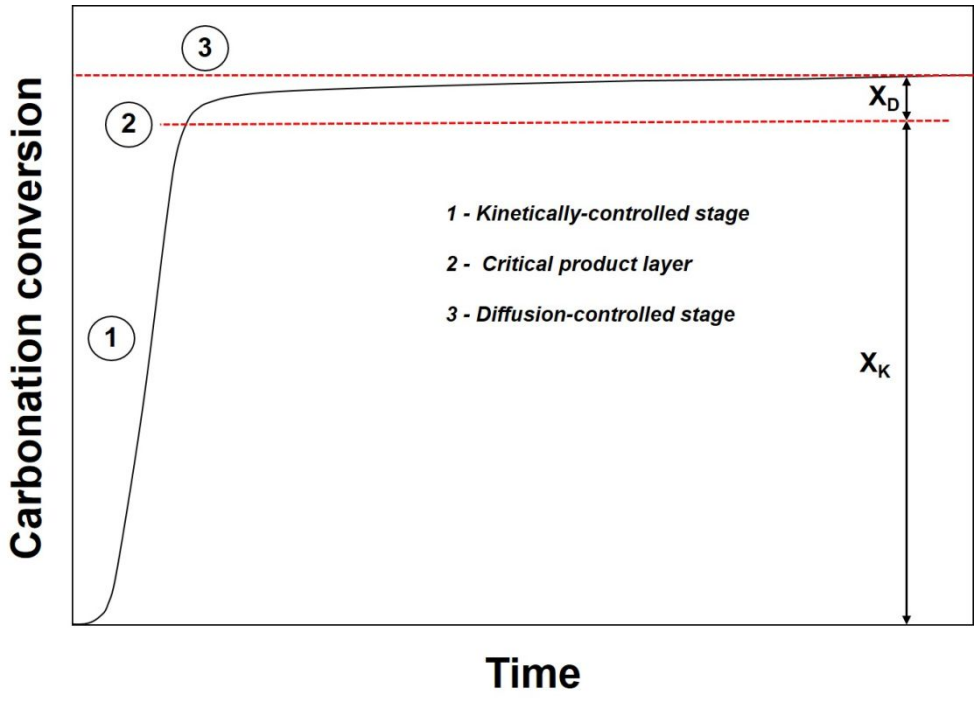

Figure 4. Carbonation reaction time evolution. X_K = CaO conversion in the kinetically controlled stage; X_D = CaO conversion in the diffusion-controlled stage.

Therefore, CaO is observed to undergo a dramatic decline in its carbonation activity over multiple carbonation/calcination cycles, which is ascribable to the CaO deactivation caused by sintering, pore pugging and agglomeration.[77] This issue has been object of intense research activity especially in the framework of CO_2 capture applications[88–90] and most recently also for TCS applications,[19,91–93] in which it is tightly linked to the achievable energy density. In particular, several solutions have been proposed to limit the CaO deactivation,[94] such: hydration, thermal activation, synthesis of Ca-based sorbents with enhanced activity and use of fine $CaO/CaCO_3$ particles.

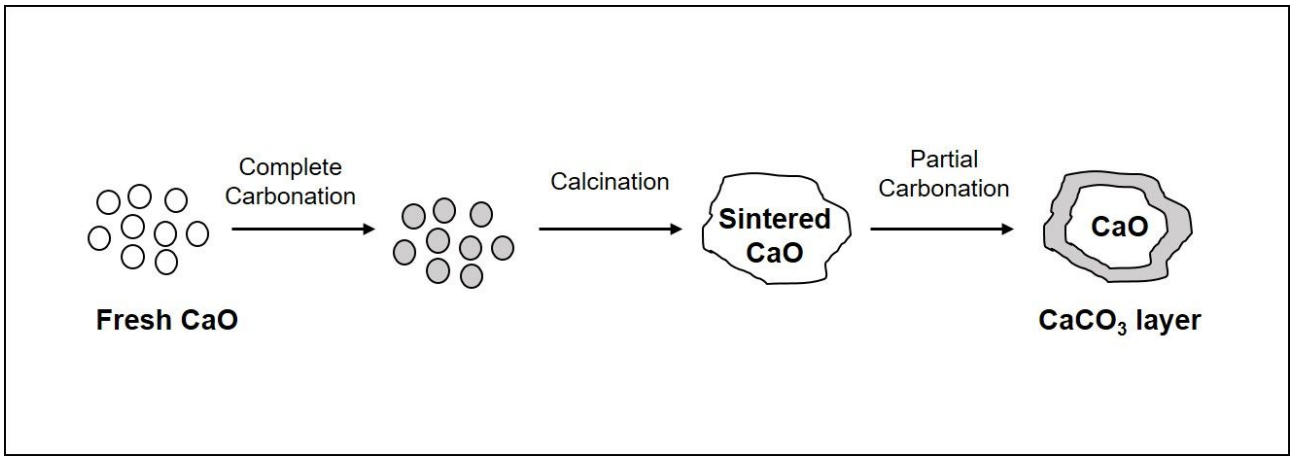

Figure 5. CaO sintering process.

3.1.1.1 Hydration

It has been shown that hydration can be used as an intermediate step to reactivate the sorbent [95] to due to an improvement of the morphological features of the sorbent particles, in terms of both surface area and particle distribution. Indeed, the penetration of H_2O molecules in the inner core of the spent sorbent results in its and reactivation,[96] occurring according to Eqs. 3 and 4:

$$CaO_{(s)} + H_2O_{(l)} \leftrightarrow Ca(OH)_{2(s)} + \Delta H \ (\Delta H = -67 \text{ kJ mol}^{-1}) \quad (3)$$

$$CaO_{(s)} + H_2O_{(g)} \leftrightarrow Ca(OH)_{2(s)} + \Delta H \quad (\Delta H = -104 \text{ kJ mol}^{-1}) \quad (4)$$

More specifically, when hydrated, CaO is converted to $Ca(OH)_2$, which causes an increase in the molar volume (CaO = 16.9 cm^3 mol^{-1}; $Ca(OH)_2$ = 33.7 cm^3 mol^{-1}) and a decrease in density (CaO = 3.32 g cm^{-3}; $Ca(OH)_2$ 2.20 g cm^{-3}).[97] Then, the hydration step, which causes the swelling of CaO, is followed by the decomposition of the produced hydrate, which leads to the formation of fractures inside the core of material; hence, porosity and surface area of the material are enhanced allowing an easier diffusion of CO_2 during the carbonation steps (i.e. pore blockage phenomena are reduced [1]).

In particular, it has been shown that CaO formed after the calcination is characterized by a structure and reactivity similar to the original one, thus meaning that the CaO cyclic stability can be remarkably

enhanced with hydration.[98] It is also noteworthy that hydration positively affects the reactive performances not only of natural lime/limestone,[95,99–102] but also dolomite[103] and synthetic sorbents.[102]

Hydration can be achieved in either wet (water hydration) or dry mode (steam hydration). In the former mode, water at a low temperature is used to soak the sorbent; in the latter, steam is used to hydrate the sorbent.[104,105] Besides these two modes, hydration can be also performed using other substances, such as ethanol solution with water.[106] Among them, it has been shown that water hydration is the most effective solution in terms of recovered sorbent activity[107] and reaction kinetics (i.e. wet hydration is typically faster than steam hydration).[96] Specifically, wet hydration typically occurs in tens of minutes, whereas, dry hydration takes place in a few hours.[96] However, hydration with water has the major shortcoming of dramatically reducing the mechanical strength of the regenerated sorbent, thus resulting in a higher tendency for particle attrition as compared to steam-hydrated sorbents.[108] Besides, wet hydration suffers from practical difficulties due to the high energy penalty associated with the necessity to dry humid hydrated lime.[96]

In spite of being more attractive from the practical point of view,[107] steam hydration is crucially limited by the high energy requirements needed for steam generation; the economics of the process becomes a major concern especially if steam is specifically produced for the sorbent reactivation only.[96] Therefore, the high energy penalty due to the steam generation can reduced by exploiting the recovered heat within the process to produce steam. Also concerning the economics of the process, Zeman[97] showed that, besides the obvious improvement of the sorbent activity, lime hydration can indeed make the process more cost-effective due to the reduction of the sorbent replacement (i.e. the need of fresh sorbent makeup, to counteract the deactivated sorbent, is remarkably limited). Specifically, when hydrated, the lime inventory can be reduced of about 40% with respect to the un-hydrated case.[109]

The hydration method can be also classified according to the stage in which it is carried out: during carbonation (in the carbonator),[99–103] during calcination (in the calciner)[95,110–114] and in a separate stage (in a separate hydrator). [97,110,115–119] Results of hydration studies performed in different position (carbonator, calciner or separate hydrator) are summarized in Table 5. In this framework, it is also important to underline that the thermicity of the hydration/de-hydration reaction should be taken into account when defining its position in the process. De-hydration (reverse of Eqs. 3-4) is, indeed, an exothermic reaction, meaning that it requires heat to occur.[96] Thermodynamically speaking, the best solution would be performing the hydration in a separate reactor rather than in in either the calciner or carbonator.[105] As a matter of fact, if the decomposition of $Ca(OH)_2$ is carried out in the carbonator, the heat released due to the exothermic carbonation reaction can be exploited, even though a reduction of the carbonation rate may be observed.[120] On the contrary, if the decomposition of $Ca(OH)_2$ is carried out in the calciner, wherein the endothermic calcination reaction takes place, additional external energy is required.[96]

Table 5. Main results available on CaO/CaO-based sorbent reactivation via wet/dry hydration.

Position	Atmosphere	Conversion	T_{carb}/T_{calc}	Ref.
Pre-treatment	Ethanol/water	$X_1 = 0.91$; $X_{15} = 0.51$	700/920 °C	[106]
Separate	Water (every 18 cycles)	$X_1 = 0.70$; $X_{18} = 0.56$; $X_{37} = 0.74$	650/900 °C	[121]
During calcination	Steam	$X_1 = 0.78$; $X_{15} = 0.38$	780/960 °C	[122]
	water (from cycle 15)	$X_{16} = 0.90$; $X_{30} = 0.40$		
Separate	Steam (every 5 cycles)	$X_1 = 0.65$; $X_{15} = 0.50$	650/900 °C	[123]
Pre-treatment	Water	$X_1 = 0.78$; $X_{40} = 0.30$	700/950 °C	[124]
Separate	Steam	$X_1 = 0.65$; $X_{15} = 0.49$	650/900 °C	[120]
Separate	Steam (every cycle)	$X_1 = 0.74$; $X_{15} = 0.64$	650/900 °C	[125]
Separate	Steam (after cycle 20)	$X_1 = 0.75$; $X_{15} = 0.62$	650/850 °C	[117]

X_i = carbonation conversion degree at the i-th cycle; T_{carb}/T_{calc}= carbonation/calcination temperature

Clearly, the effectiveness of the hydration treatment becomes lower and lower with increasing the number of the carbonation/calcination cycles, which is due to the sorbent becoming severely sintered (reduction of the sorbent pore size and surface area).[96,126] In this framework it must be considered that the hydration of CaO is a topotactic reaction, meaning that the orientation of the parent crystal (CaO) determines the orientations and microstructural structures of the product crystals ($Ca(OH)_2$).[127] Therefore, since the parent phase controls both the kinetic and the microstructural characteristics of the product phase, the hydration effectiveness in the reactivating the sorbent is highly affected by the severity of the calcination conditions (temperature and/or time).[127] As a consequence, for the hydration method to be effective, the sorbents to be hydrated should not be severely sintered, i.e. hydration should be preferentially used in case of processes with mild calcination conditions.[105,117]

3.1.1.2 Synthesis of CaO-based sorbents with enhanced activity

The strong vulnerability of CaO-based sorbents to sintering phenomena is the result of the low Tammann temperature (T_t, temperature at which sintering starts) of $CaCO_3$.[83] Therefore, a promising technological solution to limit the sintering-induced reactivity decline of CaO-based sorbents over multiple carbonation/calcination cycles is by improving the sorbent stability by means of the introduction/doping of an inert and refractory material (such as Al_2O_3, SiO_2, TiO_2, ZrO_2, Y_2O_3, MgO, etc.), characterized by a high T_t (Table 6);[92,93,96,128,129] the inert materials is, therefore, able to induce a higher resistance to sintering phenomena and leads to a better multicycle stability.[130] The multicyclic carbonation performances of CaO-based sorbents stabilized with different inert materials are summarized in Table 6 and Table 7.

The inert support can be incorporated in the sorbent following two different strategies, as clearly illustrated in Fig. 6, i.e. either homogeneously distributing the support and CaO the sorbent or coating the CaO grains by a layer of support (according to a core-in-shell structure). In both cases, the role played by the inert additives is to induce a stable framework, thus resisting the sintering phenomena, i.e. limiting the natural occurring agglomeration of the CaO grains and, therefore, keeping the original

sorbent porous structure.[83] Support materials can be further classified according to their type of interaction with CaO; they can either strongly interact with CaO, forming mixed oxides (such as in the case of Al_2O_3, ZrO_2, and SiO_2, etc.) (Table 7), or not react with CaO, not forming metal oxides (such as in the case of MgO, Y_2O_3, CeO_2, etc.) (Table 8).[83]

Table 6. T_t of CaO, $CaCO_3$, and commonly used sintering-stabilizer supports.

Compound	T_t (°C)	Ref.
CaO	1170	131
$CaCO_3$	533	132
Al_2O3	900	131
SiO_2	664	131
Ca_2SiO_4	929	133
ZrO_2	1221	131
MgO	1276	92
Y_2O_3	1083	134
CeO_2	1064	135

Among the materials forming mixed oxide with CaO, Al_2O_3 is also one of the most commonly used support, thanks to its quite high T_t (900 °C, Table 6), low cost and good mechanical strength.[83] The multicyclic performances of Al_2O_3-supported CaO-based sorbents are summarized in Table 7. When Al_2O_3 is incorporated into CaO-based sorbents different Ca-Al mixed oxides (such as $Ca_3Al_2O_6$,[136] $Ca_5Al_6O_{14}$,[137] $Ca_9Al_6O_{18}$[138] and $Ca_{12}Al_{14}O_{33}$)[139] are formed, as also shown in Table 7; as a consequence, these CaO particles are stabilized thanks to an increased sintering resistance during the multicyclic operations. It is important to underline that the achievable multicyclic performance of the Al_2O_3-stabilized sorbent is greatly affected by the synthesis procedure since it determines how the CaO and Al_2O_3 (or Ca−Al mixed oxides) are distributed in the final material.[83] In this framework, a

great variety of synthesis methods have been proposed for the synthesis of Al_2O_3-supported CaO-based sorbents, such as wet mixing,[140] co-precipitation[141] and sol−gel,[142] chemical vapor deposition,[136] atomic layer deposition,[143] etc.

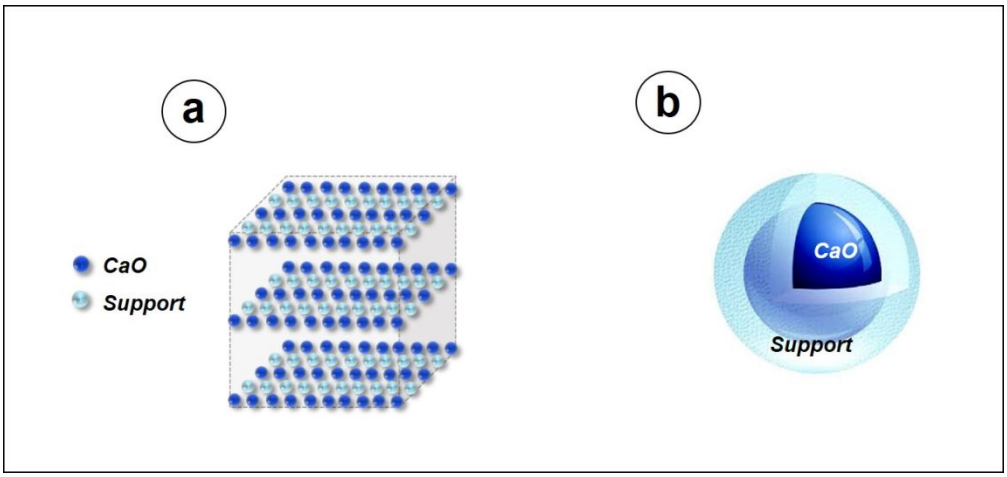

Figure 6. Incorporation of inert and refractory supports into CaO-based sorbents according to two different strategies: (a) CaO and the support are homogeneously distributed in the sorbent; (b) a layer of the support is coated on the CaO grain.

Table 7. Multicyclic carbonation performances, in terms of initial and residual CO_2 uptake, of CaO-based sorbents stabilized with inert materials forming mixed oxides with CaO.

Support	Synthesis method	Mixed oxide[a]	Temperature Carb./Calcin.	CO_2 %vol. Carb./Calcin.	Testing conditions[b]	CO_2 uptake (g_{CO_2} g^{-1}_{sorb}) *initial - last*	Ref.
Al_2O_3							
%wt Al_2O_3							
9	wet mixing	$Ca_{12}Al_{14}O_{33}/Ca_3A_{l2}O_6$	650/850 ˚C	20/0	TGA - 100 cycles	0.60 – 0.34	140
9	carbon gel templating	$Ca_{12}Al_{14}O_{33}$	750/750 ˚C	55/0	TGA - 30 cycles	0.53 – 0.55	144
18	flame spray pyrolysis	$Ca_{12}Al_{14}O_{33}$	850/950 ˚C	100/30	TGA - 100 cycles	0.37 – 0.25	145
5	dry mixing	$Ca_3Al_2O_6$	650/900 ˚C	15/70	TGA - 20 cycles	0.32 – 0.14	93
15	atomic layer deposition	$Ca_{12}Al_{14}O_{33}/Ca_3A_{l2}O_6$	650/900 ˚C	20/100	TGA - 10 cycles	0.40 – 0.41	143
9	chemical vapor deposition	$Ca_3Al_2O_6$	650/950 ˚C	20/100	TGA - 20 cycles	0.62 – 0.41	136
10	sol-gel	$Ca_5A_6O_{14}$	650/800 ˚C	15/0	TGA - 50 cycles	0.55 – 0.45	137
34	sol-gel	$Ca_3Al_2O_6$	650/850 ˚C	15/0	TGA -100 cycles	0.51 – 0.41	146
ZrO_2							
%wt $CaZrO_3$							
34	sol-gel	-	650/850 ˚C	15/0	TGA – 50 cycles	0.48 – 0.46	128

34	sol-gel	-	650/920 ˚C	10/80	Fluidized bed – 20 cycles	0.44 – 0.31	128
26	sol-gel	-	900/900 ˚C	80/0	TGA – 20 cycles	0.65 – 0.65	147
29	sol-gel	-	650/800 ˚C	50/0	TGA – 90 cycles	0.45 – 0.34	148
76	flame spry pyrolysis	-	700/700 ˚C	50/50	TGA – 1200 cycles	0.11 – 0.11	149
58	flame spry pyrolysis	-	700/700 ˚C	30/0	TGA – 100 cycles	0.21 – 0.21	150
10	citrate sol-gel	-	650/780 ˚C	100/0	TGA – 10 cycles	0.71 – 0.69	151
29	sol-gel	-	650/900 ˚C	15/0	TGA – 30 cycles	0.44 – 0.45	152
29	spray drying	-	650/950 ˚C	90/90	TGA – 100 cycles	0.60 – 0.45	153
SiO_2							
%wt SiO_2							
70	wet impregnation	Ca_2SiO_4	650/850 ˚C	15/0	TGA – 80 cycles	0.17 – 0.07	154
9	one-pot synthesis route	-	650/850 ˚C	100/0	TGA – 50 cycles	0.57 – 0.26	155
20	dry mixing	Ca_2SiO_4/ $CaSiO_3$	650/850 ˚C	15/0	TGA – 100 cycles	0.50 – 0.18	156
33	wet mixing	-	700/910 ˚C	100/0	TGA – 40 cycles	0.48 – 0.42	157
10	freeze drying	Ca_2SiO_4	700/920 ˚C	100/100	TGA – 30 cycles	0.46 – 0.21	158

[a]identified by the XRD analysis on the as-synthesized sorbents
[b]TGA = Thermogravimetric analyzer

Among these, chemical vapor deposition[136] and atomic layer deposition[143] make it possible to coat the CaO grains with a very thin Al_2O_3 layer (< 3 nm),[159] thus minimizing the amount Al_2O_3 required for structural stabilization of the sorbent and, in turn, maximizing the amount of CaO, i.e. the active phase for CO_2 sorption. The effect of using wet mixing, co-precipitation, and sol−gel auto-combustion as synthesis method has been investigated by Wang et. al.[160] The Authors showed that the CO_2 uptake and cyclic stability were improved when Al_2O_3 was incorporated via wet mixing; on the contrary, a drop in CO_2 uptake and an improvement in cyclic stability were observed with the Al_2O_3 incorporation via co-precipitation or sol−gel. The obtained results were explained referring to the relative amounts of Tetrahedral-coordinated AlO_4 (reported to affect the stability of sorbents) and octahedral-coordinated AlO_6 (reported to affect the CO_2 uptake capacity) present in the sorbents when different synthesis methods were used; in particular, the wet mixing method yielded sorbents only containing AlO_4 groups with two tetrahedral environments, whereas, the co-precipitation and sol−gel methods yielded sorbents only containing octahedral-coordinated AlO_6 located on the surface of the particle. However, in spite of the different synthesis methods, the Al_2O_3-stabilized CaO-based sorbents are always characterized by improved multicyclic performances with respect to the raw CaO, as clearly shown in Table 7. Aiming at finding the most effective inert support, several stabilized CaO-based sorbents were synthesized by Hu et al.[161] using different wet mixing procedure. The Authors ranked the tested supports as follows: Y_2O_3 >Al_2O_3 > MnO_2 ≈ MgO ≈ La_2O_3 ≈ Yb_2O_3 ≈ Nd_2O_3 > TiO_2 ≈ CeO_2 ≈ ZrO_2 ≈ SiO_2 ≈ Pr_6O_{11}. It was also pointed out that the obtained ranking can be tightly linked to both the support melting point and the stabilized-sorbent surface area.

ZrO_2-supported CaO-based sorbents have been also widely developed using different synthesis methods, as a result of the high T_t of ZrO_2 (1221 °C, Table 6). Differently from Al_2O_3 and SiO_2 supports, CaO and ZrO_2 have a quite simple interaction, only leading to the formation of $CaZrO_3$.[83] The analysis of Table 7 clearly shows that ZrO_2-supported CaO-based sorbents are characterized by enhanced multicyclic stability, particularly for high ZrO_2 mass ratio. For instance, Koirala et al.[149] found that the ZrO_2-stabilized sorbent (with 78%wt of $CaZrO_3$) kept its CO_2 uptake (0.11 $g_{CO2}/g_{sorbent}$)

over 1200 cycles without any significant decline. The Authors, however, pointed out that, in spite of the remarkable multicyclic stability, the great amount of CaZrO3 decreased the CaO reactivity, thus leading to a limited CO_2 uptake.

SiO_2 is another widely available and cost-effective support material that has been greatly used to produce stabilized CaO-based sorbents,[162] with nanostructured silica serving to both enhance the dispersion of CaO agglomerates and alleviate the sintering phenomena.[154,163] In this case, it has been shown that the beneficial effect is ascribable to the interaction between SiO2 and CaO, which leads to the formation of calcium silicates (Ca_2SiO_4) providing a greater thermal stability of the CaO skeleton and, in turn, a higher multicycle effective conversion when compared with raw limestone.[68] Indeed, Ca_2SiO_4 (characterized by a T_t of 929 °C, which is higher than that of SiO_2, 664 °C, Table 6) undergoes a phase transformation (α′- Ca2SiO4 ↔ β-Ca2SiO4) due to the temperature swing of the CaL process, which causes a volume expansion of the sorbent counteracting the sintering phenomena.[131]

Among the supports not forming metal oxides with CaO, MgO (T_t = 1276, Table 6) is considered one of the most promising additive to increase the CaO multicyclic stability thanks to its wide availability and low cost[164,165] As a matter of fact, dolomite [$CaMg(CO_3)_2$], which is a naturally occurring CO_2 sorbent combining $MgCO_3$ and $CaCO_3$, has been proved to be a good CaO precursor, yielding more stable CaO conversion performnces over multiple cycles thanks to the presence of the inert MgO that successfully separate the reactive CaO particles.[166,167] Besides the spacing effect, MgO has a much higher sintering temperature (1289 °C) as compared to CaO (527 °C), thus also limiting the tendency susceptibility of raw lime to sintering and, consequently, enhancing its durability.[168]

Table 8. Multicyclic carbonation performances, in terms of initial and residual CO_2 uptake e, of CaO-based sorbents stabilized with inert materials not forming mixed oxides with CaO.

Support	Synthesis method	Temperature Carb./Calcin.	CO_2 %vol. Carb./Calcin.	Testing conditions[b]	CO_2 uptake (g_{CO_2} g^{-1}_{sorb}) *initial - last*	Ref.
MgO						
%wt MgO						
16	carbon gel templating	650/900 ˚C	24/0	TGA – 10 cycles	0.60 – 0.55	[169]
8	one-pot recrystallization	650/900 ˚C	20/100	TGA – 10 cycles	0.67 – 0.47	[170]
15	wet mechanochemical activation	650/900 ˚C	20/100	TGA – 30 cycles	0.65 – 0.30	[171]
25	wet mixing	650/900 ˚C	15/0	TGA – 24 cycles	0.60 – 0.56	[168]
25	wet mixing	650/850 ˚C	20/0	TGA – 50 cycles	0.35 – 0.27	[172]
41	wet mixing	650/900 ˚C	100/0	dual fixed bed – 10 cycles	0.40 – 0.28	[173]
34	sol-gel	650/850 ˚C	15/0	TGA – 100 cycles	0.46 – 0.32	[174]
20	wet mixing	600/900 ˚C	15/0	fixed bed – 10 cycles	0.26 – 0.25	[175]
26	dry mixing	758/850 ˚C	100/0	dual fixed bed – 50 cycles	0.66 – 0.53	[176]
6	sol-gel	675/950 ˚C	15/80	TGA – 50 cycles	0.70 – 0.58	[177]
26	wet mixing	650/850 ˚C	15/0	TGA – 50 cycles	0.52 – 0.40	[178]

Y_2O_3						
%wt Y_2O_3						
20	calcination	650/850 ˚C	20/0	TGA – 10 cycles	0.58 – 0.57	[134]
20	calcination	650/950 ˚C	25/100	TGA – 10 cycles	0.57 – 0.49	[134]
CeO_2						
Ca/Ce						
15	sol–gel combustion	600/700 ˚C	50/0	TGA – 18 cycles	0.59 – 0.59	[135]

CaO = CO_2 uptake of about 0.1 $g_{CO2}/g_{sorbent}$ after 20 cycles, corresponding to a loss of approximately 80% of its initial uptake [133]

As clearly shown in Table 8, regardless of the specific synthesis method, the MgO-supported CaO-based sorbents are always characterized by enhanced cyclic stability with respect to the raw limestone (i.e. CO_2 uptake of about 0.1 $g_{CO2}/g_{sorbent}$ after 20 cycles, corresponding to a loss of approximately 80% of its initial uptake).[133] In this context, the general consensus is that the MgO-stabilization effect can be greatly improved if the mixing of MgO and CaO is performed at the nanoscale.[83] Huang et al.[179] homogeneously dispersed and mixed MgO nanoparticles (50 - 100 nm) with CaO grains on the particle surface, thus obtaining a good sintering resistance and improved multicyclic stability.

As inferable from Table 8, the cyclic stability of the MgO-stabilized sorbents is also clearly influenced by the amount of MgO (i.e. the MgO-to-CaO weight ratio) in CaO-based sorbent.[96] In particular, it has been demonstrated that the amount of MgO in the sorbent should be sufficiently high to obtain an effective and stable reactive performances. Typically, it is also reported that, regardless of the MgO/CaO ratio, the specific surface area and pore volume of the MgO-stabilized sorbent are higher than those of the original; nonetheless, increasing the amount of MgO yields a reduction in the specific surface area.[180] It was also demonstrated that there is typically an optimum MgO/CaO ratio, able to maximize the multicyclic CO_2 uptake capacity; this is due to the fact that above a certain amount of MgO its sintering resistance is lost.[168,181]

Besides MgO, Y_2O_3 (T_t = 1083 °C) is also reported to be effectively stabilize CaO-based sorbents, i.e. limiting their tendency to sintering.[83] Y_2O_3 nanoparticles were homogeneously distributed on the CaO particles by Zhang et al.[134] The Authors observed an enhancement of the reaction kinetics in the kinetically controlled stage and a linear correlation between the maximum carbonation rate and the volume of specific pores (smaller than 220 nm). Two different synthesis methods, thermal decomposition and wet impregnation, were used by Derevschikov et al.[182] to synthesize Y_2O_3-stabilized CaO-based sorbents. No significant difference in the multicyclic performances were observed, thus indicating that the performances of Y_2O_3-supported CaO-based sorbents are not significantly affected by the specific synthesis procedure.

CeO_2 (T_t = 1064 °C, Table 6) has been also successfully incorporated, as stabilizer, in CaO-based sorbents. Besides its high T_t, the incorporation of CeO_2 is also reported to provide great oxygen mobility and vacancy generation;[183] i.e. CO_2 diffusion and O_2−mobility are facilitated, thus positively affecting the carbonation reaction.[184] CeO_2-supported CaO-based sorbents with different Ca/Ce molar ratio were synthesized via the sol−gel method by different Authors.[135,150,185] The CeO_2-stabilized sorbents showed a loose-shell-connected cross-linking structure with CeO_2 acting as physical barrier to the CaO crystallites, which prevents their growth and sintering.[135]

Summing up, the choice of the support material must be made considering two different perspectives: the sorbent multicyclic stability and the sorbent activity towards CO_2. As a matter of fact, the CaO-based sorbents stabilized with materials that react with CaO and form metal oxides are typically characterized by better multicyclic stability. The presence of the metal oxides is indeed crucial in acting as stable framework, thus contrasting the sintering phenomena and easing the decline in the CO_2 uptake with the increasing number of cycles. However, in spite of the enhanced multicyclic-stability, the formed metal oxides reduce the CaO activity, thus causing a decrease of the intrinsic CO2 sorption capacity. Therefore, the selection of each sorbent is necessarily the result of a compromise between the mitigation of CO_2 uptake decline and the reduction of CaO activity.

In light of the above considerations, CaO-based sorbents have been also stabilized simultaneously incorporating more than one inert material, thus exploiting the synergistic effect played by different support materials on both the CO_2 uptake capacity and multicyclic stability. In this context, different synthesis methods and materials have been investigated, as summarized in Table 9. For instance, TiO_2 and Al_2O_3 were simultaneously used by Peng et al.[186] obtaining a hierarchical core−shell micro-architectured CaO-based sorbent enriched in Ca, supported by Al_2O_3 and stabilized by TiO_2. More specifically, the core of the CaO/TiO_2−Al_2O_3 sorbent contained the Al_2O_3 micron-sized particle, whereas its surface is coated with TiO_2 nanoparticles, thus avoiding the reaction between CaO and Al_2O_3. Likewise, He et al. synthesized a Y_2O_3/MgO-stabilized CaO-based sorbent via a sol−gel method.[187] In this case, Y_2O_3 was selected to induce an enhancement of the cyclic stability, whereas,

MgO was selected to improve the CO_2 uptake capacity (by means of an increased porous space for the carbonation reaction to take place). A spray drying approach was, similarly, proposed by Sun et al.[188] to produce Al_2O_3/MgO-stabilized CaO-based sorbents, obtaining good results in terms of both enhanced multicyclic CO_2 sorption performances and CO_2 uptake (which was found to be larger than that typical of Al_2O_3-stabilized CaO-based sorbents).

Even though showing very promising results in terms of multi-cyclic stability, the use of novel sintering-resistant sorbents implies the necessity to take into account the higher costs of raw materials, with respect to the use of natural limestone, and the economics and environmental impact of the synthesis process. Moreover, it should be pointed out the vast majority of all the synthetic sorbents reported in the literature are produced in fine powdered form only, which poses a clear handling/processing issue.

In this context, aiming at reducing the cost of sorbent synthesis, the use of industrial wastes and/or natural mineral clays, containing high T_t compounds, have been also proposed as promising support materials to enhance the CaO-based sorbent performances, thus also alleviating the land-filling issues and environmental and health concerns associated with industrial waste disposal.[83] For example, fly ash (mainly consisting of SiO_2 and Al_2O_3) is a common solid waste in coal-fired power plants that have been successfully used as cheap and environmental-friendly support material to produce CaO-stabilized sorbents.[189,190] As for the use of natural mineral clays, sepiolite [$Mg_4Si_6O_{15}(OH)_2 \cdot 6H_2O$], characterized by favorable structural features, i.e. continuous two-dimensional tetrahedral sheet morphology with high surface area and porosity, was successfully used by Shin et al.[191] to produce sepiolite-stabilized CaO-based sorbents.

Table 9. Multicyclic carbonation performances, in terms of initial and residual CO_2 uptake, of CaO-based sorbents stabilized with two different inert materials.

Support	Synthesis method	Temperature Carb./Calcin.	CO_2 %vol. Carb./Calcin.	Testing conditions[b]	CO_2 uptake (g_{CO2} g^{-1}_{sorb}) *initial - last*	Ref.
ZrO_2 - CeO_2	precipitation	800/800 ˚C	100/0	TGA – 14 cycles	0.55 – 0.60	[192]
Al_2O_3 - CeO_2	wet mixing	850/850 ˚C	100/0	dual fixed bed – 30 cycles	0.60 – 0.57	[193]
MgO - Al_2O_3	sol-gel	650/900 ˚C	20/100	TGA – 10 cycles	0.52 – 0.39	[194]
MgO - Al_2O_3	wet mixing	758/758 ˚C	100/0	TGA – 130 cycles	0.62 – 0.45	[195]
MgO - Al_2O_3	spray drying	650/900 ˚C	15/40	TGA – 25 cycles	0.58 – 0.35	[188]
CeO_2 – MnO_2	sol-gel	600/700 ˚C	50/0	TGA – 40 cycles	0.61 – 0.61	[195]
Y_2O_3 - ZrO_2	wet impregnations	675/850 ˚C	100/0	TGA – 20 cycles	0.23 – 0.11	[196]
Al_2O_3 - Y_2O_3	Pechini	650/900 ˚C	20/100	TGA – 30 cycles	0.64 – 0.38	[197]
Y_2O_3 - MgO	sol-gel	650/900 ˚C	15/0	TGA – 122 cycles	0.47 – 0.31	[187]
CeO_2 – Al_2O_3	templating method	650/900 ˚C	15/0	TGA – 104 cycles	0.55 – 0.44	[186]

CaO = CO_2 uptake of about 0.1 $g_{CO2}/g_{sorbent}$ after 20 cycles, corresponding to a loss of approximately 80% of its initial uptake[133]

3.1.1.3 The use of fine $CaO/CaCO_3$ particles

It is well-known that, besides crystallinity,[198] morphology[129,199] and the inclusion of additives,[88,200] also particle size[201,202] has a great impact on the role in the multicycle performances of Ca-based sorbents. In particular, large or highly crystalline particles are characterized by considerably slower calcination kinetics, thus implying the necessity to use higher temperatures to completely regenerate CaO in relatively short residence times.[19,77,91,203,204] Moreover, large particles suffer from pore diffusion and pore-plugging, which lead to hindered carbonation performances.[91,205,206] On the contrary, small particles are capable of fast calcination at lower temperatures, which, in turn, yields improved multicyclic stability.[202] In other words, the sintering and pore-plugging issues and, in turn, the decline of the CaO multi-cyclic activity, can be also remarkably limited if the CaO particle dimension is reduced,[19,91,207] also through milling the original limestone.[93,208] In this context, it is also noteworthy that using small particles would results in an easier integration of the CaL process with the solar energy due to a decreased cost of materials for the construction of the solar receiver, thanks to the possibility to perform the calcination at lower temperatures.[209] The effect of the particle size on the multicyclic stability, in terms of residual carbonation conversion (X_r), of limestone is summarized in Table 10.

Benitez-Guerriero et al.[91] and Ortiz et al.[19] have shown that the residual CaO multi-cyclic conversion of natural limestone can be increased from 0.18 to 0.45 if the limestone particle size is decreased below 45 μm. Interestingly, it has been also pointed out that the dependence of the multi-cycle CaO conversion on the CaO particle size derives from the relative thickness of the $CaCO_3$ product layer as compared to the size of the pores generated in the CaO skeleton after the fast reaction-controlled stage of the carbonation reaction.[19] More specifically, the thickness of the $CaCO_3$ product layer can become larger than 100 nm, whereas the pores formed inside the CaO skeleton are typically smaller than 50 nm under TCS-CSP operating conditions (i.e. high-temperature/high-P_{CO_2} carbonation and

low-temperature/low- P_{CO_2} calcination), which means that coarse CaO particles are affected by severe pore-plugging.[19,91] Moreover, in the case of coarse particles, those pores getting plugged by the $CaCO_3$ product layer are more prone to sinter in the following calcination steps, thus additionally decreasing the CaO surface area available for carbonation.[19,91] On the contrary, fine particles (< 45 μm), whose main feature is the higher surface to volume ratio as compared to coarser particles, have been shown to limit the entity of the pore-plugging phenomena, due to their pores being fully accessible to the CO_2 molecules.[19,91]

In spite of its evident benefits in terms of multi-cyclic stability, the use of fine sorbent particles in real large-scale reactors brings major practical challenges and handling/processing issues; indeed, the intrinsic fine particle cohesiveness leads to severe agglomeration and, in turn, hindrance of reaction efficiency due to poor and heterogeneous gas/solid contact and mass/heat transfer.[210–214] In this context, Raganati et al[77,203,215] and Valverde et al.[216] successfully demonstrated that the use of high-intensity acoustic waves makes it possible to actually use fine limestone particles in fluidized bed reactors also enhancing their carbonation performances under both CCS and TCS-CSP operating conditions. More specifically, the acoustic perturbation exhibits a much stronger effect in the initial fast stage of the carbonation reaction, i.e. when the reaction is mainly controlled by the gas-solid interaction between the CO_2 molecules and the CaO surface. The acoustic perturbation is also capable of alleviating the sintering-induced CaO deactivation, thus obtaining a the CaO residual carbonation conversion (X_{20} = 0.55,[77] Table 9) larger than that reported for coarser particles for coarser limestone particles (X_{20} = 0.41)[19,91] and even stabilized CaO-based sorbents (X_{20} = 0.46).[19,92]

Aiming at addressing the elutriation issues arising from the use of powdered CaO-based materials, granulation has been proposed as viable technique to prepare CaO-based pelletized sorbents with enhanced mechanical stability.[217–219] Five types of granulation methods are currently available: the extrusion method,[220] spheronization method,[221] wrapped shell method,[222] extrusion-spheronization

method,[223] and casting method.[224] Recently, Zhang et al.[225] thoroughly reviewed and summarized the principles and main features of different granulation methods, also analyzing the effects on the mechanical and reaction performances. Briefly, they pointed out that the extrusion, extrusion-spheronization and casting methods with external force are capable of compacting the sorbent structure, thus improving the sorbent compressive strength, but, at the same time, the initial CO_2 uptake capacity of the pelletized sorbent is reduced. On the contrary, the spheronization method and casting method without the external force can be used to shape the sorbent into pellets, thus to decreasing the attrition phenomena, without affecting the CO_2 uptake performance. The pellets prepared by the wrapped shell method are characterized by different performances primarily depending on the specific structures of the shells.

Table 10. Effect of particle size on the residual effective conversion (X_r) of limestone at different CaL conditions.

CaO precursor	Mean particle size (μm)	Calcination (T – Atmosphere)	Carbonation (T – Atmosphere)	Residual CaO conversion (X_r)[a]	
Limestone					
	> 45	725 ˚C - He (100 %vol.)	850 ˚C - CO_2 (100 %vol.)	0.18 (X_{20})[b]	91
	< 45	252 ˚C – He (100 %vol.)	850 ˚C - CO_2 (100 %vol.)	0.41 (X_{20})[b]	91
	3.19	725 ˚C – He (100 %vol.)	850 ˚C - CO_2 (100 %vol.)	0.51 (X_{20} = 0.6)[b]	202
	> 160	725 ˚C – He (100 %vol.)	850 ˚C - CO_2 (100 %vol.)	0.21 (X_{20})[b]	92
	> 160	950 ˚C – CO_2 (100 %vol.)	850 ˚C - CO_2 (100 %vol.)	0.18 (X_{20})[b]	92
	> 200	1000 ˚C – CO_2 (100 %vol.)	850 ˚C - CO_2 (100 %vol.)	0.13 (X_{11})[b]	226
	45 - 160	725 ˚C – He (100 %vol.)	850 ˚C - CO_2 (100 %vol.)	0.15 (X_{50})[b]	68
	4	750 ˚C – N_2 (100 %vol.)	850 ˚C - CO_2/N_2 (70/30 %vol.)	0.50 (X_{20} = 0.55)[b]	77
	1 - 10	725 ˚C – He (100 %vol.)	850 ˚C - CO_2 (100 %vol.)	0.48 (X_{20} = 0.58)[b]	227
Dolomite					
	> 45	725 ˚C - He (100 %vol.)	850 ˚C - CO_2 (100 %vol.)	0.42 (X_{20})[b]	91
	< 45	252 ˚C – He (100 %vol.)	850 ˚C - CO_2 (100 %vol.)	0.41 (X_{20})[b]	91

	> 160	725 ˚C – He (100 %vol.)	850 ˚C - CO_2 (100 %vol.)	0.47 (X_{20})[b]	92
	> 160	950 ˚C – CO_2 (100 %vol.)	850 ˚C - CO_2 (100 %vol.)	0.39 (X_{20})[b]	92
	> 200	1000 ˚C – CO_2 (100 %vol.)	850 ˚C - CO_2 (100 %vol.)	0.20 (X_{11})[b]	226
Dolomite/Limestone					
	268	725 ˚C – He (100 %vol.)	850 ˚C - CO_2 (100 %vol.)	0.53 (X_{11})[b]	129
	221	725 ˚C – He (100 %vol.)	850 ˚C - CO_2 (100 %vol.)	0.69 (X_{11})[b]	129
Chalk					
	7	725 ˚C – He (100 %vol.)	850 ˚C - CO_2 (100 %vol.)	0.38 (X_{20} = 0.44)[b]	202
Marble					
	> 45	725 ˚C - He (100 %vol.)	850 ˚C - CO_2 (100 %vol.)	0.16 (X_{20})[b]	91
	< 45	725 ˚C - He (100 %vol.)	850 ˚C - CO_2 (100 %vol.)	0.40 (X_{20})[b]	91
	11	725 ˚C – He (100 %vol.)	850 ˚C - CO_2 (100 %vol.)	0.27 (X_{20} = 0.40)[b]	202
$Ca_3Al_2O_6/CaCO_3$					
	> 160	725 ˚C – He (100 %vol.)	850 ˚C - CO_2 (100 %vol.)	0.41 (X_{20})[b]	92
	> 160	950 ˚C – CO_2 (100 %vol.)	850 ˚C - CO_2 (100 %vol.)	0.18 (X_{20})[b]	92
$ZrO_2/CaCO_3$					

	> 160	725 ˚C – He (100 %vol.)	850 ˚C - CO_2 (100 %vol.)	0.46 (X_{20})[b]	92
	> 160	950 ˚C – CO_2 (100 %vol.)	850 ˚C - CO_2 (100 %vol.)	0.37 (X_{20})[b]	92
	> 200	1000 ˚C – He (100 %vol.)	850 ˚C - CO_2 (100 %vol.)	0.33 (X_{20})[b]	226

[a] X_r = evaluated as the value the CaO carbonation conversion converges asymptotically after a very large number of cycles.
[b] X_y = CaO carbonation conversion at y-th cycle which is close to the residual value.

3.2 Alternative carbonate systems ($BaO/BaCO_3$ and $SrO/SrCO_3$)

In alternative to the more widely investigated $CaCO_3$/CaO couple, other carbonate systems have been proposed for TCS-CSP applications, such as $BaCO_3$/BaO and $SrCO_3$/SrO (Table 2).

As regards the $BaCO_3$/BaO system, $BaCO_3$ is industrially produced from naturally mined barite ($BaSO_4$) via the 'black ash' process, i.e. a reaction with coke. However, pristine $BaCO_3$ is thermodynamically very stable and has, indeed, a decomposition temperature larger than 1500 ˚C at atmospheric pressure, which is too high to be handled for commercial TCS applications.[20,228] Besides that, $BaCO_3$ is also affected by severe sintering and melting issues, which hinder the possibility to carry out cyclic operations and, in turn, its applicability for TCS.[20]

Likewise, the $SrO/SrCO_3$ system has been receiving increasing research interest due to its advantageous features for both CCS and TCS applications.[20,34,229–232] Sr is the 15th most abundant element on earth and, hence, $SrCO_3$ is widely available and rather inexpensive.[229] Besides, the system can count on higher value of both energy density (4 GJ $m_{SrCO_3}^{-3}$) and dissociation temperature (equilibrium temperature = 1175 ˚C at P_{CO_2} = 1atm)[34] with respect to the $CaCO_3$/CaO couple,[229] but still manageable from an applicative point of view. However, $SrCO_3$/SrO suffers from the same critical problem as $CaCO_3$/CaO system, i.e. the severe decline of SrCO reactivity over repeated calcination/carbonation cycles, which, also in this case, is due to sintering and pore plugging.[20,34,230]

3.2.1 Multi-cyclic decline of BrO/SrO reactivity and technological solutions

As regards the problems encountered with the pristine $BaCO_3$, i.e. its extremely high decomposition temperature, Moller et al.[228] recently proposed a thermodynamic destabilization procedure by means of the incorporation of barium orthosilicate ($BaSiO_3$). More specifically, the resulting $BaSiO_3$- $BaCO_3$ system is characterized by an improved thermodynamics, being able to successfully operate in cyclic mode at more suitable temperatures 700–1000 ˚C through the following reaction scheme:

$$BaCO_3 + BaSiO_3 = Ba_2SiO_4 + CO_2 \quad (5)$$

The Authors also evaluated the possibility to improve the performances of the $BaSiO_3$-$BaCO_3$ system by adding a second carbonate, $CaCO_3$. It was found that the presence of $CaCO_3$ in amounts ranging from 2.5 to 10 mol% made it possible to enhance the reaction kinetics by up to ten times thanks to the formation of $Ba_{2-x}Ca_{2x}SiO_4$ intermediates.

As regards the decline in the sorbent reactivity along multiple carbonation/calcination cycles due to sintering, only few studies can be found in the literature proposing strategies to alleviate the SrO/BaO deactivation and they basically consist in the introduction of inert refractory material in the structural framework of the sorbent.

After a preliminary investigation of the thermodynamics and kinetics of $CaCO_3$, $SrCO_3$ and $BaCO_3$ for TCS applications, Andre and Abanades[20] studied the effect of MgO stabilization on the cyclic

stability of the three carbonates. It was shown that the multicyclic stability of all the MgO-stabilized sorbents was clearly improved. However, while $BaCO_3$ and $CaCO_3$ still suffered some loss in their multicyclic carbonation capacity even after MgO-stabilization, the MgO-stabilized $SrCO_3$ sample did not exhibit any significant loss in its multicyclic performances. Likewise, MgO-stabilized SrO composites were tested by Gigantino et al.[233] with a focus on the effect of several aspects of the synthesis process, i.e. the type of precursor material, support contents and production method. More recently, Ammendola et al.[234] incorporated different materials (Al_2O_3, Hydroxyapatite, ZrO_2, ZrO_2-Al_2O_3 and Sr-substituted Hydroxyapatite) to increase the cycling stability of the system. Among these, Al_2O_3 was proved to be a promising sintering/agglomeration inhibitor when $SrO/SrCO_3$ is used under fluidized bed conditions.[235,236] Similarly, Amghar et al.[237] synthesized and tested the cyclic stability of different SrO-composites using ZrO_2, SiO_2 and MgO as stabilizing agents. The use of inert additives with great thermal stability and acting as "spacers" (i.e. by physically separating the sorbent particles) was also successfully proved to inhibit the sintering phenomena and, in turn, the SrO deactivation.[34,230] More specifically, $CaSO_4$/$Sr_3(PO_4)_2$ and zirconia-based sintering inhibitors were successfully added to $SrO/SrCO_3$ system by Bagherisereshki et al.[34] and Rhodes et al.,[230] showing good multi-cyclic stability of the stabilized composites with respect to the untreated material.

4 Reactor configuration

For the actual deployment of TCS for CSP applications, the design of efficient reactors goes hand in hand with the materials development/improvement. As a matter of fact, the selection of the optimum reactor configuration is strictly dependent on the nature, physicochemical properties, and working temperatures of the reagents. In the following sections, an overview is provided of the different types of solid–gas reactors proposed in the literature to carry out the carbonation and calcination reactions in the framework of TCS-CSP applications.

4.1 Solar calciner

Several types of solar-driven reactors, i.e. particle receivers, have been developed and tested at laboratory and pilot scale for carbonate-based TCS systems and recently reviewed.[7,61]

Solar-driven reactors can be classified based on the heat integration mode into the reactor, the flow pattern, and the reaction type, as proposed by Zsembinszki et al.[61]

Clearly, the selection of the most suitable heat integration mode is strongly influenced by the thermal properties (i.e. solar absorptivity) of the particles entering the solar calciner. Based on this criterion, the solar reactors can be further classified in: directly and indirectly irradiated:[7]

- In the directly irradiated ones, the solar radiation directly heated the reactants, i.e. without any intermediate surface. Therefore, from one hand, the achievable temperatures are maximized,

but, on the other, keeping the temperature homogeneity inside the reactor may be more challenging.[238] Based on this working principle, it is clear that the absorptivity of the reagents plays a crucial role in obtaining an effective radiative heat transfer.[7] Directly irradiated reactors can be either opened to air or closed by a transparent window, through which the concentrated solar radiation enters the reactor chamber.[7] In the case of closed reactors, the design of a proper window is still challenging, especially for high-temperature processes (T > 900 °C),[66] and the necessity to keep it clean during operation must be also taken into account to both limit the reduction of radiation transfer to the reaction chamber and to avoid the cracking of the windows itself.[7]

- In the indirectly irradiated reactors, the reactants are not directly heated by the concentrated solar radiation; a primary absorber is used to directly absorb the concentrated solar radiation which is then transferred, in the form of heat, to the reactants.[7] In this case, two types of configuration can be envisaged: i) a design in which the walls of the reactor chamber are irradiated by the sun; ii) a design comprising two cavities, one absorbing the solar radiation and the other acting as reaction chamber. In the former configuration, the temperature homogeneity on the wall has been indicated as one of the primary issues, since the temperature may be easily different on different spots of the wall.[7] The latter configuration, on the contrary,

is preferred for reactions in which the products are mainly in the gaseous phase, thus quickly leaving the reaction chamber; indeed, the formation of a growing product layer above the unreacted solid particles may act as an insulation layer.[239] In both configurations, the limiting factor is represented by the efficiency of the conduction through the primary absorber material.[239]

Considering that carbonates, such as limestone, are typically white materials and, hence, characterized by poor solar absorptivity[74] (16–60 %[7] with respect to values larger than 95 % for state-of-the-art solar absorber coatings),[240] the indirect heating integration mode is generally considered to be the most appropriate solution for the calcination reaction.[241] However, different works have been published focusing on boosting both the intrinsically low optical and thermal conduction properties of carbonate-based sorbents in order to improve their performances in both directly-irradiated and indirectly-irradiated systems. $CaCO_3$/graphite nano-sheets composites with enhanced thermal conductivity (60 % increase) were synthesized via wet-impregnation with a H_3BO_3 solution.[242] As a consequence of the improved thermal conductivity, the composite energy storage density (1313 kJ kg^{-1} after 50 cycles) was almost three times larger than that of the pristine limestone (452 kJ kg^{-1}). A sol-gel method was proposed by Da et al.[28] to produce CaO composites doped with binary metal element (Mn and Fe). The proposed doping strategy made it possible to enhance both the solar

absorptivity (reaching a maximum value of 89.81 % with a Ca/Mn/Fe molar ratio of 100:4:8) and multicyclic stability of the sorbent ($X_1 = X_{20} = 0.8$ due to the improved sintering resistance arising from the presence of $FeMnO_3$ and Fe_2O_3). Similarly, Teng et al. doped $CaCO_3$ with the high-solar-absorptivity Mn/Fe oxides.[243] The Mn/Fe-doped $CaCO_3$ samples showed an improved solar absorptivity of 91% in comparison to the low value, 11%, characterizing the raw $CaCO_3$ and also an enhanced carbonation conversion multicyclic stability ($X > 90\%$ in 60 cycles) and average energy density (1450 kJ/kg, i.e. 1.8 times larger than that of the raw $CaCO_3$). Likewise, Fe/Mn-doped Ca-based composites (mainly consisting of $CaCO_3$ and Ca_2FeMnO_5) were produced by Yang et al.[244] An absorptivity of 77% (in comparison to the 10.8% measured for the pure $CaCO_3$ sample) was achieved using a Ca/Fe/Mn molar ratio equal to 100:2:7. A sol-gel synthesis method (using aluminum nitrate and iron nitrate as precursors) was also proposed by Song et al.[245] to produce Fe/Al-doped $CaCO_3$ particles that showed absorptivity of 46% (in comparison to the 8% value obtained for the untreated $CaCO_3$). Mn/SiC-doped CaO pellets (absorptivity = 53% with respect to the 3% value of the un-modified CaO particles; $X_{30} = 0.48$) were synthesized by Li et al.[246] through the extrusion-spheronization method. Zheng et al.[247] synthesized a series of dark Ca-based sorbents by binary-doping the $CaCO_3$ particles with Cu/Fe/Co/Cr (to enhance the solar absorptivity) and Mn/Al (to enhance the multicyclic stability) via a sol-gel method. All the prepared composites were characterized by a spectral absorption of solar energy larger 60 % with the Cu/Mn-doped samples

showing the maximum value of energy density, 1952 kJ kg^{-1} after 20 cycles (i.e.84% larger than that of pure $CaCO_3$ particles).

Depending on needed residence time of the particles inside the reactor to achieve full decomposition, the selection of the most suitable reactor configuration can be made according to type of gas-solid contacting system, i.e. the type gas-solid flow-pattern. According to this criterion, reactors can be classified in: entrained beds, stacked beds and fluidized beds:[7,61]

- In entrained bed reactors, specifically cyclones, the particles are dragged across the reactor.
- In stacked bed reactors, the solid particles are placed in the form of a bed (which can be fixed, mobile, or rotary) and the they are not moved by the gas flow.
- In fluidized bed reactors, the gas flows through the particles creating a suspension.

Pros/cons and performances of the solar-driven stacked, fluidized beds and entrained beds solar receivers are summarized in Table 11 and Table 12, respectively.

Table 11. Comparison of solar receivers based on different types of gas-solid flow-pattern.

Reactor type	Advantages	Disadvantages
Stacked		
Fixed bed	• Low cost • Easy design • Easy construction • Easy operation • Widely studied	• Poor heat/mass transfer • High pressure drop • Difficult implementation in solar reactors for continuous operations • Non-uniform irradiance distribution on the particle bed
Mobile bed	○ High heat/mass transfer	○ Non-uniform irradiance distribution on the particle bed ○ Complex hydrodynamics ○ Difficult implementation in solar reactors
Rotary kiln	• High heat/mass transfer • High versatility • Co-current and counter-current flow	• Difficult scale-up • High risk of mechanical maintenance (due to rotary elements) • Difficult integration in large-scale solar towers (due to the horizontal design)
Fluidized		
Fluidized bed	○ High heat/mass transfer	○ Difficult implementation in solar reactors

	○ Minimized hot/cold spots ○ Widely used at industrial scale	○ Particle attrition ○ Erosion of internal components ○ Complex hydrodynamics ○ Energy consumption for fluidization
Entrained		
Cyclone	• Continuous feed • Separate solid and gas products	• Solid deposition on the walls • Erosion of the reactor window

Table 12. Summary of the data reported for different types of solar-driven entrained, fixed and fluidized bed calcination reactors.

	Heat integration	System type	Operation mode	Power (kW)	T_{max} °C	Mass flow kg h^{-1}	Thermal efficiency (%)	Chemical efficiency (%)	Conversion degree (%)	Particle size (μm)	Length/diameter (mm)	Ref.
Stacked												
Rotary kiln	Direct	Open	Continuous/batch	1.5	1500	0.28	10 - 30	15	30/60	200 - 315	90/20	74
Rotary kiln	Direct	Open	Continuous	10	1150	1.30	-	20	98	2000-3000	600/350	33
Rotary kiln	Direct	Open	Continuous	14	997	9.60/6.20	22/17	15/20	73/95	1-176	735/240	248
Rotary kiln	Direct	Open	Continuous	14	980	5	22	17	55	1-176	735/240	249
Rotary kiln	Indirect	Cavity	Continuous	2	1000	1.29	-	-	-	200-315	66/52.5	73
Rotary kiln	Indirect	Cavity	Continuous	0.75	1027	0.16	-	16.60	100	50-100	400/20	250
Rotary kiln	Indirect	Tube	Continuous	10.60	1127	4	22	35	98	2000-3000	225/252	251,252
Entrained												
Cyclone	Direct	Open	Continuous	3	1027	0.60	34	9	53-94	1-5	300/200	253,254
Cyclone	Direct	Open	Continuous	54	9000	25	73	9	15	10	800/540	255
Cyclone	Direct	Closed	Continuous	4.76	1145	0.18		7-10	83	6	210/120	256,257
Fluidized												
Fluidized bed	Direct	Closed	Batch	1.75	1300	-	20-40	20	100	200-315	300/35	74

Fluidized bed	Direct	Closed	Batch	75	875	-	-	-	71	-	250/22	[258]
Fluidized bed	Direct	Closed	Batch	3.20	950	-	-	-	88	420-590	100/100	[71,259]
Fluidized bed	Direct	Closed	Batch	2	1175	-	-	-	-	250	120/10	[260]
Fluidized bed	Indirect	Cavity	Continuous	25	800	9.40	-	6.60	100	60-220	1000/80	[261]
Fluidized bed	Indirect	Cavity	Continuous	55	915	20	12	17	95.20	10-300	1000/80	[262]

4.1.1 Entrained bed

In solar entrained bed reactors, the solid and gaseous phases are injected in co-current flow, usually horizontally or downward, and subsequently separated creating a cyclone or a vortex flow inside the reactor. This reactor configuration has the advantage of providing high heat transfer coefficients (up to 200–400 W m^{-2} K^{-1} for particles with a diameter between 150–300 μm)[263] and high heating rates, but still assuring a good control of the reaction conditions. However, it has the disadvantages of quite short residence time (a few seconds) and high sensitivity to the particle dimensions.[264] Therefore, the geometry of the cavity and the injection of the gaseous and solid reactants represent the most critical design challenges.[238] An open solar directly irradiated entrained bed reactor was designed by Imhof[253] and Steinfeld et al.[254] to carry out the calcination of $CaCO_3$ particles with a size of 1–5 μm, as a consequence of the technical issues deriving from the quartz window needed for the closed configuration. The reactor consisted of an open truncated cavity (30 cm height) whose inner walls were insulated by a ceramic layer. More specifically, the proposed reactor configuration consists of an open cyclone gas separator in which: the solid and the gaseous reactants are injected through a tangential slot; a high-tangential-velocity vortex is created by the gas stream, thus producing a high centrifugal force that moves the entrained particles to the cyclone wall where they drop down and are removed from the gaseous stream, which leaves the cyclone through the gas outlet channel. A temperature higher than 1000 ˚C and a total efficiency of 43% with $CaCO_3$ calcination conversion

degree of 53 % – 94% were achieved with this reactor configuration.[254] Aiming at increasing the particle residence time, thus counteracting the poor optical properties of $CaCO_3$ for the absorption of the solar radiation, the solar cyclone reactor was combined with a fluidized bed reactor.[253] Later on, the concept of the reactor developed by Imhof[253] was modified, placing cyclone vertically with the solar radiation entering from the bottom, and its size increased.[255] A $CaCO_3$ calcination conversion degree of 32 – 85 % with a thermal efficiency of 73 % and a chemical efficiency of 15% were obtained. Even though not for TCS applications, Nikulshina et al.[256,257] developed a 5 kW closed directly irradiated solar entrained bed reactor to perform the $CaCO_3$ calcination reactor in combination with the CH_4 reforming and obtained a chemical efficiency of 7 - 10% and a $CaCO_3$ calcination conversion degree of 83 %. A possible future optimization of the reactor design was also proposed envisaging the limitation of the conduction losses and re-radiation through the reactor insulation and the reactor aperture, respectively.

4.1.2 Stacked bed

As regards the stacked bed reactors, the fixed bed ones are characterized by the simplest and most economic design, construction and operation; indeed, they are typically used to carry out preliminary tests at the lab-scale level in order to obtain preliminary information (e.g. the reaction temperature, kinetics constants, etc.) on different types of chemical processes.[238] However, in spite of these favorable features, fixed bed reactors suffer from poor heat and transfer coefficients, which lead to

high thermal gradient inside the bed (i.e. hot/cold spots) that causes, in turn, a non-homogeneous conversion of the reactant.[238] Besides that, continuous operation is not feasible in fixed bed reactors; therefore, after the calcination reaction completion, a reloading of the feedstock is needed, thus causing additional thermal losses during cooling and heating stages before and after restocking [250]. Even though some papers are available in the literature on the use of solar-driven fixed bed reactors, none of them refers to the calcination reactions of carbonates. For example, closed directly irradiated fixed bed reactors were used for the solar-driven H_2 production via H_2O/CO_2 splitting.[265–267] Likewise, also indirectly irradiated fixed bed reactors have been developed for the solar-driven steam gasification of coal[268] and carbon waste.[269]

Also in the framework of the stacked bed reactors, mobile bed reactors can provide a better temperature control and distribution as compared to fixed bed reactors, also allowing the possibility to perform the process in a continuous operation mode.[61] As for the fixed bed configuration, no solar mobile bed reactor has been proposed in the literature to carry out the calcination reaction. Both directly[270] and indirectly[271] irradiated mobile bed reactor has been developed for the thermal reduction of ZnO.

As regards the rotary reactors, the solid particles are fed into a rotating receiver, wherein a centrifugal force is generated, thus distributing the particles on the walls.[241] Rotary reactors, which are widely

used in a variety of industrial processes (e.g. cement production and the food industry) can count on relatively high heat/mass transfer coefficients; however, a significant amount of energy is required to rotate the kiln.[238] As regards the directly irradiated configuration, a solar rotary reactor, with a 5° inclination relative to the horizontal axis, was proposed for the $CaCO_3$ calcination by Flamant et al.,[74] obtaining a total efficiency of 25 – 45 % with a $CaCO_3$ calcination degree of 30-60%. Likewise, a 10kW horizontal rotary kiln was proposed Meier et al.[33] to produce high purity lime through the solar-driven limestone calcination reaction. More specifically, the reaction chamber, characterized by a conical shape, is located with an inclination of 5° inside the horizontal kiln, whose movement is driven by rubber wheels, powered by an electric motor. The reactor was operated for more than 100 h at 1150 °C obtaining a $CaCO_3$ calcination degree larger than 98 % with a chemical efficiency of 20 %. A solar rotary kiln, in both the open and closed configurations, was designed by Moumin et al.[248] to perform the calcination of cement raw meal in the form of cohesive fine particles. As regards the closed configuration, clogging issues in the suction system and severe particle deposition on the window forced the Authors to interrupt the test. On the contrary, the test was concluded with the open configuration obtaining a $CaCO_3$ calcination degree of 24 – 99 % with a total efficiency of 19 - 40% and a chemical efficiency of 8 – 20 %. Similarly, the solar rotary kiln designed by Tescari et al.[249] was reported to achieve a total efficiency of 39 % and a chemical efficiency of 17 %. As regards the indirectly irradiated configuration, an optimized version of the directly irradiated solar rotary kiln

calciner of Flamant et al.[74] was proposed by Badie et al.[73] More specifically, a more even distribution inside the reactor was achieved using a stainless steel tube along the center axial line of the chamber; the tube, directly exposed to the solar radiation, acted as the indirect heating source for the reactor. A 10.6 kW indirectly irradiated rotary kiln calciner with a multi-tube absorber and a preheating chamber was designed by Meier et al.[251,252] to produce high purity lime from 2 – 3 mm limestone particles. The calcination reaction was successfully performed at a temperature of 1127 ˚C obtaining a chemical efficiency of 30 - 35%. An indirectly irradiated rotary kiln, consisting of a tube crossing an absorber cavity with a circular front aperture, was also proposed by Abanades and André.[250] In particular, the cavity was separated from the ambient atmosphere by means of a transparent hemispherical window, from which the solar radiation entered the cavity. $CaCO_3$ particles (50 – 100 μm) were successfully calcined with a conversion degree up to 100 % with a chemical efficiency of about 17 %.

4.1.3 Fluidized bed

Among all the different types of reactor configurations, fluidized beds are particularly suitable as solar receiver since they can count on the main benefit of remarkably high heat transfer coefficients (on the order of hundreds of W m^{-2} K^{-1}), high thermal diffusivities (on the order of 10^{-2} m^2 s^{-1}), efficient solids mixing, easily adaptable residence time and possibility of continuous operation (in circulating fluidized bed mode), deriving from the peculiar motion of particles inside the bed.[7,272] In this framework, it was also reported that thermal diffusivity and surface-to-bed heat transfer

efficiency in fluidized bed reactors may be remarkably increased using non-conventional design and operation, like those based on uneven or unsteady (pulsed) fluidization.[272] Besides that, the particle residence time in fluidized beds is increased with respect to entrained bed reactors, which is advantageous for slow-kinetics reactions.[238] Directly irradiated fluidized beds with a closed configuration, wherein the solar radiation enters the reaction chamber through a transparent window, are typically characterized by higher thermal efficiency and operating temperatures, and lower thermal inertia with respect to the indirectly irradiated fluidized beds.[238] However, the success of this type of configuration strictly depends on the ability to keep the glass window clean and scratch-free and thus limiting reduction in the medium transmittance and efficiency, and avoiding the erosion of the internal components of the reactor.[273] In this framework, Flamant et al.[74] successfully calcined limestone particles (0.2–0.315 mm) in a directly irradiated fluidized bed batch reactor, whose walls are made of transparent silica, obtaining a thermal efficiency of 20-40% and a chemical efficiency of 20 %. Nikulshina et al.[258] designed a directly irradiated fluidized batch bed reactor, consisting of a quartz tube located at the focal plane of a high-flux solar simulator (75 kW), to perform consecutively perform the $CaO/CaCO_3$ carbonation/calcination reactions for the capture of CO_2 from air. Full calcination at a maximum temperature of 850 ˚C was achieved with uniform irradiance and temperature distribution inside the bed, and good solid–gas contacting efficiency; however, a progressive decrease in the CaO particle dimensions was observed with increasing number of cycles

due to the friction caused by the SiO_2 particles used as inert materials to enhance the fluidization process. Likewise, a directly irradiated fluidized bed batch reactor was designed by Tregambi et al.[71,259] to perform CaL tests for both TCS and CCS; a solar simulator with a total power of about 3 kW was used, consisting of an array of short arc Xe-lamps and elliptical reflectors incident on the bed surface. A decline in the material performances due to sintering phenomena was observed from the fourth cycle. A lab-scale fountain-like solar receiver was coupled with a double pipe heat exchanger by Tregambi et al.[260] The peculiar design, consisting of two concentric tubes, allows the particles to circulate from the inner tube to the space in between the tubes. In indirectly irradiated fluidized beds, the solar radiation irradiates a cavity or an arrangement of tubes from which the heat is transferred to the fluidizing particle bed (with the fluidizing gas enhancing the heat transfer from the irradiated surface to the particles).[61] Even though the indirectly irradiated configuration is simpler from the constructive point of view, the irradiated surface may easily suffer from severe thermo-mechanical stress.[7] Moreover, temperature and conversion inhomogeneity among the absorber tubes in different parts of the cavity may be another issue of indirectly irradiated fluidized beds.[7] An indirectly irradiated fluidized bed continuous reactor, consisting of four compartments in series, to perform dolomite ($CaMg(CO_3)_2$) calcination was modeled and tested by Esence et al.[261] The solar radiation (radiant power of 25 kW) was directed to the front wall of the reactor and preheated air, injected from the bottom of the reactor, was used as fluidizing gas. The compartmentation of the bed

was shown to homogenize the particle residence time distribution and product conversion. A chemical efficiency of 6.6 % was achieved. The dolomite was only partially decomposed; $MgCO_3$ was totally converted, whereas $CaCO_3$ could not be totally decomposed since the temperature was not sufficiently high with respect to the P_{CO_2} in the reactor. A similar fluidized bed continuous calciner with higher radiant power (55 kW) was more recently proposed by Esence et al.[262] A 95 % calcination conversion degree with a chemical efficiency of 17 % and a total efficiency of 29 % were reported.

4.2 Carbonator

Aiming at achieving a proper reaction between the sorbent and the CO_2 during the carbonation reaction, the carbonator reactor must be very carefully designed in order to assure the release of the previously stored energy. It is noteworthy that, in contrast to the calcination reaction, the carbonation reaction is not complete with the carbonation conversion degree decreasing with increasing number of cycle down to a residual value, which is strongly dependent on the operating conditions (temperature and pressure) inside the reactor.[65] In particular, an industrial-scale carbonator must be designed in order to provide some crucial features:[65] i) high enough particle residence time for the particles to be able to reach the set temperature and, thus, achieve a proper carbonation conversion degree; ii) limited thermal gradients, which would cause conversion non-homogeneity; iii) homogeneity of heat transfer to the reactor wall; iv) limited temperature gradient between the reactor

and the particles fed to the reactor in order to avoid undesired cooling effects (i.e. cold-spot with reduced reaction efficiency); v) limited particle attrition and agglomeration phenomena.

On the basis of the above-mentioned requirements of a large-scale carbonator, fluidized beds and entrained beds have been indicated as the most promising reactor configurations.[274] A summary of the available bench- and pilot-scale carbonator reactors is reported in Table 13.

As a matter of fact, the original concept of the CaL process, when applied for CCS, envisaged the use of a twin fluidized reactor (calciner and carbonator)[275] and a huge number of works are available in the literature about the modeling of fluidized bed carbonators for CCS.[258,276–278] Moreover, most of the existing CaL pilot plants for CO_2 capture use fluidized bed reactors.[279] On the contrary, only few studies are available on the modeling of carbonator for TCS applications.[84,274] Ortiz et al.[280] showed that the carbonator size of a 100-MWth CSP-CaL plant could be remarkably reduced (solids inventory ~ 128 – 234 kg MWe^{-1}) in comparison with a post-combustion (solids inventory ~1300 kg MWe^{-1})[281] large-scale carbonator, thanks to enhanced carbonation kinetics and higher multicycle CaO carbonation conversion at TCS operating conditions.[91,282] Alovisio et al.[84] and Ortiz et al. [283] investigated several CSP-CaL integration schemes, all of which rely on the use of a pressurized fluidized bed carbonator, aiming at maximizing the efficiency of power cycle integration in the carbonator zone. More recently, Bailera et al.[274] have modelled an internal co-current entrained flow

carbonator for CaL-CSP applications under three different configurations: i) a single reactor; ii) two carbonation reactors operating in parallel, with the total inlet mass flow equally divided and diverted among them; iii) two carbonator reactors in series with intermediate cooling. Considering that the reduction of the particle size is one of the available solutions to limit the multicyclic decline in the sorbent carbonation reactivity,[91] assisted-fluidization techniques were proposed to counteract the intrinsic cohesive behavior (leading to agglomeration and plugging phenomena) of fine particles (< 50 μm), i.e. thus actually obtaining a proper fluidization regime that is not achievable in ordinary fluidized bed reactors.[210] Even though only at lab-scale, Valverde et al.[70] and Raganati et al.[77,215] successfully designed sound-assisted fluidized bed carbonators, showing that the application of high-intensity acoustic fields could enhance the carbonation efficiency for both CCS and TCS applications, respectively.

Also regarding the possibility to use fine sorbent particles, which are intrinsically difficult to handle in fluidized bed reactors, entrained flow reactors with fine particles were successfully used in the cracking industry.[284] Wang et al.[285] tested an entrained bed carbonator, operated at 450 – 650 °C, for the simultaneous CO_2/SO_2 capture in the framework of a 120-kWth pilot plant. Almost 100 % CO_2 capture levels were obtained using fine particles of mass median diameter of 3 μm; coarser particles (size in the range 3 - 600 μm) were also tested, obtaining a significant decrease of the CO_2 capture

efficiency. Likewise, Hanak et al. [286], proposing a similar reactor configuration for the carbonator, showed that the reduction of the particle size could enhance carbonation efficiency, due to the increase of the surface-to-volume ratio. More recently, Plou et al. [287] obtained CO_2 capture efficiencies larger than 90 % in a kW-scale carbonator with a particle residence time lower than 5 s. However, in spite of the favorable feature of being capable of handling fine sorbent particles, the entrained flow bed reactors are characterized by heat transfer coefficients as high as 100 – 200 W $m^{-2}K^{-1}$ [288], remarkably lower than the values typical of fluidized bed reactors (500–800 W $m^{-2}K^{-1}$).[289,290] Recently, Turrado et al.[291] tested a downer carbonator (height = 6 m, diameter = 0.1 m), with the solid and the gaseous phases flowing co-currently, for CO_2 capture. It was observed that the carbonation kinetics is enhanced at higher CO_2 concentrations. This is relevant for a CSP-TCS CaL integration scheme, where the carbonation reaction is performed under a pure CO_2 atmosphere, as clearly discussed by Ortiz et al.[280] As a matter of fact, carbonators are tested/simulated at ambient pressure for CCS applications,[86] whereas, high-pressure (3 – 5 bar) carbonation would result in the improvement of the the TCS efficiency by the direct integration with a CO_2 Brayton cycle.[81,283]

Table 13. Summary of the data reported for different types of carbonator reactors.

	Purpose	Size (kW_{th})	T °C	Length/diameter (m)	Ref.
Fluidized					
Bubbling fluidized bed	CCS	1900	750	3.30/4.20	292
Fluidized bed	CCS	1000	620 - 660	8.66/0.59	293
Circulating fluidized bed	CCS	1700	600-715	15/0.65	294
Bubbling fluidized bed	CCS	100	750	3/0.1	295
Circulating fluidized bed	CCS	10	630	12.40/0.07	296
Bubbling fluidized bed	CCS	3	650	2.5/0.10	297
Bubbling fluidized bed	CCS	10	630	1/0.15	286
Circulating fluidized bed	CCS	25	650	4.20/0.10	298
Bubbling fluidized bed	CCS	0.10	650	3/0.10	299
Circulating fluidized bed	CCS	1000	650	8.60/0.60	300
Entrained					
Entrained bed	CCS	25	600-650	4.30/0.10	301,302

5 Techno-economic analysis and life cycle analysis

This section presents a discussion on the cost of the CaL process for TCS, being the $CaCO_3$/CaO pair the only carbonate system investigated so far at scale larger than the lab-scale. However, it should be considered that the number of experimental researches on the pilot-scale TCS-CaL for CSP plants (TRL 4–5) is still very limited.[303,304] Indeed, most of the works available in the literature are based on lab-scale studies, focused on the improvement of the process performance by: i) enhancing the kinetics and multicyclic conversion of both natural[91,202] and synthetic Ca-based raw materials;[207,243,305] varying the process conditions (e.g. CO_2 partial pressure at reactors, temperature, particle size, etc.).[72,207,306] Likewise, innovative process integration schemes have been also proposed, achieving thermal-to-electric efficiencies of up to 32 – 48 %.[19,307] In this framework, the idea of integrating a CSP plant with a CaL-TCS system, although promising, is still in the research and development stage; the recently completed SOCRATCES project (Horizon 2020, Grant Agreement no. 727348)[304] can be considered as a reference of the current state of the art. Therefore, it is still not possible to provide an economic estimation which would be satisfactorily accurate at a commercial scale. On the contrary, the extent of the research on the techno-economic analysis is much larger when CaL is applied for CCS purposes (i.e. to capture CO_2 from the flue gas of coal-fired power plants). However, considering that the equipment is basically the same for both CCS and TCS

applications (they mainly differ in the operating conditions), the results obtained for the CaL-CCS applications can be used as an initial reference for CSP-CaL.

In this framework, Hanak et al.[308] estimated that the cost of the CaL process, retrofitting a 580 MW coal-fired power plant, is 2100–2300 € kW^{-1}. Mantripragada et al.[309] demonstrated that the highest cost of the plant is represented by the cost of the carbonator/calciner reactors together with the cost of solids handling systems. In line with this, the capital costs of the calciner/carbonator fluidized bed reactors have been estimated in several works[309–312] applying exponential functions and using the flue gas volume flow rate, reactor volume or heat input to the calciner as scaling parameter. Michalski et al.[313] performed the economic assessment of a CaL combustion-based power plant, reporting a capital cost of 2573.5 € kW^{-1}. More specifically, this work provided a detailed procedure to estimate the capital cost of the main CaL process equipment applying a bottom up approach: calciner/carbonator reactors, heat exchangers, fans and CO_2 compressor, steam cycle as power block, coolers and CO_2 turbine.

With reference to the CaL for TCS-CSP applications, Bayon et al.[314] provided a techno-economic analysis of seventeen different gas-solid systems. In particular, the evaluation of the total cost of the storage took into account the costs of the feedstock, vessels, pumps, compressors and particles conveyor, whereas, notably, it did not consider the costs of the reactors. The Authors pointed out that

the greatest impact on the capital cost of the system was due to the cost of raw materials and the energy consumption of auxiliary equipment. Among all the analyzed systems, eight, comprising the $CaCO_3$/CaO couple, were proved to hold high potential for commercial applications. Interestingly, it was reported that the CaL process is one of the most promising, being characterized by one of the of the lowest capital cost (~54 \$ $kWht^{-1}$). Similarly, Muto et al.[315,316] analyzed a CaL-TCS process using a synthetic sorbent (characterized by high stability X = 0.4), reporting a total cost of 47 \$ $kWht^{-1}$. In particular, it was shown that, while the overall cost of the process is slightly affected by the sorbent cost, it is, instead, greatly impacted by the costs deriving from the heat exchanger reactor and auxiliary equipment, including compressors and gas storage. Therefore, great research effort must be devoted to improve the efficiency of the integration of the CSP-CaL scheme, including storage systems, solids transportation and gas separation. In this direction, Tesio et al.[307] provided the energy and economic analysis/optimization of the CaL-TCS process, considering three different thermodynamic cycles for the power block: the supercritical CO_2 Brayton cycle, steam Rankine cycle (SRC) and high-temperature Organic Rankine Cycles (ORC). The economic assessment showed that the power block based on the supercritical CO_2 cycle (CO_2 Brayton cycle) was the optimal option, providing the best energy performances, even though the steam Rankine cycles can count on a remarkably simpler plant layout. More specifically, it was shown that that 86 % of the total investment capital was represented by the solar and calciner sides. Based on these results, the Authors pointed out that the selection of a

high-performing power block is a crucial aspect in the integration process; indeed, implementing an expensive supercritical CO_2 power cycle, in spite of being nearly three times more expensive than standard SRC/ORC cycles, is still economically convenient in terms of the overall capital costs of the plant. Ortiz et al.[19,65] published two reviews on the CaL technology for TCS applications with a focus on its pros and cons and the challenges to be addressed for the process to reach a commercial scale[65] and on the issues related to the scale-up.[19] In both the reviews, the Authors pointed out that a better estimation of the costs of TCS-CaL in real CSP plants is strictly related to a better understanding and knowledge of the solar receiver (calciner), including a scaling-up analysis from the pilot to the commercial scale based on the real challenges and solutions found during the prototype testing.

As regards the analysis of the environmental impact, LCA (life cycle assessment) approach can be useful to analyze a process throughout its life cycle in order to improve its overall environmental performance and system design.[317] Different works, available in the literature, used the LCA analysis to evaluate the environmental performance of CSP plants;[318–320] Cavallaro et al.[321] demonstrated that that the overall environmental impact produced by the entire life cycle of a CSP plant is lower with respect to traditional fossil fuel power plants. In particular, Lamnatou and Chemisana[319] reported that CSP plants have estimated CO_{2eq} emissions lower than 40 kg MWh^{-1} with an Energy Payback Time (EPBT, defined as the period of time required for the plant to generate an amount of energy at least

equivalent to the amount of energy used for the construction of the plant[317]) of around 15 months. Only very recently, Colelli et al.[317] presented a paper on the life cycle and environmental assessment of CaL-TCS in CSP plants. In particular, the Authors analyzed two different TCS-CaL layouts, representing the state-of the-art concepts for daily and seasonal storage: i) CSP-CaL with high-temperature storage of the calcination products (conceived for daily storage); CSP-CaL with ambient temperature storage of calcination products (conceived for seasonal storage). The obtained results were very promising, the analysis of all the considered parameters evidencing that these novel storage systems have no particular potentially harmful effects on the environment. More specifically, it was reported that, while the plant construction represents a high energy demand for the process, the operation/maintenance of the plant, on the contrary, has only a limited impact over the life cycle of the plant thanks to the low water consumption and the low environmental impact of the limestone, being the sole raw material in the whole process. With reference to the two analyzed storage configurations, the major difference was found in the higher energy consumption required during the construction stage of the hot storage system, which results in a slightly longer EPBT and a larger impact on global warming. The results obtained were also compared to those reported for molten salt-based CSP plants, showing a remarkable reduction (up to 50%) in the associated CO_2 emissions, whereas, the EPBT is longer.

6 Challenges and perspectives

Based on the discussion presented in in the previous sections, it is clear that, among all of the available technological solutions, TCS based on carbonates systems hold great potential for future applications in CSP plants, due to several distinctive favorable features. However, it is also evident that the state of the art of the currently available technologies needs serious enhancements in different directions, i.e. material improvement/development, reactor design and process integration, thus implying that a multidisciplinary approach must be used.

With reference to the materials, metal carbonates can rely on the following key advantages:

- high energy density (~3–4 GJ m^{-3}), roughly 10 times larger than sensible heat storage systems (i.e., molten salts), which makes it possible to maximize the storage capacity;
- high working temperatures (> 800 ˚C), meaning that heat is released through a remarkably high-temperature exothermic reaction; this makes it possible to integrate the system with high-efficiency power cycles, such as combined cycles, supercritical Rankine cycles or Brayton Cycles;
- carbonates are generally quite cheap and abundant (i.e. available at large-scale) materials;
- carbonates are also non-toxic, non-corrosive, non-flammable, and non-explosive materials, which can be easily and stably stored also at ambient temperature; this makes it possible to

remarkably limit electricity consumption, also eliminating the risks derived from the solidification of salts.

However, in spite of the above-mentioned favorable features, metal carbonates also suffer from important problems related to their handling at high-temperature, which requires an in-depth investigation especially when scaling up the technology. In particular, the main challenge for a metal carbonates based TCS process is related to the progressive sorbent deactivation over multi-cyclic operations. Indeed, the sorbent carbonation reactivity drops with the number of calcination-carbonation cycles, mainly due to sintering and pore-plugging phenomena, thus severely compromising the operation of the CSP plant. More specifically, after few carbonation/calcination cycles, the system tends to achieve a low residual carbonation conversion (depending on the both the sorbent properties, such as the particle size, and on the operating conditions, i.e. temperature, pressure and atmosphere composition), which ends up limiting the amount of heat released during carbonation reaction and, in turn, the energy density of the system. So far, different solutions have been proposed to address this issue, such as hydration, development of synthetic sorbents with enhanced activity and use of fine sorbent particles. Clearly, in spite of the of the intense research activity devoted to limiting the multi-cyclic sorbent deactivation, further investigation is still required. In particular, hydration can be used to improve the multi-cyclic stability of cheap natural calcium-containing minerals, but this goes at the expense of their mechanical stability (natural limestones are generally weak and they

become even weaker when thermally pre-treated or hydrated). Therefore, future research activities should be focused on understanding how to prevent/limit attrition caused by hydration/thermal pretreatment (e.g. research on optimal hydration frequency, position and time). On the contrary, synthetic sorbents can be produced with very specific and enhanced physico-chemical features (e.g. improved attrition/sintering resistance and, consequently, multicyclic stability), by means of the introduction/doping of an inert and refractory material characterized by high T_t (e.g. Al_2O_3, ZrO_2, MgO, etc); however, this clearly goes at the expense of the economics and environmental impact of the whole process. Likewise, even though the use of fine sorbent particles may be beneficial in terms of multi-cyclic stability and reaction kinetics, it brings major practical challenges and handling/processing issues, i.e. cohesiveness leading to severe agglomeration and, in turn, hindrance of reaction efficiency, in real industrial-scale reactor. On the whole, all the reviewed strategies are capable of improving the sorbent multi-cyclic stability in comparison to their pristine equivalents, however, some important issues still need to be dealt with. First of all, it is noteworthy that, in the framework of the material development research field, maybe too much attention has been devoted to attempt novel synthesis methods to produce cutting-edge materials with very high reactivity and exceptional multicyclic stability without taking into account other factors that play a crucial role in the feasibility of their application in real industrial-scale processes, such as economic viability, environmental friendliness and operating complexity of the proposed synthesis methods. For example, some of the synthesis routes proposed in the literature are way to complex and/or the precursors are way too expensive, thus strongly hindering their use for industrial production. Likewise, most of the proposed synthetic sorbents are produced in fine powdered form (even down to the nano-scale) and tested in analytical-scale instrument (e.g. thermobalance, etc., which are far

from the operating conditions existing in an industrial-scale reactor) only completely neglecting the major practical problems associated with the use of fine powders in in real large-scale reactors (where particles with well-defined shape and morphologies are generally necessary). In this context, palletization may be proposed as a simple and viable technological solution. However, it must be taken into account that palletization is often reported to either completely or partially destroy the porous structure of the synthesized sorbents, thus leading to a remarkable reduction of the reactive performances of the pelletized sorbents with respect to the as-synthesized powdered counterparts. In light of these concerns, some general recommendations should be followed in the future when developing new sorbents. First of all, it is necessary to perform a LCA and techno-economic analysis of the whole synthesis procedure, which is hardly available in the current literature; knowing the cost of a newly-synthesized material as compared to the pristine equivalent is of utmost importance for an objective assessment of the material potential. For example, if the cost of the developed sorbent is dramatically larger than the raw counterpart, it is most likely that not even a lower makeup rate, coming from to the enhanced multicyclic stability, of the synthetic sorbent may make it economically competitive. Secondly, the synthetic sorbents must be tested and assessed under industrially-relevant conditions, in terms of both process operating variables (temperature, pressure and atmosphere) and fluid-dynamic conditions, namely more testing should be performed in lab-scale and pilot-scale reactors in order to approach the real industrial conditions.

Besides the issues and open challenges related to the materials, it is also important to point out that the design of the reactors, for both the solar-driven endothermic calcination reaction and the exothermic carbonation reaction, and their integration in the CSP plant represent a key point of the TCS-CSP system; the optimization of the reactor concept remains, indeed, one of the most remarkable open challenge needing to be solved before the carbonate-based TCS systems for CSP can be industrially deployed.

As regards the solar-driven calciner design, the literature review has highlighted that two main characteristics should be taken into account when assessing the different reactor concepts: the particle erosion of internal components, walls, windows and particle-particle erosion (due to the collision between particles) and dust formation when comparing different gas-solid contacting modes (entrained, stacked and fluidized beds); the sorbent particle absorptivity when comparing the and direct and indirect irradiation modes. With reference to the former feature, it is widely known that carbonate particles are typically very fragile and intrinsically prone to attrition phenomena; therefore, reactor designs that promote the fast movement of the sorbent particles, i.e. fluidized, entrained and rotary beds, are strongly affected by particle erosion and dust formation. As regards the latter feature, carbonate-based sorbents are characterized by relatively low values of solar absorptivity and, hence, the use of indirectly-irradiated reactors may be helpful with reference to this specific issue. Indeed,

the indirect irradiation mode would avoid the necessity to directly and poorly absorb the solar radiation via the low-absorptivity carbonate particle, thus also implying the lack of need for a transparent window, which may easily incur in degradation and cracking. Cleary, if the indirectly-irradiated reactors can count, on one hand, on good heat transfer efficiency through radiation, thanks to the use of a high-absorptivity primary absorber material, from the other hand, they suffer from re-radiation losses and very challenging distribution of radiation across the irradiated surface and very high reactor wall temperatures. Therefore, special attention must be devoted to the optimization of the other heat transfer mechanisms, namely conduction and convection. In this regards, even though rotary kilns and mobile bed reactors have been successfully tested for TCS-CSP applications, fluidized bed reactor may represent one of the most viable option, thanks to some of their distinctive features, such as the high heat/mass transfer coefficients (on the order of hundreds of W m^{-2} K^{-1}), high thermal diffusivities (on the order of 10^{-2} m^2 s^{-1}), good solids mixing, possibility of continuous operation in circulating configuration, adjustable residence time with long permanence in high-temperature zones. On the contrary, directly-irradiated solar-driven calciners are characterized by a high sensitivity to the sorbent particle solar absorptivity. Therefore, more work must be devoted to the development of sorbent with enhanced optical properties.

As regards the carbonator, even though a great research effort has been devoted to the study of reactor (especially fluidized beds) concepts for CCS applications, only few studies are currently available on the development of carbonation reactors to be specifically used in TCS-CSP applications. Based on these few studies, it appears that fluidized beds and entrained beds may be the most promising solutions, thanks to the high mass and heat transfer coefficients allowing to achieve high carbonation efficiencies. Moreover, considering that the use of fine sorbent particles is one of the available solutions to limit the multicyclic decline in the sorbent carbonation reactivity, assisted-fluidization techniques were successfully proved, even though only at lab-scale, to successfully counteract the intrinsic cohesive behavior of fine particles, thus actually making it possible to achieve a proper fluidization regime. Therefore, in light of the positive results obtained from the lab-scale testing, further effort may be needed to bring these technologies to the large-scale fluidized bed reactors

Finally, it must be highlighted that that the number of experimental researches on the pilot-scale carbonate-based TCS systems for CSP plants (TRL 4–5) is still very limited; indeed, most of the works available in the literature are performed at lab-scale and are focused on the improvement of the process performance by enhancing the kinetics and multicyclic conversion of both natural and synthetic Ca-based raw materials and varying the process conditions (e.g. CO_2 partial pressure at reactors, temperature, particle size, etc.). Therefore, there is a clear need of research on the economic

feasibility and scalability of the process. Further work and analysis are also required to better evaluate the environmental impact of carbonate-based TCS systems when integrated in a CSP plant.

7 Conclusions

This study reviews the state-of-the-art of carbonate-based systems for thermochemical energy storage (TCS) focusing on their suitability for potential application and integration in concentrating solar power (CSP) plants.

It is well-known that dispatchability is a major technological challenge of CSP plant and, therefore, increasing research interest has been focused in TCS systems as a potential alternative to molten salts to store solar energy. In this framework, alkaline-earth metal carbonates, namely their reversible calcination/carbonation reaction with CO_2 used as a means to store/release energy, are recognized to be very promising candidates due to their very advantageous features: wide availability, low cost, high volumetric density (> 1 GJ m^{-3}), relatively high operating temperatures (> 800 ˚C), non-toxic and non-corrosive chemical nature, no occurrence of any side reactions involving the production of undesired by-products.

However, in spite of these promising features, carbonate-based TCS systems still suffers from a relatively low level of maturity, i.e. most of the available literature is still limited to the lab-scale. Therefore, aiming at bringing carbonate-based TCS systems from fundamental research to real-scale

applications, the use of a multidisciplinary approach with further research efforts in different directions is needed, i.e. material improvement/development, reactor design and process integration.

After a brief introduction, in which the general topic of energy storage is discussed indicating the different available technological solutions, in the second section of this review the main concepts of TCS are presented; all the distinctive features that a potential heat storage material should have been also highlighted and discussed. Then, the most promising carbonate-based systems to be applied for TCS-CSP applications are reviewed, paying particular attention to one of the main issues affecting these systems, namely the dramatic decline in the carbonation activity over multiple carbonation/calcination cycles due to sintering, pore pugging and agglomeration. Hence, the different technological solutions proposed to limit the sorbent deactivation and, in turn, increase the sorbent multi-cyclic stability are reviewed in details. The third section reviews the different types of solid-gas reactors that can be used to perform the calcination and carbonation reactions, highlighting their strengths and limitations. Finally, the fourth section presents a discussion on the cost of the CaL process for TCS.

References

(1) André, L.; Abanades, S. Investigation of Metal Oxides, Mixed Oxides, Perovskites and Alkaline Earth Carbonates/Hydroxides as Suitable Candidate Materials for High-Temperature Thermochemical Energy Storage Using Reversible Solid-Gas Reactions. *Mater. Today Energy* **2018**, *10*, 48–61. https://doi.org/10.1016/J.MTENER.2018.08.007.

(2) Medrano, M.; Gil, A.; Martorell, I.; Potau, X.; Cabeza, L. F. State of the Art on High-Temperature Thermal Energy Storage for Power Generation. Part 2-Case Studies. *Renew. Sustain. Energy Rev.* **2010**, *14* (1), 56–72. https://doi.org/10.1016/J.RSER.2009.07.036.

(3) Rodat, S.; Abanades, S.; Boujjat, H.; Chuayboon, S. On the Path toward Day and Night Continuous Solar High Temperature Thermochemical Processes: A Review. *Renew. Sustain. Energy Rev.* **2020**, *132*, 110061. https://doi.org/10.1016/j.rser.2020.110061.

(4) Sunku Prasad, J.; Muthukumar, P.; Desai, F.; Basu, D. N.; Rahman, M. M. A Critical Review of High-Temperature Reversible Thermochemical Energy Storage Systems. *Appl. Energy* **2019**, *254* (October 2018), 113733. https://doi.org/10.1016/j.apenergy.2019.113733.

(5) Gil, A.; Medrano, M.; Martorell, I.; Lázaro, A.; Dolado, P.; Zalba, B.; Cabeza, L. F. State of the Art on High Temperature Thermal Energy Storage for Power Generation. Part 1-Concepts, Materials and Modellization. *Renew. Sustain. Energy Rev.* **2010**, *14*, 31–55. https://doi.org/10.1016/j.rser.2009.07.035.

(6) Lilliestam, J.; Labordena, M.; Patt, A.; Pfenninger, S. Empirically Observed Learning Rates for Concentrating Solar Power and Their Responses to Regime Change. **2017**, 12. https://doi.org/10.1038/nenergy.2017.94.

(7) Alvarez Rivero, M.; Rodrigues, D.; Pinheiro, C. I. C.; Cardoso, J. P.; Mendes, L. F. Solid–Gas Reactors Driven by Concentrated Solar Energy with Potential Application to Calcium Looping: A Comparative Review. *Renew. Sustain. Energy Rev.* **2022**, *158*, 112048.

https://doi.org/10.1016/j.rser.2021.112048.

(8) Weinstein, L. A.; Loomis, J.; Bhatia, B.; Bierman, D. M.; Wang, E. N.; Chen, G. Concentrating Solar Power. *Chem. Rev.* **2015**, *115* (23), 12797–12838. https://doi.org/10.1021/acs.chemrev.5b00397.

(9) Chen, X.; Zhang, Z.; Qi, C.; Ling, X.; Peng, H. State of the Art on the High-Temperature Thermochemical Energy Storage Systems. *Energy Convers. Manag.* **2018**, *177*, 792–815. https://doi.org/10.1016/j.enconman.2018.10.011.

(10) Zhang, H.; Benoit, H.; Gauthier, D.; Degrève, J.; Baeyens, J.; López, I. P.; Hemati, M.; Flamant, G. Particle Circulation Loops in Solar Energy Capture and Storage: Gas–Solid Flow and Heat Transfer Considerations. *Appl. Energy* **2016**, *161*, 206–224. https://doi.org/10.1016/j.apenergy.2015.10.005.

(11) Benoit, H.; Spreafico, L.; Gauthier, D.; Flamant, G. Review of Heat Transfer Fluids in Tube-Receivers Used in Concentrating Solar Thermal Systems: Properties and Heat Transfer Coefficients. *Renew. Sustain. Energy Rev.* **2016**, *55*, 298–315. https://doi.org/10.1016/j.rser.2015.10.059.

(12) Carrillo, A. J.; González-Aguilar, J.; Romero, M.; Coronado, J. M. Solar Energy on Demand: A Review on High Temperature Thermochemical Heat Storage Systems and Materials. *Chem. Rev.* **2019**, *119* (7), 4777–4816. https://doi.org/10.1021/acs.chemrev.8b00315.

(13) Shahabuddin, M.; Alim, M. A.; Alam, T.; Mofijur, M.; Ahmed, S. F.; Perkins, G. A Critical Review on the Development and Challenges of Concentrated Solar Power Technologies. *Sustain. Energy Technol. Assessments* **2021**, *47*, 101434. https://doi.org/10.1016/j.seta.2021.101434.

(14) Kuravi, S.; Trahan, J.; Goswami, D. Y.; Rahman, M. M.; Stefanakos, E. K. Thermal Energy Storage Technologies and Systems for Concentrating Solar Power Plants. *Prog. Energy*

Combust. Sci. **2013**, *39* (4), 285–319. https://doi.org/10.1016/j.pecs.2013.02.001.

(15) Zhang, H.; Baeyens, J.; Cáceres, G.; Degrève, J.; Lv, Y. Thermal Energy Storage: Recent Developments and Practical Aspects. *Prog. Energy Combust. Sci.* **2016**, *53*, 1–40. https://doi.org/10.1016/j.pecs.2015.10.003.

(16) André, L.; Abanades, S. Recent Advances in Thermochemical Energy Storage via Solid–Gas Reversible Reactions at High Temperature. *Energies* **2020**, *13* (22), 5859. https://doi.org/10.3390/en13225859.

(17) Khan, M. I.; Asfand, F.; Al-Ghamdi, S. G. Progress in Research and Technological Advancements of Thermal Energy Storage Systems for Concentrated Solar Power. *J. Energy Storage* **2022**, *55*, 105860. https://doi.org/10.1016/j.est.2022.105860.

(18) Alva, G.; Liu, L.; Huang, X.; Fang, G. Thermal Energy Storage Materials and Systems for Solar Energy Applications. *Renew. Sustain. Energy Rev.* **2017**, *68*, 693–706. https://doi.org/10.1016/J.RSER.2016.10.021.

(19) Ortiz, C.; Valverde, J. M.; Chacartegui, R.; Perez-Maqueda, L. A.; Giménez, P. The Calcium-Looping (CaCO3/CaO) Process for Thermochemical Energy Storage in Concentrating Solar Power Plants. *Renew. Sustain. Energy Rev.* **2019**, *113*, 109252. https://doi.org/10.1016/j.rser.2019.109252.

(20) André, L.; Abanades, S. Evaluation and Performances Comparison of Calcium, Strontium and Barium Carbonates during Calcination/Carbonation Reactions for Solar Thermochemical Energy Storage. *J. Energy Storage* **2017**, *13*, 193–205. https://doi.org/10.1016/j.est.2017.07.014.

(21) Liu, L.; Zhou, Z.; Zhou, Y.; Peng, D.; Liu, X.; Xu, M. Co2.8Mg0.2O4 as a Promising Thermochemical Energy Storage Material with Lower Reduction Onset Temperature and Higher Energy Density. *J. Energy Storage* **2022**, *55*, 105594.

https://doi.org/10.1016/j.est.2022.105594.

(22) Peng, X.; Root, T. W.; Maravelias, C. T. Storing Solar Energy with Chemistry: The Role of Thermochemical Storage in Concentrating Solar Power. *Green Chem.* **2017**, *19* (10), 2427–2438. https://doi.org/10.1039/C7GC00023E.

(23) Ervin, G. Solar Heat Storage Using Chemical Reactions. *J. Solid State Chem.* **1977**, *22* (1), 51–61. https://doi.org/10.1016/0022-4596(77)90188-8.

(24) Abedin, A. H. A Critical Review of Thermochemical Energy Storage Systems. *Open Renew. Energy J.* **2011**, *4* (1), 42–46. https://doi.org/10.2174/1876387101004010042.

(25) Aydin, D.; Casey, S. P.; Riffat, S. The Latest Advancements on Thermochemical Heat Storage Systems. *Renew. Sustain. Energy Rev.* **2015**, *41*, 356–367. https://doi.org/10.1016/j.rser.2014.08.054.

(26) Peng, X.; Bajaj, I.; Yao, M.; Maravelias, C. T. Solid-Gas Thermochemical Energy Storage Strategies for Concentrating Solar Power: Optimization and System Analysis. *Energy Convers. Manag.* **2021**, *245*, 114636. https://doi.org/10.1016/j.enconman.2021.114636.

(27) Department, U. S.; of Energy: Washington, D. Concentrating Solar Power: Efficiently Leveraging Equilibrium Mechanisms for Engineering New Thermochemical Storage | Department of Energy https://www.energy.gov/eere/solar/concentrating-solar-power-efficiently-leveraging-equilibrium-mechanisms-engineering-new (accessed Mar 22, 2022).

(28) Da, Y.; Xuan, Y.; Teng, L.; Zhang, K.; Liu, X.; Ding, Y. Calcium-Based Composites for Direct Solar-Thermal Conversion and Thermochemical Energy Storage. *Chem. Eng. J.* **2020**, *382*, 122815. https://doi.org/10.1016/j.cej.2019.122815.

(29) Yang, Y.; Li, Y.; Yan, X.; Zhao, J.; Zhang, C. Development of Thermochemical Heat Storage Based on CaO/CaCO3 Cycles: A Review. *Energies* **2021**, *14* (20), 6847.

https://doi.org/10.3390/en14206847.

(30) Khosa, A. A.; Xu, T.; Xia, B. Q.; Yan, J.; Zhao, C. Y. Technological Challenges and Industrial Applications of CaCO3/CaO Based Thermal Energy Storage System – A Review. *Sol. Energy* **2019**, *193*, 618–636. https://doi.org/10.1016/j.solener.2019.10.003.

(31) Han, X.; Wang, L.; Ling, H.; Ge, Z.; Lin, X.; Dai, X.; Chen, H. Critical Review of Thermochemical Energy Storage Systems Based on Cobalt, Manganese, and Copper Oxides. *Renew. Sustain. Energy Rev.* **2022**, *158*, 112076. https://doi.org/10.1016/j.rser.2022.112076.

(32) Pardo, P.; Deydier, A.; Anxionnaz-Minvielle, Z.; Rougé, S.; Cabassud, M.; Cognet, P. A Review on High Temperature Thermochemical Heat Energy Storage. *Renew. Sustain. Energy Rev.* **2014**, *32*, 591–610. https://doi.org/10.1016/j.rser.2013.12.014.

(33) Meier, A.; Bonaldi, E.; Cella, G. M.; Lipinski, W.; Wuillemin, D.; Palumbo, R. Design and Experimental Investigation of a Horizontal Rotary Reactor for the Solar Thermal Production of Lime. *Energy* **2004**, *29* (5–6), 811–821. https://doi.org/10.1016/S0360-5442(03)00187-7.

(34) Bagherisereshki, E.; Tran, J.; Lei, F.; AuYeung, N. Investigation into SrO/SrCO3 for High Temperature Thermochemical Energy Storage. *Sol. Energy* **2018**, *160*, 85–93. https://doi.org/10.1016/j.solener.2017.11.073.

(35) Yan, T.; Wang, R. Z.; Li, T. X.; Wang, L. W.; Fred, I. T. A Review of Promising Candidate Reactions for Chemical Heat Storage. *Renew. Sustain. Energy Rev.* **2015**, *43*, 13–31. https://doi.org/10.1016/j.rser.2014.11.015.

(36) Schaube, F.; Wörner, A.; Tamme, R. High Temperature Thermochemical Heat Storage for Concentrated Solar Power Using Gas-Solid Reactions. *J. Sol. Energy Eng. Trans. ASME* **2011**, *133* (3). https://doi.org/10.1115/1.4004245/456215.

(37) Yan, J.; Zhao, C. Y. Thermodynamic and Kinetic Study of the Dehydration Process of

CaO/Ca(OH) 2 Thermochemical Heat Storage System with Li Doping. *Chem. Eng. Sci.* **2015**, *138*, 86–92. https://doi.org/10.1016/j.ces.2015.07.053.

(38) Møller, K.; Sheppard, D.; Ravnsbæk, D.; Buckley, C.; Akiba, E.; Li, H.-W.; Jensen, T. Complex Metal Hydrides for Hydrogen, Thermal and Electrochemical Energy Storage. *Energies* **2017**, *10* (10), 1645. https://doi.org/10.3390/en10101645.

(39) Rönnebro, E.; Whyatt, G.; Powell, M.; Westman, M.; Zheng, F.; Fang, Z. Metal Hydrides for High-Temperature Power Generation. *Energies* **2015**, *8* (8), 8406–8430. https://doi.org/10.3390/en8088406.

(40) Ward, P. A.; Teprovich, J. A.; Liu, Y.; He, J.; Zidan, R. High Temperature Thermal Energy Storage in the CaAl2 System. *J. Alloys Compd.* **2018**, *735*, 2611–2615. https://doi.org/10.1016/j.jallcom.2017.10.191.

(41) Wierse, M.; Werner, R.; Groll, M. Magnesium Hydride for Thermal Energy Storage in a Small-Scale Solar-Thermal Power Station. *J. Less Common Met.* **1991**, *172–174* (PART 3), 1111–1121. https://doi.org/10.1016/S0022-5088(06)80018-4.

(42) Felderhoff, M.; Bogdanović, B. High Temperature Metal Hydrides as Heat Storage Materials for Solar and Related Applications. *Int. J. Mol. Sci.* **2009**, *10* (1), 325–344. https://doi.org/10.3390/ijms10010325.

(43) Reilly, J. J.; Wiswall, R. H. The Reaction of Hydrogen with Alloys of Magnesium and Nickel and the Formation of Mg2NiH4. *Inorg. Chem.* **1968**, *7* (11), 2254–2256. https://doi.org/10.1021/IC50069A016/ASSET/IC50069A016.FP.PNG_V03.

(44) Friedlmeier, G.; Wierse, M.; Groll, M. Titanium Hydride for High-Temperature Thermal Energy Storage in Solar-Thermal Power Stations. *Zeitschrift fur Phys. Chemie* **1994**, *183* (Part_1_2), 175–183. https://doi.org/10.1524/ZPCH.1994.183.PART_1_2.175/MACHINEREADABLECITATIO

N/RIS.

(45) Neises, M.; Tescari, S.; de Oliveira, L.; Roeb, M.; Sattler, C.; Wong, B. Solar-Heated Rotary Kiln for Thermochemical Energy Storage. *Sol. Energy* **2012**, *86* (10), 3040–3048. https://doi.org/10.1016/j.solener.2012.07.012.

(46) Agrafiotis, C.; Roeb, M.; Sattler, C. Cobalt Oxide-Based Structured Thermochemical Reactors/Heat Exchangers for Solar Thermal Energy Storage in Concentrated Solar Power Plants. In *Volume 1: Combined Energy Cycles, CHP, CCHP, and Smart Grids; Concentrating Solar Power, Solar Thermochemistry and Thermal Energy Storage; Geothermal, Ocean, and Emerging Energy Technologies; Hydrogen Energy Technologies; Low/Zero Emission Power Plants an*; American Society of Mechanical Engineers, 2014; Vol. 1. https://doi.org/10.1115/ES2014-6336.

(47) Agrafiotis, C.; Roeb, M.; Sattler, C. Exploitation of Thermochemical Cycles Based on Solid Oxide Redox Systems for Thermochemical Storage of Solar Heat. Part 4: Screening of Oxides for Use in Cascaded Thermochemical Storage Concepts. *Sol. Energy* **2016**, *139*, 695–710. https://doi.org/10.1016/j.solener.2016.04.034.

(48) Miguel, S. Á. de; Gonzalez-Aguilar, J.; Romero, M. 100-Wh Multi-Purpose Particle Reactor for Thermochemical Heat Storage in Concentrating Solar Power Plants. *Energy Procedia* **2014**, *49*, 676–683. https://doi.org/10.1016/j.egypro.2014.03.073.

(49) Fahim, M. A.; Ford, J. D. Energy Storage Using the BaO2□BaO Reaction Cycle. *Chem. Eng. J.* **1983**, *27* (1), 21–28. https://doi.org/10.1016/0300-9467(83)80042-2.

(50) Jafarian, M.; Arjomandi, M.; Nathan, G. J. Thermodynamic Potential of Molten Copper Oxide for High Temperature Solar Energy Storage and Oxygen Production. *Appl. Energy* **2017**, *201*, 69–83. https://doi.org/10.1016/J.APENERGY.2017.05.049.

(51) Dunn, R.; Lovegrove, K.; Burgess, G. A Review of Ammonia-Based Thermochemical

Energy Storage for Concentrating Solar Power. *Proc. IEEE* **2012**, *100* (2), 391–400. https://doi.org/10.1109/JPROC.2011.2166529.

(52) Pelay, U.; Luo, L.; Fan, Y.; Stitou, D.; Rood, M. Thermal Energy Storage Systems for Concentrated Solar Power Plants. *Renew. Sustain. Energy Rev.* **2017**, *79*, 82–100. https://doi.org/10.1016/J.RSER.2017.03.139.

(53) Prieto, C.; Cooper, P.; Fernández, A. I.; Cabeza, L. F. Review of Technology: Thermochemical Energy Storage for Concentrated Solar Power Plants. *Renew. Sustain. Energy Rev.* **2016**, *60*, 909–929. https://doi.org/10.1016/j.rser.2015.12.364.

(54) Felderhoff, M.; Urbanczyk, R.; Peil, S. Thermochemical Heat Storage for High Temperature Applications-A Review. *Green* **2013**, *3* (2), 113–123. https://doi.org/10.1515/GREEN-2013-0011/MACHINEREADABLECITATION/RIS.

(55) Wu, J.; Long, X. F. Research Progress of Solar Thermochemical Energy Storage. *Int. J. Energy Res.* **2015**, *39* (7), 869–888. https://doi.org/10.1002/er.3259.

(56) André, L.; Abanades, S.; Flamant, G. Screening of Thermochemical Systems Based on Solid-Gas Reversible Reactions for High Temperature Solar Thermal Energy Storage. *Renew. Sustain. Energy Rev.* **2016**, *64*, 703–715. https://doi.org/10.1016/j.rser.2016.06.043.

(57) Prieto, C.; Cooper, P.; Fernández, A. I.; Cabeza, L. F. Review of Technology: Thermochemical Energy Storage for Concentrated Solar Power Plants. *Renew. Sustain. Energy Rev.* **2016**, *60*, 909–929. https://doi.org/10.1016/J.RSER.2015.12.364.

(58) Pan, Z. H.; Zhao, C. Y. Gas–Solid Thermochemical Heat Storage Reactors for High-Temperature Applications. *Energy* **2017**, *130*, 155–173. https://doi.org/10.1016/J.ENERGY.2017.04.102.

(59) Liu, D.; Xin-Feng, L.; Bo, L.; Si-quan, Z.; Yan, X. Progress in Thermochemical Energy

Storage for Concentrated Solar Power: A Review. *Int. J. Energy Res.* **2018**, *42* (15), 4546–4561. https://doi.org/10.1002/ER.4183.

(60) Yuan, Y.; Li, Y.; Zhao, J. Development on Thermochemical Energy Storage Based on CaO-Based Materials: A Review. *Sustainability* **2018**, *10* (8), 2660. https://doi.org/10.3390/su10082660.

(61) Zsembinszki, G.; Sole, A.; Barreneche, C.; Prieto, C.; Fernández, A. I.; Cabeza, L. F. Review of Reactors with Potential Use in Thermochemical Energy Storage in Concentrated Solar Power Plants. *Energies* **2018**, *11* (9). https://doi.org/10.3390/en11092358.

(62) Fedunik-Hofman, L.; Bayon, A.; Donne, S. W. Kinetics of Solid-Gas Reactions and Their Application to Carbonate Looping Systems. *Energies* **2019**, *12* (15), 2981. https://doi.org/10.3390/en12152981.

(63) Yan, Y.; Wang, K.; Clough, P. T.; Anthony, E. J. Developments in Calcium/Chemical Looping and Metal Oxide Redox Cycles for High-Temperature Thermochemical Energy Storage: A Review. *Fuel Processing Technology*. Elsevier B.V. March 1, 2020. https://doi.org/10.1016/j.fuproc.2019.106280.

(64) Zhao, Y.; Zhao, C. Y.; Markides, C. N.; Wang, H.; Li, W. Medium- and High-Temperature Latent and Thermochemical Heat Storage Using Metals and Metallic Compounds as Heat Storage Media: A Technical Review. *Appl. Energy* **2020**, *280*. https://doi.org/10.1016/J.APENERGY.2020.115950.

(65) Ortiz, C.; Valverde, J. M.; Chacartegui, R.; Pérez-Maqueda, L. A.; Gimenez-Gavarrell, P. Scaling-up the Calcium-Looping Process for CO2 Capture and Energy Storage. *KONA Powder Part. J.* **2021**, *38* (38), 189–208. https://doi.org/10.14356/kona.2021005.

(66) Bellan, S.; Kodama, T.; Gokon, N.; Matsubara, K. A Review on High-temperature Thermochemical Heat Storage: Particle Reactors and Materials Based on Solid–Gas

Reactions. *WIREs Energy Environ.* **2022**, *11* (5). https://doi.org/10.1002/wene.440.

(67) Perry, R.; Green, D. Perry's Chemical Engineers' Handbook, 6th Edn. *McGraw-Hill, New York* **1997**, *6*, 641–672.

(68) Benitez-Guerrero, M.; Valverde, J. M.; Perejon, A.; Sanchez-Jimenez, P. E.; Perez-Maqueda, L. A. Low-Cost Ca-Based Composites Synthesized by Biotemplate Method for Thermochemical Energy Storage of Concentrated Solar Power. *Appl. Energy* **2018**, *210*, 108–116. https://doi.org/10.1016/J.APENERGY.2017.10.109.

(69) Edwards, S. E. B.; Materić, V. Calcium Looping in Solar Power Generation Plants. *Sol. Energy* **2012**, *86* (9), 2494–2503. https://doi.org/10.1016/j.solener.2012.05.019.

(70) Valverde, J. M.; Raganati, F.; Quintanilla, M. a. S.; Ebri, J. M. P.; Ammendola, P.; Chirone, R. Enhancement of CO2 Capture at Ca-Looping Conditions by High-Intensity Acoustic Fields. *Appl. Energy* **2013**, *111*, 538–549. https://doi.org/10.1016/j.apenergy.2013.05.012.

(71) Tregambi, C.; Salatino, P.; Solimene, R.; Montagnaro, F. An Experimental Characterization of Calcium Looping Integrated with Concentrated Solar Power. *Chem. Eng. J.* **2018**, *331* (May 2017), 794–802. https://doi.org/10.1016/j.cej.2017.08.068.

(72) Valverde, J. M.; Medina, S. Reduction of Calcination Temperature in the Calcium Looping Process for CO 2 Capture by Using Helium: In Situ XRD Analysis. *ACS Sustain. Chem. Eng.* **2016**, *4* (12), 7090–7097. https://doi.org/10.1021/acssuschemeng.6b01966.

(73) Badie, J. M.; Bonet, C.; Faure, M.; Flamant, G.; Foro, R.; Hernandez, D. 52 Decarbonation of Calcite and Phosphate Rock in Solar Chemical Reactors. *Chem. Eng. Sci.* **1980**, *35* (1–2), 413–420. https://doi.org/10.1016/0009-2509(80)80114-X.

(74) Flamant, G.; Hernandez, D.; Bonet, C.; Traverse, J. P. Experimental Aspects of the Thermochemical Conversion of Solar Energy; Decarbonation of CaCO3. *Sol. Energy* **1980**,

24 (4), 385–395. https://doi.org/10.1016/0038-092X(80)90301-1.

(75) Barker, R. The Reactivity of Calcium Oxide towards Carbon Dioxide and Its Use for Energy Storage. *J. Appl. Chem. Biotechnol.* **1974**, *24* (4–5), 221–227. https://doi.org/10.1002/JCTB.2720240405.

(76) Raganati, F.; Chirone, R.; Ammendola, P. Preliminary Study on Sound Assisted Calcium Looping for TCES in CSP Applications. *Chem. Eng. Trans.* **2019**, *74*, 427–432. https://doi.org/10.3303/CET1974072.

(77) Raganati, F.; Chirone, R.; Ammendola, P. Calcium-Looping for Thermochemical Energy Storage in Concentrating Solar Power Applications: Evaluation of the Effect of Acoustic Perturbation on the Fluidized Bed Carbonation. *Chem. Eng. J.* **2020**, *392* (December 2019), 123658. https://doi.org/10.1016/j.cej.2019.123658.

(78) Sakellariou, K. G.; Karagiannakis, G.; Criado, Y. A.; Konstandopoulos, A. G. Calcium Oxide Based Materials for Thermochemical Heat Storage in Concentrated Solar Power Plants. *Sol. Energy* **2015**, *122*, 215–230. https://doi.org/10.1016/j.solener.2015.08.011.

(79) Karasavvas, E.; Panopoulos, K. D.; Papadopoulou, S.; Voutetakis, S. Design of an Integrated CSP-Calcium Looping for Uninterrupted Power Production Through Energy Storage. *Chem. Eng. Trans.* **2018**, *70*, 2131–2136. https://doi.org/10.3303/CET1870356.

(80) Ortiz, C. Thermochemical Energy Storage Based on Carbonates: A Brief Overview. *Energies* **2021**, *14* (14), 4336. https://doi.org/10.3390/en14144336.

(81) Chacartegui, R.; Alovisio, A.; Ortiz, C.; Valverde, J. M.; Verda, V.; Becerra, J. A. Thermochemical Energy Storage of Concentrated Solar Power by Integration of the Calcium Looping Process and a CO 2 Power Cycle. *Appl. Energy* **2016**, *173*, 589–605. https://doi.org/10.1016/j.apenergy.2016.04.053.

(82) Ortiz, C.; Romano, M. C.; Valverde, J. M.; Binotti, M.; Chacartegui, R. Process Integration of Calcium-Looping Thermochemical Energy Storage System in Concentrating Solar Power Plants. *Energy* **2018**, *155*, 535–551. https://doi.org/10.1016/j.energy.2018.04.180.

(83) Chen, J.; Duan, L.; Sun, Z. Review on the Development of Sorbents for Calcium Looping. *Energy and Fuels* **2020**, *34* (7), 7806–7836. https://doi.org/10.1021/acs.energyfuels.0c00682.

(84) Alovisio, A.; Chacartegui, R.; Ortiz, C.; Valverde, J. M.; Verda, V. Optimizing the CSP-Calcium Looping Integration for Thermochemical Energy Storage. *Energy Convers. Manag.* **2017**, *136*, 85–98. https://doi.org/10.1016/j.enconman.2016.12.093.

(85) Sarrion, B.; Valverde, J. M.; Perejon, A.; Perez-Maqueda, L.; Sanchez-Jimenez, P. E. On the Multicycle Activity of Natural Limestone/Dolomite for Thermochemical Energy Storage of Concentrated Solar Power. *Energy Technol.* **2016**, *4* (8), 1013–1019. https://doi.org/10.1002/ente.201600068.

(86) Dean, C. C.; Blamey, J.; Florin, N. H.; Al-Jeboori, M. J.; Fennell, P. S. The Calcium Looping Cycle for CO2 Capture from Power Generation, Cement Manufacture and Hydrogen Production. *Chem. Eng. Res. Des.* **2011**, *89* (6), 836–855. https://doi.org/10.1016/j.cherd.2010.10.013.

(87) Blamey, J.; Anthony, E. J.; Wang, J.; Fennell, P. S. The Calcium Looping Cycle for Large-Scale CO2 Capture. *Prog. Energy Combust. Sci.* **2010**, *36* (2), 260–279. https://doi.org/10.1016/j.pecs.2009.10.001.

(88) Erans, M.; Manovic, V.; Anthony, E. J. Calcium Looping Sorbents for CO2 Capture. *Appl. Energy* **2016**, *180*, 722–742. https://doi.org/10.1016/j.apenergy.2016.07.074.

(89) Dou, B.; Song, Y.; Liu, Y.; Feng, C. High Temperature CO2 Capture Using Calcium Oxide Sorbent in a Fixed-Bed Reactor. *J. Hazard. Mater.* **2010**, *183* (1–3), 759–765. https://doi.org/10.1016/j.jhazmat.2010.07.091.

(90) Perejón, A.; Miranda-Pizarro, J.; Pérez-Maqueda, L. A.; Valverde, J. M. On the Relevant Role of Solids Residence Time on Their CO 2 Capture Performance in the Calcium Looping Technology. *Energy* **2016**, *113*, 160–171. https://doi.org/10.1016/j.energy.2016.07.028.

(91) Benitez-Guerrero, M.; Sarrion, B.; Perejon, A.; Sanchez-Jimenez, P. E.; Perez-Maqueda, L. A.; Manuel Valverde, J. Large-Scale High-Temperature Solar Energy Storage Using Natural Minerals. *Sol. Energy Mater. Sol. Cells* **2017**, *168* (November 2016), 14–21. https://doi.org/10.1016/j.solmat.2017.04.013.

(92) Sarrión, B.; Perejón, A.; Sánchez-Jiménez, P. E.; Pérez-Maqueda, L. A.; Valverde, J. M. Role of Calcium Looping Conditions on the Performance of Natural and Synthetic Ca-Based Materials for Energy Storage. *J. CO2 Util.* **2018**, *28*, 374–384. https://doi.org/10.1016/j.jcou.2018.10.018.

(93) Benitez-Guerrero, M.; Valverde, J. M.; Sanchez-Jimenez, P. E.; Perejon, A.; Perez-Maqueda, L. A. Calcium-Looping Performance of Mechanically Modified Al2O3-CaO Composites for Energy Storage and CO2 Capture. *Chem. Eng. J.* **2018**, *334*, 2343–2355. https://doi.org/10.1016/j.cej.2017.11.183.

(94) Han, R.; Wang, Y.; Xing, S.; Pang, C.; Hao, Y.; Song, C.; Liu, Q. Progress in Reducing Calcination Reaction Temperature of Calcium-Looping CO2 Capture Technology: A Critical Review. *Chem. Eng. J.* **2022**, *450*, 137952. https://doi.org/10.1016/j.cej.2022.137952.

(95) Wang, Y.; Lin, S.; Suzuki, Y. Limestone Calcination with CO2 Capture (II): Decomposition in CO2/Steam and CO2/N2 Atmospheres. *Energy & Fuels* **2008**, No. Ii, 2326–2331.

(96) Salaudeen, S. A.; Acharya, B.; Dutta, A. CaO-Based CO2 Sorbents: A Review on Screening, Enhancement, Cyclic Stability, Regeneration and Kinetics Modelling. *J. CO2 Util.* **2018**, *23*, 179–199. https://doi.org/10.1016/j.jcou.2017.11.012.

(97) ZEMAN, F. Effect of Steam Hydration on Performance of Lime Sorbent for CO2 Capture.

Int. J. Greenh. Gas Control **2008**, *2* (2), 203–209. https://doi.org/10.1016/S1750-5836(07)00115-6.

(98) Valverde, J. M.; Medina, S. Limestone Calcination under Calcium-Looping Conditions for CO 2 Capture and Thermochemical Energy Storage in the Presence of H 2 O: An in Situ XRD Analysis. *Phys. Chem. Chem. Phys.* **2017**, *19* (11), 7587–7596. https://doi.org/10.1039/C7CP00260B.

(99) Sato, S.; Lin, S. Y.; Suzuki, Y.; Hatano, H. Hydrogen Production from Heavy Oil in the Presence of Calcium Hydroxide☆. *Fuel* **2003**, *82* (5), 561–567. https://doi.org/10.1016/S0016-2361(02)00328-9.

(100) Lin, S.; Harada, M.; Suzuki, Y.; Hatano, H. Hydrogen Production from Coal by Separating Carbon Dioxide during Gasification. *Fuel* **2002**, *81* (16), 2079–2085. https://doi.org/10.1016/S0016-2361(02)00187-4.

(101) Lin, S. Y.; Suzuki, Y.; Hatano, H.; Harada, M. Hydrogen Production from Hydrocarbon by Integration of Water-Carbon Reaction and Carbon Dioxide Removal (HyPr-RING Method). *Energy and Fuels* **2001**, *15* (2), 339–343. https://doi.org/10.1021/EF000089U/ASSET/IMAGES/LARGE/EF000089UF00010.JPEG.

(102) Manovic, V.; Anthony, E. J. Carbonation of CaO-Based Sorbents Enhanced by Steam Addition. *Ind. Eng. Chem. Res.* **2010**, *49* (19), 9105–9110. https://doi.org/10.1021/ie101352s.

(103) Dobner, S.; Sterns, L.; Graff, R. A.; Squires, A. M. Cyclic Calcination and Recarbonation of Calcined Dolomite. *Ind. Eng. Chem. Process Des. Dev.* **1977**, *16* (4), 479–486. https://doi.org/10.1021/I260064A008/ASSET/I260064A008.FP.PNG_V03.

(104) Wang, A.; Deshpande, N.; Fan, L. S. Steam Hydration of Calcium Oxide for Solid Sorbent

Based CO2 Capture: Effects of Sintering and Fluidized Bed Reactor Behavior. *Energy and Fuels* **2015**, *29* (1), 321–330. https://doi.org/10.1021/EF502021D/ASSET/IMAGES/LARGE/EF-2014-02021D_0011.JPEG.

(105) Blamey, J.; Zhao, M.; Manovic, V.; Anthony, E. J.; Dugwell, D. R.; Fennell, P. S. A Shrinking Core Model for Steam Hydration of CaO-Based Sorbents Cycled for CO2 Capture. *Chem. Eng. J.* **2016**, *291*, 298–305. https://doi.org/10.1016/J.CEJ.2016.01.086.

(106) Li, Y.-J.; Zhao, C.-S.; Qu, C.-R.; Duan, L.-B.; Li, Q.-Z.; Liang, C. CO2 Capture Using CaO Modified with Ethanol/Water Solution during Cyclic Calcination/Carbonation. *Chem. Eng. Technol.* **2008**, *31* (2), 237–244. https://doi.org/10.1002/ceat.200700371.

(107) Sun, H.; Wu, C.; Shen, B.; Zhang, X.; Zhang, Y.; Huang, J. Progress in the Development and Application of CaO-Based Adsorbents for CO2 Capture—a Review. *Mater. Today Sustain.* **2018**, *1–2*, 1–27. https://doi.org/10.1016/j.mtsust.2018.08.001.

(108) Coppola, A.; Palladino, L.; Montagnaro, F.; Scala, F.; Salatino, P. Reactivation by Steam Hydration of Sorbents for Fluidized-Bed Calcium Looping. *Energy & Fuels* **2015**, *29* (7), 4436–4446. https://doi.org/10.1021/acs.energyfuels.5b00413.

(109) Laursen, K.; Duo, W.; Grace, J. R.; Lim, C. J. Cyclic Steam Reactivation of Spent Limestone. *Ind. Eng. Chem. Res.* **2004**, *43* (18), 5715–5720. https://doi.org/10.1021/IE030795T/ASSET/IMAGES/LARGE/IE030795TF00006.JPEG.

(110) Sun, P.; Grace, J. R.; Lim, C. J.; Anthony, E. J. Investigation of Attempts to Improve Cyclic CO2 Capture by Sorbent Hydration and Modification. *Ind. Eng. Chem. Res.* **2008**, *47* (6), 2024–2032. https://doi.org/10.1021/IE070335Q/ASSET/IMAGES/MEDIUM/IE070335QE00002.GIF.

(111) Hughes, R. W.; Lu, D. Y.; Anthony, E. J.; Macchi, A. Design, Process Simulation and

Construction of an Atmospheric Dual Fluidized Bed Combustion System for in Situ CO2 Capture Using High-Temperature Sorbents. *Fuel Process. Technol.* **2005**, *86* (14–15), 1523–1531. https://doi.org/10.1016/j.fuproc.2005.01.006.

(112) Wang, Y.; Lin, S.; Suzuki, Y. Limestone Calcination with CO2 Capture (III): Characteristics of Coal Combustion during Limestone Decomposition. *Energy and Fuels* **2009**, *23* (5), 2804–2809. https://doi.org/10.1021/EF801105J/ASSET/IMAGES/LARGE/EF-2008-01105J_0014.JPEG.

(113) Wang, Y.; Lin, S.; Suzuki, Y. Experimental Study on CO2 Capture Conditions of a Fluidized Bed Limestone Decomposition Reactor. *Fuel Process. Technol.* **2010**, *91* (8), 958–963. https://doi.org/10.1016/j.fuproc.2009.07.011.

(114) Wang, Y.; Thomson, W. J. The Effects of Steam and Carbon Dioxide on Calcite Decomposition Using Dynamic X-Ray Diffraction. *Chem. Eng. Sci.* **1995**, *50* (9), 1373–1382. https://doi.org/10.1016/0009-2509(95)00002-M.

(115) Han, L.; Wang, Q.; Ma, Q.; Guan, J.; Luo, Z.; Cen, K. Hydration Reactivation of CaO-Based Sorbent for Cyclic Calcination- Carbonation Reactions. *Proc. 20th Int. Conf. Fluid. Bed Combust.* **2009**, 726–731. https://doi.org/10.1007/978-3-642-02682-9_112/COVER.

(116) Kuramoto, K.; Fujimoto, S.; Morita, A.; Shibano, S.; Suzuki, Y.; Hatano, H.; Shi-Ying, L.; Harada, M.; Takarada, T. Repetitive Carbonation-Calcination Reactions of Ca-Based Sorbents for Efficient CO2 Sorption at Elevated Temperatures and Pressures. *Ind. Eng. Chem. Res.* **2003**, *42* (5), 975–981. https://doi.org/10.1021/IE0207111/ASSET/IMAGES/LARGE/IE0207111F00007.JPEG.

(117) Manovic, V.; Anthony, E. J. Steam Reactivation of Spent CaO-Based Sorbent for Multiple CO 2 Capture Cycles. *Environ. Sci. Technol.* **2007**, *41* (4), 1420–1425. https://doi.org/10.1021/es0621344.

(118) Manovic, V.; Anthony, E. J. Sequential SO2/CO2 Capture Enhanced by Steam Reactivation of a CaO-Based Sorbent. *Fuel* **2008**, *87* (8–9), 1564–1573. https://doi.org/10.1016/j.fuel.2007.08.022.

(119) Manovic, V.; Anthony, E. J. Thermal Activation of CaO-Based Sorbent and Self-Reactivation during CO 2 Capture Looping Cycles. *Environ. Sci. Technol.* **2008**, *42* (11), 4170–4174. https://doi.org/10.1021/es800152s.

(120) Arias, B.; Grasa, G. S.; Abanades, J. C. Effect of Sorbent Hydration on the Average Activity of CaO in a Ca-Looping System. *Chem. Eng. J.* **2010**, *163* (3), 324–330. https://doi.org/10.1016/j.cej.2010.08.009.

(121) Yin, J.; Zhang, C.; Qin, C.; Liu, W.; An, H.; Chen, G.; Feng, B. Reactivation of Calcium-Based Sorbent by Water Hydration for CO2 Capture. *Chem. Eng. J.* **2012**, *198–199*, 38–44. https://doi.org/10.1016/j.cej.2012.05.078.

(122) Li, C.-C.; Cheng, J.-Y.; Liu, W.-H.; Huang, C.-M.; Hsu, H.-W.; Lin, H.-P. Enhancement in Cyclic Stability of the CO2 Adsorption Capacity of CaO-Based Sorbents by Hydration for the Calcium Looping Cycle. *J. Taiwan Inst. Chem. Eng.* **2014**, *45* (1), 227–232. https://doi.org/10.1016/j.jtice.2013.06.019.

(123) Martínez, I.; Grasa, G.; Murillo, R.; Arias, B.; Abanades, J. C. Evaluation of CO 2 Carrying Capacity of Reactivated CaO by Hydration. *Energy & Fuels* **2011**, *25* (3), 1294–1301. https://doi.org/10.1021/ef1015582.

(124) Wang, K.; Guo, X.; Zhao, P.; Zhang, L.; Zheng, C. CO2 Capture of Limestone Modified by Hydration–Dehydration Technology for Carbonation/Calcination Looping. *Chem. Eng. J.* **2011**, *173* (1). https://doi.org/10.1016/j.cej.2011.07.057.

(125) Rong, N.; Wang, Q.; Fang, M.; Cheng, L.; Luo, Z.; Cen, K. Steam Hydration Reactivation of CaO-Based Sorbent in Cyclic Carbonation/Calcination for CO 2 Capture. *Energy & Fuels*

2013, *27* (9), 5332–5340. https://doi.org/10.1021/ef4007214.

(126) Coppola, A.; Salatino, P.; Montagnaro, F.; Scala, F. Hydration-Induced Reactivation of Spent Sorbents for Fluidized Bed Calcium Looping (Double Looping). *Fuel Process. Technol.* **2014**, *120*, 71–78. https://doi.org/10.1016/j.fuproc.2013.12.004.

(127) Kudłacz, K.; Rodriguez-Navarro, C. The Mechanism of Vapor Phase Hydration of Calcium Oxide: Implications for CO2 Capture. *Environ. Sci. Technol.* **2014**, *48* (20), 12411–12418. https://doi.org/10.1021/ES5034662/SUPPL_FILE/ES5034662_SI_001.PDF.

(128) Antzara, A. N.; Arregi, A.; Heracleous, E.; Lemonidou, A. A. In-Depth Evaluation of a ZrO2 Promoted CaO-Based CO2 Sorbent in Fluidized Bed Reactor Tests. *Chem. Eng. J.* **2018**, *333*, 697–711. https://doi.org/10.1016/j.cej.2017.09.192.

(129) Sánchez Jiménez, P. E.; Perejón, A.; Benítez Guerrero, M.; Valverde, J. M.; Ortiz, C.; Pérez Maqueda, L. A. High-Performance and Low-Cost Macroporous Calcium Oxide Based Materials for Thermochemical Energy Storage in Concentrated Solar Power Plants. *Appl. Energy* **2019**, *235*, 543–552. https://doi.org/10.1016/j.apenergy.2018.10.131.

(130) Broda, M.; Kierzkowska, A. M.; Müller, C. R. Influence of the Calcination and Carbonation Conditions on the CO 2 Uptake of Synthetic Ca-Based CO 2 Sorbents. *Environ. Sci. Technol.* **2012**, *46* (19), 10849–10856. https://doi.org/10.1021/es302757e.

(131) Zhao, M.; Shi, J.; Zhong, X.; Tian, S.; Blamey, J.; Jiang, J.; Fennell, P. S. A Novel Calcium Looping Absorbent Incorporated with Polymorphic Spacers for Hydrogen Production and CO 2 Capture. *Energy Environ. Sci.* **2014**, *7* (10), 3291–3295. https://doi.org/10.1039/C4EE01281J.

(132) Chen, J.; Duan, L.; Donat, F.; Müller, C. R.; Anthony, E. J.; Fan, M. Self-Activated, Nanostructured Composite for Improved CaL-CLC Technology. *Chem. Eng. J.* **2018**, *351*, 1038–1046. https://doi.org/10.1016/j.cej.2018.06.176.

(133) Su, C.; Duan, L.; Donat, F.; Anthony, E. J. From Waste to High Value Utilization of Spent Bleaching Clay in Synthesizing High-Performance Calcium-Based Sorbent for CO2 Capture. *Appl. Energy* **2018**, *210*, 117–126. https://doi.org/10.1016/j.apenergy.2017.10.104.

(134) Zhang, X.; Li, Z.; Peng, Y.; Su, W.; Sun, X.; Li, J. Investigation on a Novel CaO–Y2O3 Sorbent for Efficient CO2 Mitigation. *Chem. Eng. J.* **2014**, *243*, 297–304. https://doi.org/10.1016/j.cej.2014.01.017.

(135) Wang, S.; Fan, S.; Fan, L.; Zhao, Y.; Ma, X. Effect of Cerium Oxide Doping on the Performance of CaO-Based Sorbents during Calcium Looping Cycles. *Environ. Sci. Technol.* **2015**, *49* (8), 5021–5027. https://doi.org/10.1021/ES5052843/ASSET/IMAGES/LARGE/ES-2014-052843_0010.JPEG.

(136) Han, R.; Gao, J.; Wei, S.; Su, Y.; Qin, Y. Development of Highly Effective CaO@Al2O3 with Hierarchical Architecture CO2 Sorbents via a Scalable Limited-Space Chemical Vapor Deposition Technique. *J. Mater. Chem. A* **2018**, *6* (8), 3462–3470. https://doi.org/10.1039/C7TA09960F.

(137) Xu, P.; Zhou, Z.; Zhao, C.; Cheng, Z. Catalytic Performance of Ni/CaO-Ca 5 Al 6 O 14 Bifunctional Catalyst Extrudate in Sorption-Enhanced Steam Methane Reforming. *Catal. Today* **2016**, *259*, 347–353. https://doi.org/10.1016/j.cattod.2015.05.026.

(138) Chen, X.; Yang, L.; Zhou, Z.; Cheng, Z. Core-Shell Structured CaO-Ca9Al6O18@Ca5Al6O14/Ni Bifunctional Material for Sorption-Enhanced Steam Methane Reforming. *Chem. Eng. Sci.* **2017**, *163*, 114–122. https://doi.org/10.1016/j.ces.2017.01.036.

(139) Ma, X.; Li, Y.; Qian, Y.; Wang, Z. A Carbide Slag-Based, Ca12Al14O33-Stabilized Sorbent Prepared by the Hydrothermal Template Method Enabling Efficient CO2 Capture. *Energies* **2019**, *12* (13), 2617. https://doi.org/10.3390/en12132617.

(140) Zhang, M.; Peng, Y.; Sun, Y.; Li, P.; Yu, J. Preparation of CaO–Al2O3 Sorbent and CO2

Capture Performance at High Temperature. *Fuel* **2013**, *111*, 636–642. https://doi.org/10.1016/j.fuel.2013.03.078.

(141) Florin, N. H.; Blamey, J.; Fennell, P. S. Synthetic CaO-Based Sorbent for CO 2 Capture from Large-Point Sources. *Energy & Fuels* **2010**, *24* (8), 4598–4604. https://doi.org/10.1021/ef100447c.

(142) Xu, P.; Xie, M.; Cheng, Z.; Zhou, Z. CO2 Capture Performance of CaO-Based Sorbents Prepared by a Sol-Gel Method. *Ind. Eng. Chem. Res.* **2013**, *52* (34), 12161–12169. https://doi.org/10.1021/IE401600E/ASSET/IMAGES/LARGE/IE-2013-01600E_0014.JPEG.

(143) Kurlov, A.; Armutlulu, A.; Donat, F.; Studart, A. R.; Müller, C. R. CaO-Based CO2 Sorbents with a Hierarchical Porous Structure Made via Microfluidic Droplet Templating. *Ind. Eng. Chem. Res.* **2020**, *59* (15), 7182–7188. https://doi.org/10.1021/ACS.IECR.9B05996/ASSET/IMAGES/LARGE/IE9B05996_0002.JPEG.

(144) Broda, M.; Müller, C. R. Synthesis of Highly Efficient, Ca-Based, Al2O3-Stabilized, Carbon Gel-Templated CO2 Sorbents. *Adv. Mater.* **2012**, *24* (22), 3059–3064. https://doi.org/10.1002/adma.201104787.

(145) Koirala, R.; Reddy, G. K.; Smirniotis, P. G. Single Nozzle Flame-Made Highly Durable Metal Doped ca-Based Sorbents for CO 2 Capture at High Temperature. *Energy and Fuels* **2012**, *26* (5), 3103–3109. https://doi.org/10.1021/EF3004015/ASSET/IMAGES/LARGE/EF-2012-004015_0005.JPEG.

(146) Angeli, S. D.; Martavaltzi, C. S.; Lemonidou, A. A. Development of a Novel-Synthesized Ca-Based CO2 Sorbent for Multicycle Operation: Parametric Study of Sorption. *Fuel* **2014**, *127*, 62–69. https://doi.org/10.1016/j.fuel.2013.10.046.

(147) Sultana, K. S.; Tran, D. T.; Walmsley, J. C.; Rønning, M.; Chen, D. CaO Nanoparticles

Coated by ZrO 2 Layers for Enhanced CO 2 Capture Stability. *Ind. Eng. Chem. Res.* **2015**, *54* (36), 8929–8939. https://doi.org/10.1021/acs.iecr.5b00423.

(148) Broda, M.; Müller, C. R. Sol–Gel-Derived, CaO-Based, ZrO2-Stabilized CO2 Sorbents. *Fuel* **2014**, *127*, 94–100. https://doi.org/10.1016/j.fuel.2013.08.004.

(149) Koirala, R.; Gunugunuri, K. R.; Pratsinis, S. E.; Smirniotis, P. G. Effect of Zirconia Doping on the Structure and Stability of CaO-Based Sorbents for CO 2 Capture during Extended Operating Cycles. *J. Phys. Chem. C* **2011**, *115* (50), 24804–24812. https://doi.org/10.1021/jp207625c.

(150) Lu, H.; Khan, A.; Pratsinis, S. E.; Smirniotis, P. G. Flame-Made Durable Doped-CaO Nanosorbents for CO 2 Capture. *Energy & Fuels* **2009**, *23* (2), 1093–1100. https://doi.org/10.1021/ef8007882.

(151) Yoon, H. J.; Lee, K. B. Introduction of Chemically Bonded Zirconium Oxide in CaO-Based High-Temperature CO2 Sorbents for Enhanced Cyclic Sorption. *Chem. Eng. J.* **2019**, *355*, 850–857. https://doi.org/10.1016/j.cej.2018.08.148.

(152) Zhao, C.; Zhou, Z.; Cheng, Z. Sol–Gel-Derived Synthetic CaO-Based CO 2 Sorbents Incorporated with Different Inert Materials. *Ind. Eng. Chem. Res.* **2014**, *53* (36), 14065–14074. https://doi.org/10.1021/ie502559t.

(153) Zhao, M.; He, X.; Ji, G.; Song, Y.; Zhao, X. Zirconia Incorporated Calcium Looping Absorbents with Superior Sintering Resistance for Carbon Dioxide Capture from in Situ or Ex Situ Processes. *Sustain. Energy Fuels* **2018**, *2* (12), 2733–2741. https://doi.org/10.1039/C8SE00413G.

(154) Sanchez-Jimenez, P. E.; Perez-Maqueda, L. A.; Valverde, J. M. Nanosilica Supported CaO: A Regenerable and Mechanically Hard CO2 Sorbent at Ca-Looping Conditions. *Appl. Energy* **2014**, *118*, 92–99. https://doi.org/10.1016/j.apenergy.2013.12.024.

(155) Li, C.-C.; Wu, U.-T.; Lin, H.-P. Cyclic Performance of CaCO 3 @mSiO 2 for CO 2 Capture in a Calcium Looping Cycle. *J. Mater. Chem. A* **2014**, *2* (22), 8252–8257. https://doi.org/10.1039/C4TA00516C.

(156) Valverde, J. M.; Perejon, A.; Perez-Maqueda, L. A. Enhancement of Fast CO 2 Capture by a Nano-SiO 2 /CaO Composite at Ca-Looping Conditions. *Environ. Sci. Technol.* **2012**, *46* (11), 6401–6408. https://doi.org/10.1021/es3002426.

(157) Huang, C.-H.; Chang, K.-P.; Yu, C.-T.; Chiang, P.-C.; Wang, C.-F. Development of High-Temperature CO2 Sorbents Made of CaO-Based Mesoporous Silica. *Chem. Eng. J.* **2010**, *161* (1–2), 129–135. https://doi.org/10.1016/j.cej.2010.04.045.

(158) Zhao, M.; Song, Y.; Ji, G.; Zhao, X. Demonstration of Polymorphic Spacing Strategy against Sintering: Synthesis of Stabilized Calcium Looping Absorbents for High-Temperature CO 2 Sorption. *Energy & Fuels* **2018**, *32* (4), 5443–5452. https://doi.org/10.1021/acs.energyfuels.8b00648.

(159) Armutlulu, A.; Awais Naeem, M.; Liu, H.-J.; Min Kim, S.; Kierzkowska, A.; Fedorov, A.; Müller, C. R.; Armutlulu, A.; Naeem, M. A.; Kim, S. M.; et al. Multishelled CaO Microspheres Stabilized by Atomic Layer Deposition of Al2O3 for Enhanced CO2 Capture Performance. *Adv. Mater.* **2017**, *29* (41), 1702896. https://doi.org/10.1002/ADMA.201702896.

(160) Wang, N.; Feng, Y.; Liu, L.; Guo, X. Effects of Preparation Methods on the Structure and Property of Al-Stabilized CaO-Based Sorbents for CO 2 Capture. *Fuel Process. Technol.* **2018**, *173*, 276–284. https://doi.org/10.1016/j.fuproc.2018.02.005.

(161) Hu, Y.; Liu, W.; Chen, H.; Zhou, Z.; Wang, W.; Sun, J.; Yang, X.; Li, X.; Xu, M. Screening of Inert Solid Supports for CaO-Based Sorbents for High Temperature CO2 Capture. *Fuel* **2016**, *181*, 199–206. https://doi.org/10.1016/j.fuel.2016.04.138.

(162) Koirala, R.; Reddy, G. K.; Lee, J. Y.; Smirniotis, P. G. Influence of Foreign Metal Dopants on the Durability and Performance of Zr/Ca Sorbents during High Temperature CO2 Capture. *http://dx.doi.org/10.1080/01496395.2013.836672* **2013**, *49* (1), 47–54. https://doi.org/10.1080/01496395.2013.836672.

(163) Soria-Hoyo, C.; Valverde, J. M.; Van Ommen, J. R.; Sánchez-Jiménez, P. E.; Pérez-Maqueda, L. A.; Sayagués, M. J. Synthesis of a Nanosilica Supported CO2 Sorbent in a Fluidized Bed Reactor. *Appl. Surf. Sci.* **2015**, *328*, 548–553. https://doi.org/10.1016/j.apsusc.2014.12.106.

(164) SILABAN, A.; NARCIDA, M.; HARRISON, D. P. CHARACTERISTICS OF THE REVERSIBLE REACTION BETWEEN CO 2 (g) AND CALCINED DOLOMITE. *Chem. Eng. Commun.* **1996**, *146* (1), 149–162. https://doi.org/10.1080/00986449608936487.

(165) Albrecht, K. O.; Wagenbach, K. S.; Satrio, J. A.; Shanks, B. H.; Wheelock, T. D. Development of a CaO-Based CO2 Sorbent with Improved Cyclic Stability. *Ind. Eng. Chem. Res.* **2008**, *47* (20), 7841–7848. https://doi.org/10.1021/IE8007743/ASSET/IMAGES/LARGE/IE-2008-007743_0004.JPEG.

(166) Sun, J.; Yang, Y.; Guo, Y.; Xu, Y.; Li, W.; Zhao, C.; Liu, W.; Lu, P. Stabilized CO2 Capture Performance of Wet Mechanically Activated Dolomite. *Fuel* **2018**, *222*, 334–342. https://doi.org/10.1016/J.FUEL.2018.02.162.

(167) Wang, K.; Hu, X.; Zhao, P.; Yin, Z. Natural Dolomite Modified with Carbon Coating for Cyclic High-Temperature CO2 Capture. *Appl. Energy* **2016**, *165*, 14–21. https://doi.org/10.1016/j.apenergy.2015.12.071.

(168) Liu, W.; Feng, B.; Wu, Y.; Wang, G.; Barry, J.; Diniz da Costa, J. C. Synthesis of Sintering-Resistant Sorbents for CO 2 Capture. *Environ. Sci. Technol.* **2010**, *44* (8), 3093–3097. https://doi.org/10.1021/es903436v.

(169) Naeem, M. A.; Armutlulu, A.; Kierzkowska, A.; Müller, C. R. Development of High-Performance CaO-Based CO2 Sorbents Stabilized with Al2O3 or MgO. *Energy Procedia* **2017**, *114*, 158–166. https://doi.org/10.1016/j.egypro.2017.03.1158.

(170) Broda, M.; Kierzkowska, A. M.; Müller, C. R. Development of Highly Effective CaO-Based, MgO-Stabilized CO 2 Sorbents via a Scalable "One-Pot" Recrystallization Technique. *Adv. Funct. Mater.* **2014**, *24* (36), 5753–5761. https://doi.org/10.1002/adfm.201400862.

(171) Kurlov, A.; Broda, M.; Hosseini, D.; Mitchell, S. J.; Pérez-Ramírez, J.; Müller, C. R. Mechanochemically Activated, Calcium Oxide-Based, Magnesium Oxide-Stabilized Carbon Dioxide Sorbents. *ChemSusChem* **2016**, *9* (17), 2380–2390. https://doi.org/10.1002/cssc.201600510.

(172) Lan, P.; Wu, S. Synthesis of a Porous Nano-CaO/MgO-Based CO 2 Adsorbent. *Chem. Eng. Technol.* **2014**, *37* (4), 580–586. https://doi.org/10.1002/ceat.201300709.

(173) Chen, H.; Zhao, C. Development of a CaO-Based Sorbent with Improved Cyclic Stability for CO2 Capture in Pressurized Carbonation. *Chem. Eng. J.* **2011**, *171* (1), 197–205. https://doi.org/10.1016/j.cej.2011.03.091.

(174) Antzara, A.; Heracleous, E.; Lemonidou, A. A. Development of CaO-Based Mixed Oxides as Stable Sorbents for Post-Combustion CO2 Capture Via Carbonate Looping. *Energy Procedia* **2014**, *63*, 2160–2169. https://doi.org/10.1016/j.egypro.2014.11.235.

(175) Phromprasit, J.; Powell, J.; Assabumrungrat, S. Metals (Mg, Sr and Al) Modified CaO Based Sorbent for CO 2 Sorption/Desorption Stability in Fixed Bed Reactor for High Temperature Application. *Chem. Eng. J.* **2016**, *284*, 1212–1223. https://doi.org/10.1016/j.cej.2015.09.038.

(176) Li, L.; King, D. L.; Nie, Z.; Howard, C. Magnesia-Stabilized Calcium Oxide Absorbents with Improved Durability for High Temperature CO 2 Capture. *Ind. Eng. Chem. Res.* **2009**, *48* (23), 10604–10613. https://doi.org/10.1021/ie901166b.

(177) Chen, H.; Zhang, P.; Duan, Y.; Zhao, C. Reactivity Enhancement of Calcium Based Sorbents by Doped with Metal Oxides through the Sol–Gel Process. *Appl. Energy* **2016**, *162*, 390–400. https://doi.org/10.1016/j.apenergy.2015.10.035.

(178) Luo, C.; Zheng, Y.; Xu, Y.; Ding, N.; Shen, Q.; Zheng, C. Wet Mixing Combustion Synthesis of CaO-Based Sorbents for High Temperature Cyclic CO2 Capture. *Chem. Eng. J.* **2015**, *267*, 111–116. https://doi.org/10.1016/j.cej.2015.01.005.

(179) Huang, L.; Zheng, Q.; Louis, B.; Wang, Q. A Facile Solvent/Nonsolvent Preparation of Sintering-Resistant MgO/CaO Composites for High-Temperature CO 2 Capture. *Energy Technol.* **2018**, *6* (12), 2469–2478. https://doi.org/10.1002/ente.201800300.

(180) Daud, F. D. M.; Vignesh, K.; Sreekantan, S.; Mohamed, A. R. Improved CO2 Adsorption Capacity and Cyclic Stability of CaO Sorbents Incorporated with MgO. *New J. Chem.* **2016**, *40* (1), 231–237. https://doi.org/10.1039/C5NJ02081F.

(181) Guo, M.; Zhang, L.; Yang, Z.; Tang, Q. Removal of CO2 by CaO/MgO and CaO/Ca9Al 6O18 in the Presence of SO2. *Energy and Fuels* **2011**, *25* (11), 5514–5520. https://doi.org/10.1021/EF201072X/ASSET/IMAGES/LARGE/EF-2011-01072X_0015.JPEG.

(182) Derevschikov, V. S.; Lysikov, A. I.; Okunev, A. G. High Temperature CaO/Y2O3 Carbon Dioxide Absorbent with Enhanced Stability for Sorption-Enhanced Reforming Applications. *Ind. Eng. Chem. Res.* **2011**, *50* (22), 12741–12749. https://doi.org/10.1021/IE2015334/ASSET/IMAGES/LARGE/IE-2011-015334_0007.JPEG.

(183) Venkataswamy, P.; Rao, K. N.; Jampaiah, D.; Reddy, B. M. Nanostructured Manganese Doped Ceria Solid Solutions for CO Oxidation at Lower Temperatures. *Appl. Catal. B Environ.* **2015**, *162*, 122–132. https://doi.org/10.1016/J.APCATB.2014.06.038.

(184) Guo, H.; Feng, J.; Zhao, Y.; Wang, S.; Ma, X. Effect of Micro-Structure and Oxygen

Vacancy on the Stability of (Zr-Ce)-Additive CaO-Based Sorbent in CO 2 Adsorption. *J. CO2 Util.* **2017**, *19*, 165–176. https://doi.org/10.1016/j.jcou.2017.03.015.

(185) Yanase, I.; Maeda, T.; Kobayashi, H. The Effect of Addition of a Large Amount of CeO2 on the CO2 Adsorption Properties of CaO Powder. *Chem. Eng. J.* **2017**, *327*, 548–554. https://doi.org/10.1016/j.cej.2017.06.140.

(186) Peng, W.; Xu, Z.; Luo, C.; Zhao, H. Tailor-Made Core-Shell CaO/TiO2-Al2O3 Architecture as a High-Capacity and Long-Life CO2 Sorbent. *Environ. Sci. Technol.* **2015**, *49* (13), 8237–8245. https://doi.org/10.1021/ACS.EST.5B01415/SUPPL_FILE/ES5B01415_SI_001.PDF.

(187) He, D.; Qin, C.; Zhang, Z.; Pi, S.; Ran, J.; Pu, G. Investigation of Y2O3/MxOy-Incorporated Ca-Based Sorbents for Efficient and Stable CO2 Capture at High Temperature. *Ind. Eng. Chem. Res.* **2018**, *57* (34), 11625–11635. https://doi.org/10.1021/ACS.IECR.8B02064/ASSET/IMAGES/LARGE/IE-2018-020647_0014.JPEG.

(188) Sun, J.; Yang, Y.; Guo, Y.; Zhao, C.; Zhang, J.; Liu, W.; Lu, P. Stabilized Performance of Al-Decorated and Al/Mg Co-Decorated Spray-Dried CaO-Based CO 2 Sorbents. *Chem. Eng. Technol.* **2019**, *42* (6), 1283–1292. https://doi.org/10.1002/ceat.201900012.

(189) Chen, H.; Khalili, N. Fly-Ash-Modified Calcium-Based Sorbents Tailored to CO2 Capture. *Ind. Eng. Chem. Res.* **2017**, *56* (7), 1888–1894. https://doi.org/10.1021/ACS.IECR.6B04234/ASSET/IMAGES/LARGE/IE-2016-042349_0005.JPEG.

(190) Chen, H.; Khalili, N.; Li, J. Development of Stabilized Ca-Based CO2 Sorbents Supported by Fly Ash. *Chem. Eng. J.* **2018**, *345*, 312–319. https://doi.org/10.1016/j.cej.2018.03.162.

(191) Shi, J.; Li, Y.; Zhang, Q.; Ma, X.; Duan, L.; Zhou, X. CO2 Capture Performance of a Novel Synthetic CaO/Sepiolite Sorbent at Calcium Looping Conditions. *Appl. Energy* **2017**, *203*,

412–421. https://doi.org/10.1016/j.apenergy.2017.06.050.

(192) Hlaing, N. N.; Sreekantan, S.; Othman, R.; Hinode, H.; Kurniawan, W.; Thant, A. A.; Mohamed, A. R.; Salim, C. A Novel (Zr–Ce) Incorporated Ca(OH) 2 Nanostructure as a Durable Adsorbent for CO 2 Capture. *Mater. Lett.* **2014**, *133*, 204–207. https://doi.org/10.1016/j.matlet.2014.07.043.

(193) Sun, H.; Li, Y.; Yan, X.; Zhao, J.; Wang, Z. Thermochemical Energy Storage Performance of Al2O3/CeO2 Co-Doped CaO-Based Material under High Carbonation Pressure. *Appl. Energy* **2020**, *263*, 114650. https://doi.org/10.1016/j.apenergy.2020.114650.

(194) Kim, S. M.; Kierzkowska, A. M.; Broda, M.; Müller, C. R. Sol-Gel Synthesis of MgAl2O4-Stabilized CaO for CO2 Capture. *Energy Procedia* **2017**, *114*, 220–229. https://doi.org/10.1016/j.egypro.2017.03.1164.

(195) Li, L.; King, D. L.; Nie, Z.; Li, X. S.; Howard, C. MgAl 2 O 4 Spinel-Stabilized Calcium Oxide Absorbents with Improved Durability for High-Temperature CO 2 Capture. *Energy & Fuels* **2010**, *24* (6), 3698–3703. https://doi.org/10.1021/ef100245q.

(196) Sedghkerdar, M. H.; Mahinpey, N.; Soleimanisalim, A. H.; Sun, Z.; Chen, Z.; Lim, J.; Kaliaguine, S. Core-Shell Structured CaO-Based Pellets Protected by Mesoporous Ceramics Shells for High-Temperature CO 2 Capture. *Can. J. Chem. Eng.* **2016**, *94* (11), 2038–2044. https://doi.org/10.1002/cjce.22626.

(197) Naeem, M. A.; Armutlulu, A.; Imtiaz, Q.; Müller, C. R. CaO-Based CO 2 Sorbents Effectively Stabilized by Metal Oxides. *ChemPhysChem* **2017**, *18* (22), 3280–3285. https://doi.org/10.1002/cphc.201700695.

(198) Biasin, A.; Segre, C. U.; Strumendo, M. CaCO 3 Crystallite Evolution during CaO Carbonation: Critical Crystallite Size and Rate Constant Measurement by In-Situ Synchrotron Radiation X-Ray Powder Diffraction. *Cryst. Growth Des.* **2015**, *15* (11), 5188–

5201. https://doi.org/10.1021/acs.cgd.5b00563.

(199) Ma, X.; Li, Y.; Yan, X.; Zhang, W.; Zhao, J.; Wang, Z. Preparation of a Morph-Genetic CaO-Based Sorbent Using Paper Fibre as a Biotemplate for Enhanced CO2 Capture. *Chem. Eng. J.* **2019**, *361*, 235–244. https://doi.org/10.1016/j.cej.2018.12.061.

(200) Khosa, A. A.; Zhao, C. Y. Heat Storage and Release Performance Analysis of CaCO3/CaO Thermal Energy Storage System after Doping Nano Silica. *Sol. Energy* **2019**, *188*, 619–630. https://doi.org/10.1016/j.solener.2019.06.048.

(201) Khinast, J.; Krammer, G. F.; Brunner, C.; Staudinger, G. Decomposition of Limestone: The Influence of CO2 and Particle Size on the Reaction Rate. *Chem. Eng. Sci.* **1996**, *51* (4), 623–634. https://doi.org/10.1016/0009-2509(95)00302-9.

(202) Benitez-Guerrero, M.; Valverde, J. M.; Sanchez-Jimenez, P. E.; Perejon, A.; Perez-Maqueda, L. A. Multicycle Activity of Natural CaCO 3 Minerals for Thermochemical Energy Storage in Concentrated Solar Power Plants. *Sol. Energy* **2017**, *153*, 188–199. https://doi.org/10.1016/j.solener.2017.05.068.

(203) Raganati, F.; Ammendola, P. Carbonation Kinetics of Fine CaO Particles in a Sound-Assisted Fluidized Bed for Thermochemical Energy Storage. *KONA Powder Part. J.* **2022**, *39* (39), 240–250. https://doi.org/10.14356/kona.2022007.

(204) Valverde, J. M.; Sanchez-Jimenez, P. E.; Perez-Maqueda, L. A. Relevant Influence of Limestone Crystallinity on CO 2 Capture in The Ca-Looping Technology at Realistic Calcination Conditions. *Environ. Sci. Technol.* **2014**, *48* (16), 9882–9889. https://doi.org/10.1021/es5014505.

(205) Grasa, G. S.; Abanades, J. C.; Alonso, M.; González, B. Reactivity of Highly Cycled Particles of CaO in a Carbonation/Calcination Loop. *Chem. Eng. J.* **2008**, *137* (3), 561–567. https://doi.org/10.1016/j.cej.2007.05.017.

(206) Grasa, G.; Murillo, R.; Alonso, M.; Abanades, J. C. Application of the Random Pore Model to the Carbonation Cyclic Reaction. *AIChE J.* **2009**, *55* (5), 1246–1255. https://doi.org/10.1002/aic.11746.

(207) Durán-Martín, J. D.; Sánchez Jimenez, P. E.; Valverde, J. M.; Perejón, A.; Arcenegui-Troya, J.; García Triñanes, P.; Pérez Maqueda, L. A. Role of Particle Size on the Multicycle Calcium Looping Activity of Limestone for Thermochemical Energy Storage. *J. Adv. Res.* **2020**, *22*, 67–76. https://doi.org/10.1016/j.jare.2019.10.008.

(208) Sánchez-Jiménez, P. E.; Valverde, J. M.; Perejón, A.; De La Calle, A.; Medina, S.; Pérez-Maqueda, L. A. Influence of Ball Milling on CaO Crystal Growth during Limestone and Dolomite Calcination: Effect on CO2 Capture at Calcium Looping Conditions. *Cryst. Growth Des.* **2016**, *16* (12), 7025–7036. https://doi.org/10.1021/acs.cgd.6b01228.

(209) Behar, O.; Khellaf, A.; Mohammedi, K. A Review of Studies on Central Receiver Solar Thermal Power Plants. *Renew. Sustain. Energy Rev.* **2013**, *23*, 12–39. https://doi.org/10.1016/j.rser.2013.02.017.

(210) Raganati, F.; Chirone, R.; Ammendola, P. Gas–Solid Fluidization of Cohesive Powders. *Chem. Eng. Res. Des.* **2018**, *133*, 347–387. https://doi.org/10.1016/j.cherd.2018.03.034.

(211) Chirone, R.; Raganati, F.; Ammendola, P.; Barletta, D.; Lettieri, P.; Poletto, M. A Comparison between Interparticle Forces Estimated with Direct Powder Shear Testing and with Sound Assisted Fluidization. *Powder Technol.* **2018**, *323*, 1–7. https://doi.org/10.1016/j.powtec.2017.09.038.

(212) Raganati, F.; Chirone, R.; Ammendola, P. Effect of Temperature on Fluidization of Geldart's Group A and C Powders: Role of Interparticle Forces. *Ind. Eng. Chem. Res.* **2017**, *56* (44), 12811–12821. https://doi.org/10.1021/acs.iecr.7b03270.

(213) Raganati, F.; Ammendola, P.; Chirone, R. Role of Acoustic Fields in Promoting the Gas-

Solid Contact in a Fluidized Bed of Fine Particles. *KONA Powder Part. J.* **2015**, *32* (32), 23–40. https://doi.org/10.14356/kona.2015006.

(214) Seville, J. P. K.; Willett, C. D.; Knight, P. C. Interparticle Forces in Fluidisation: A Review. *Powder Technol.* **2000**, *113* (3), 261–268. https://doi.org/10.1016/S0032-5910(00)00309-0.

(215) Raganati, F.; Ammendola, P. Sound-Assisted Fluidization for Temperature Swing Adsorption and Calcium Looping: A Review. *Materials (Basel).* **2021**, *14* (3), 672. https://doi.org/10.3390/ma14030672.

(216) Raganati, F.; Ammendola, P.; Chirone, R. CO2 Adsorption on Fine Activated Carbon in a Sound Assisted Fluidized Bed: Effect of Sound Intensity and Frequency, CO2 Partial Pressure and Fluidization Velocity. *Appl. Energy* **2014**, *113*, 1269–1282. https://doi.org/10.1016/j.apenergy.2013.08.073.

(217) Zhou, Y.; Zhou, Z.; Liu, L.; She, X.; Xu, R.; Sun, J.; Xu, M. Enhanced Thermochemical Energy Storage Stability of CaO-Based Composite Pellets Incorporated with a Zr-Based Stabilizer. *Energy and Fuels* **2021**, *35* (22), 18778–18788. https://doi.org/10.1021/ACS.ENERGYFUELS.1C02788/ASSET/IMAGES/LARGE/EF1C02788_0013.JPEG.

(218) Brandt, A. R.; Yeskoo, T.; McNally, M. S.; Vafi, K.; Yeh, S.; Cai, H.; Wang, M. Q. Energy Intensity and Greenhouse Gas Emissions from Tight Oil Production in the Bakken Formation. *Energy & Fuels* **2016**, *30* (11), 9613–9621. https://doi.org/10.1021/acs.energyfuels.6b01907.

(219) Sun, J.; Liu, W.; Hu, Y.; Li, M.; Yang, X.; Zhang, Y.; Xu, M. Structurally Improved, Core-in-Shell, CaO-Based Sorbent Pellets for CO 2 Capture. *Energy & Fuels* **2015**, *29* (10), 6636–6644. https://doi.org/10.1021/acs.energyfuels.5b01419.

(220) Manovic, V.; Anthony, E. J. CaO-Based Pellets Supported by Calcium Aluminate Cements

for High-Temperature CO 2 Capture. *Environ. Sci. Technol.* **2009**, *43* (18), 7117–7122. https://doi.org/10.1021/es901258w.

(221) Chen, H.; Zhao, C.; Yang, Y.; Zhang, P. CO2 Capture and Attrition Performance of CaO Pellets with Aluminate Cement under Pressurized Carbonation. *Appl. Energy* **2012**, *91* (1), 334–340. https://doi.org/10.1016/j.apenergy.2011.09.032.

(222) Sun, J.; Liu, W.; Hu, Y.; Li, M.; Yang, X.; Zhang, Y.; Xu, M. Structurally Improved, Core-in-Shell, CaO-Based Sorbent Pellets for CO 2 Capture. *Energy & Fuels* **2015**, *29* (10), 6636–6644. https://doi.org/10.1021/acs.energyfuels.5b01419.

(223) Tong, X.; Liu, W.; Yang, Y.; Sun, J.; Hu, Y.; Chen, H.; Li, Q. A Semi-Industrial Preparation Procedure of CaO-Based Pellets with High CO2 Uptake Performance. *Fuel Process. Technol.* **2019**, *193*, 149–158. https://doi.org/10.1016/j.fuproc.2019.05.018.

(224) Hu, Y.; Liu, W.; Peng, Y.; Yang, Y.; Sun, J.; Chen, H.; Zhou, Z.; Xu, M. One-Step Synthesis of Highly Efficient CaO-Based CO2 Sorbent Pellets via Gel-Casting Technique. *Fuel Process. Technol.* **2017**, *160*, 70–77. https://doi.org/10.1016/j.fuproc.2017.02.016.

(225) Zhang, X.; Liu, W.; Zhou, S.; Li, Z.; Sun, J.; Hu, Y.; Yang, Y. A Review on Granulation of CaO-Based Sorbent for Carbon Dioxide Capture. *Chem. Eng. J.* **2022**, *446*, 136880. https://doi.org/10.1016/j.cej.2022.136880.

(226) Sarrion, B.; Sanchez-Jimenez, P. E.; Perejon, A.; Perez-Maqueda, L. A.; Valverde, J. M. Pressure Effect on the Multicycle Activity of Natural Carbonates and a Ca/Zr Composite for Energy Storage of Concentrated Solar Power. *ACS Sustain. Chem. Eng.* **2018**, *6* (6), 7849–7858. https://doi.org/10.1021/acssuschemeng.8b00981.

(227) Valverde, J. M.; Barea-López, M.; Perejón, A.; Sánchez-Jiménez, P. E.; Pérez-Maqueda, L. A. Effect of Thermal Pretreatment and Nanosilica Addition on Limestone Performance at Calcium-Looping Conditions for Thermochemical Energy Storage of Concentrated Solar

Power. *Energy and Fuels* **2017**, *31* (4), 4226–4236. https://doi.org/10.1021/ACS.ENERGYFUELS.6B03364/ASSET/IMAGES/LARGE/EF-2016-03364Z_0011.JPEG.

(228) Møller, K. T.; Williamson, K.; Buckley, C. E.; Paskevicius, M. Thermochemical Energy Storage Properties of a Barium Based Reactive Carbonate Composite. *J. Mater. Chem. A* **2020**, *8* (21), 10935–10942. https://doi.org/10.1039/d0ta03671d.

(229) Meroueh, L.; Yenduru, K.; Dasgupta, A.; Jiang, D.; AuYeung, N. Energy Storage Based on SrCO3 and Sorbents—A Probabilistic Analysis towards Realizing Solar Thermochemical Power Plants. *Renew. Energy* **2019**, *133*, 770–786. https://doi.org/10.1016/J.RENENE.2018.10.071.

(230) Rhodes, N. R.; Barde, A.; Randhir, K.; Li, L.; Hahn, D. W.; Mei, R.; Klausner, J. F.; AuYeung, N. Solar Thermochemical Energy Storage Through Carbonation Cycles of SrCO 3 /SrO Supported on SrZrO 3. *ChemSusChem* **2015**, *8* (22), 3793–3798. https://doi.org/10.1002/cssc.201501023.

(231) Miccio, F.; Murri, A. N.; Landi, E. High-Temperature Capture of CO2 by Strontium Oxide Sorbents. *Ind. Eng. Chem. Res.* **2016**, *55* (23), 6696–6707. https://doi.org/10.1021/acs.iecr.6b00184.

(232) Zare Ghorbaei, S.; Ale Ebrahim, H. Carbonation Reaction of Strontium Oxide for Thermochemical Energy Storage and CO2 Removal Applications: Kinetic Study and Reactor Performance Prediction. *Appl. Energy* **2020**, *277* (March), 115604. https://doi.org/10.1016/j.apenergy.2020.115604.

(233) Gigantino, M.; Kiwic, D.; Steinfeld, A. Thermochemical Energy Storage via Isothermal Carbonation-Calcination Cycles of MgO-Stabilized SrO in the Range of 1000–1100 °C. *Sol. Energy* **2019**, *188* (January), 720–729. https://doi.org/10.1016/j.solener.2019.06.046.

(234) Ammendola, P.; Raganati, F.; Miccio, F.; Natali, A. Preliminary Screening of SrO-Based Composites for Thermochemical Energy Storage. *Chem. Eng. Trans.* **2021**, *86* (March), 1051–1056. https://doi.org/10.3303/CET2186176.

(235) Ammendola, P.; Raganati, F.; Miccio, F.; Murri, A. N.; Landi, E. Insights into Utilization of Strontium Carbonate for Thermochemical Energy Storage. *Renew. Energy* **2020**, *157*, 769–781. https://doi.org/10.1016/j.renene.2020.05.048.

(236) Ammendola, P.; Raganati, F.; Landi, E.; Natali Murri, A.; Miccio, F. Kinetics of the Carbonation Reaction of an SrO-Al2O3 Composite for Thermochemical Energy Storage. *Chem. Eng. J.* **2021**, *420*, 129618. https://doi.org/10.1016/j.cej.2021.129618.

(237) Amghar, N.; Ortiz, C.; Perejón, A.; Valverde, J. M.; Maqueda, L. P.; Sánchez Jiménez, P. E. The SrCO3/SrO System for Thermochemical Energy Storage at Ultra-High Temperature. *Sol. Energy Mater. Sol. Cells* **2022**, *238*, 111632. https://doi.org/10.1016/j.solmat.2022.111632.

(238) Alonso, E.; Romero, M. Review of Experimental Investigation on Directly Irradiated Particles Solar Reactors. *Renew. Sustain. Energy Rev.* **2015**, *41*, 53–67. https://doi.org/10.1016/j.rser.2014.08.027.

(239) Koepf, E.; Alxneit, I.; Wieckert, C.; Meier, A. A Review of High Temperature Solar Driven Reactor Technology: 25years of Experience in Research and Development at the Paul Scherrer Institute. *Appl. Energy* **2017**, *188*, 620–651. https://doi.org/10.1016/j.apenergy.2016.11.088.

(240) Rubin, E. B.; Chen, Y.; Chen, R. Optical Properties and Thermal Stability of Cu Spinel Oxide Nanoparticle Solar Absorber Coatings. *Sol. Energy Mater. Sol. Cells* **2019**, *195*, 81–88. https://doi.org/10.1016/j.solmat.2019.02.032.

(241) Ho, C. K. A Review of High-Temperature Particle Receivers for Concentrating Solar Power.

Appl. Therm. Eng. **2016**, *109*, 958–969. https://doi.org/10.1016/j.applthermaleng.2016.04.103.

(242) Han, R.; Gao, J.; Wei, S.; Su, Y.; Sun, F.; Zhao, G.; Qin, Y. Strongly Coupled Calcium Carbonate/Antioxidative Graphite Nanosheets Composites with High Cycling Stability for Thermochemical Energy Storage. *Appl. Energy* **2018**, *231*, 412–422. https://doi.org/10.1016/j.apenergy.2018.09.142.

(243) Teng, L.; Xuan, Y.; Da, Y.; Liu, X.; Ding, Y. Modified Ca-Looping Materials for Directly Capturing Solar Energy and High-Temperature Storage. *Energy Storage Mater.* **2020**, *25*, 836–845. https://doi.org/10.1016/j.ensm.2019.09.006.

(244) Yang, L.; Huang, Z.; Huang, G. Fe- and Mn-Doped Ca-Based Materials for Thermochemical Energy Storage Systems. *Energy & Fuels* **2020**, *34* (9), 11479–11488. https://doi.org/10.1021/acs.energyfuels.0c01500.

(245) Song, C.; Liu, X.; Zheng, H.; Bao, C.; Teng, L.; Da, Y.; Jiang, F.; Li, C.; Li, Y.; Xuan, Y.; et al. Decomposition Kinetics of Al- and Fe-Doped Calcium Carbonate Particles with Improved Solar Absorbance and Cycle Stability. *Chem. Eng. J.* **2021**, *406*, 126282. https://doi.org/10.1016/j.cej.2020.126282.

(246) Li, B.; Li, Y.; Dou, Y.; Wang, Y.; Zhao, J.; Wang, T. SiC/Mn Co-Doped CaO Pellets with Enhanced Optical and Thermal Properties for Calcium Looping Thermochemical Heat Storage. *Chem. Eng. J.* **2021**, *423*, 130305. https://doi.org/10.1016/j.cej.2021.130305.

(247) Zheng, H.; Song, C.; Bao, C.; Liu, X.; Xuan, Y.; Li, Y.; Ding, Y. Dark Calcium Carbonate Particles for Simultaneous Full-Spectrum Solar Thermal Conversion and Large-Capacity Thermochemical Energy Storage. *Sol. Energy Mater. Sol. Cells* **2020**, *207*, 110364. https://doi.org/10.1016/j.solmat.2019.110364.

(248) Moumin, G.; Tescari, S.; Sundarraj, P.; de Oliveira, L.; Roeb, M.; Sattler, C. Solar Treatment

of Cohesive Particles in a Directly Irradiated Rotary Kiln. *Sol. Energy* **2019**, *182*. https://doi.org/10.1016/j.solener.2019.01.093.

(249) Tescari, S.; Sundarraj, P.; Moumin, G.; Duarte, J. P. R.; Agrafiotis, C.; de Oliveira, L.; Willsch, C.; Roeb, M.; Sattler, C. Solar Rotary Kiln for Continuous Treatment of Particle Material: Chemical Experiments from Micro to Milli Meter Particle Size. In *AIP Conference Proceedings*; 2020; Vol. 2303. https://doi.org/10.1063/5.0029271.

(250) Abanades, S.; André, L. Design and Demonstration of a High Temperature Solar-Heated Rotary Tube Reactor for Continuous Particles Calcination. *Appl. Energy* **2018**, *212*, 1310–1320. https://doi.org/10.1016/j.apenergy.2018.01.019.

(251) Meier, A.; Bonaldi, E.; Cella, G. M.; Lipinski, W. Multitube Rotary Kiln for the Industrial Solar Production of Lime. *J. Sol. Energy Eng.* **2005**, *127* (3), 386–395. https://doi.org/10.1115/1.1979517.

(252) Meier, A.; Bonaldi, E.; Cella, G. M.; Lipinski, W.; Wuillemin, D. Solar Chemical Reactor Technology for Industrial Production of Lime. *Sol. Energy* **2006**, *80* (10), 1355–1362. https://doi.org/10.1016/J.SOLENER.2005.05.017.

(253) Imhof, A. The Cyclone Reactor — an Atmospheric Open Solar Reactor. *Sol. Energy Mater.* **1991**, *24* (1–4), 733–741. https://doi.org/10.1016/0165-1633(91)90106-U.

(254) Steinfeld, A.; Imhof, A.; Mischler, D. Experimental Investigation of an Atmospheric-Open Cyclone Solar Reactor for Solid-Gas Thermochemical Reactions. *J. Sol. Energy Eng.* **1992**, *114* (3), 171–174. https://doi.org/10.1115/1.2930001.

(255) Imhof, A. Decomposition of Limestone in a Solar Reactor. *Renew. Energy* **1997**, *10* (2–3), 239–246. https://doi.org/10.1016/0960-1481(96)00072-9.

(256) NIKULSHINA, V.; HIRSCH, D.; MAZZOTTI, M.; STEINFELD, A. CO2 Capture from Air

and Co-Production of H2 via the Ca(OH)2–CaCO3 Cycle Using Concentrated Solar Power–Thermodynamic Analysis. *Energy* **2006**, *31* (12), 1715–1725. https://doi.org/10.1016/j.energy.2005.09.014.

(257) Nikulshina, V.; Halmann, M.; Steinfeld, A. Coproduction of Syngas and Lime by Combined CaCO 3 -Calcination and CH 4 -Reforming Using a Particle-Flow Reactor Driven by Concentrated Solar Radiation. *Energy & Fuels* **2009**, *23* (12), 6207–6212. https://doi.org/10.1021/ef9007246.

(258) Nikulshina, V.; Gebald, C.; Steinfeld, A. CO2 Capture from Atmospheric Air via Consecutive CaO-Carbonation and CaCO3-Calcination Cycles in a Fluidized-Bed Solar Reactor. *Chem. Eng. J.* **2009**, *146* (2), 244–248. https://doi.org/10.1016/j.cej.2008.06.005.

(259) Tregambi, C.; Solimene, R.; Montagnaro, F.; Salatino, P.; Marroccoli, M.; Ibris, N.; Telesca, A. Solar-Driven Production of Lime for Ordinary Portland Cement Formulation. *Sol. Energy* **2018**, *173*, 759–768. https://doi.org/10.1016/j.solener.2018.08.018.

(260) Tregambi, C.; Padula, S.; Galbusieri, M.; Coppola, G.; Montagnaro, F.; Salatino, P.; Troiano, M.; Solimene, R. Directly Irradiated Fluidized Bed Reactor for Thermochemical Energy Storage and Solar Fuels Production. *Powder Technol.* **2020**, *366*, 460–469. https://doi.org/10.1016/j.powtec.2020.02.045.

(261) Esence, T.; Benoit, H.; Poncin, D.; Tessonneaud, M.; Flamant, G. A Shallow Cross-Flow Fluidized-Bed Solar Reactor for Continuous Calcination Processes. *Sol. Energy* **2020**, *196*, 389–398. https://doi.org/10.1016/j.solener.2019.12.029.

(262) Esence, T.; Guillot, E.; Tessonneaud, M.; Sans, J.-L.; Flamant, G. Solar Calcination at Pilot Scale in a Continuous Flow Multistage Horizontal Fluidized Bed. *Sol. Energy* **2020**, *207*, 367–378. https://doi.org/10.1016/j.solener.2020.06.098.

(263) Szekely, J.; Carr, R. Heat Transfer in a Cyclone. *Chem. Eng. Sci.* **1966**, *21* (12), 1119–1132.

https://doi.org/10.1016/0009-2509(66)85033-9.

(264) Kiang, Y.-H. Other and Emerging Alternative Energy Technology. In *Fuel Property Estimation and Combustion Process Characterization*; Elsevier, 2018; pp 363–401. https://doi.org/10.1016/B978-0-12-813473-3.00010-6.

(265) Gokon, N.; Kodama, T.; Imaizumi, N.; Umeda, J.; Seo, T. Ferrite/Zirconia-Coated Foam Device Prepared by Spin Coating for Solar Demonstration of Thermochemical Water-Splitting. *Int. J. Hydrogen Energy* **2011**, *36* (3), 2014–2028. https://doi.org/10.1016/j.ijhydene.2010.11.034.

(266) Roeb, M.; Säck, J.-P.; Rietbrock, P.; Prahl, C.; Schreiber, H.; Neises, M.; de Oliveira, L.; Graf, D.; Ebert, M.; Reinalter, W.; et al. Test Operation of a 100kW Pilot Plant for Solar Hydrogen Production from Water on a Solar Tower. *Sol. Energy* **2011**, *85* (4), 634–644. https://doi.org/10.1016/j.solener.2010.04.014.

(267) Chueh, W. C.; Falter, C.; Abbott, M.; Scipio, D.; Furler, P.; Haile, S. M.; Steinfeld, A. High-Flux Solar-Driven Thermochemical Dissociation of CO 2 and H 2 O Using Nonstoichiometric Ceria. *Science (80-.).* **2010**, *330* (6012), 1797–1801. https://doi.org/10.1126/science.1197834.

(268) Piatkowski, N.; Steinfeld, A. Solar-Driven Coal Gasification in a Thermally Irradiated Packed-Bed Reactor. *Energy & Fuels* **2008**, *22* (3), 2043–2052. https://doi.org/10.1021/ef800027c.

(269) Piatkowski, N.; Wieckert, C.; Steinfeld, A. Experimental Investigation of a Packed-Bed Solar Reactor for the Steam-Gasification of Carbonaceous Feedstocks. *Fuel Process. Technol.* **2009**, *90* (3), 360–366. https://doi.org/10.1016/j.fuproc.2008.10.007.

(270) Koepf, E.; Advani, S. G.; Steinfeld, A.; Prasad, A. K. A Novel Beam-down, Gravity-Fed, Solar Thermochemical Receiver/Reactor for Direct Solid Particle Decomposition: Design,

Modeling, and Experimentation. *Int. J. Hydrogen Energy* **2012**, *37* (22), 16871–16887. https://doi.org/10.1016/j.ijhydene.2012.08.086.

(271) Wieckert, C.; Palumbo, R.; Frommherz, U. A Two-Cavity Reactor for Solar Chemical Processes: Heat Transfer Model and Application to Carbothermic Reduction of ZnO. *Energy* **2004**, *29* (5–6), 771–787. https://doi.org/10.1016/S0360-5442(03)00183-X.

(272) Salatino, P.; Ammendola, P.; Bareschino, P.; Chirone, R.; Solimene, R. Improving the Thermal Performance of Fluidized Beds for Concentrated Solar Power and Thermal Energy Storage. *Powder Technol.* **2016**, *290*, 97–101. https://doi.org/10.1016/j.powtec.2015.07.036.

(273) Solé, A.; Martorell, I.; Cabeza, L. F. State of the Art on Gas–Solid Thermochemical Energy Storage Systems and Reactors for Building Applications. *Renew. Sustain. Energy Rev.* **2015**, *47*, 386–398. https://doi.org/10.1016/j.rser.2015.03.077.

(274) Bailera, M.; Lisbona, P.; Romeo, L. M.; Díez, L. I. Calcium Looping as Chemical Energy Storage in Concentrated Solar Power Plants: Carbonator Modelling and Configuration Assessment. *Appl. Therm. Eng.* **2020**, *172*, 115186. https://doi.org/10.1016/j.applthermaleng.2020.115186.

(275) Shimizu, T.; Hirama, T.; Hosoda, H.; Kitano, K.; Inagaki, M.; Tejima, K. A Twin Fluid-Bed Reactor for Removal of CO2 from Combustion Processes. *Chem. Eng. Res. Des.* **1999**, *77* (1), 62–68. https://doi.org/10.1205/026387699525882.

(276) Lasheras, A.; Ströhle, J.; Galloy, A.; Epple, B. Carbonate Looping Process Simulation Using a 1D Fluidized Bed Model for the Carbonator. *Int. J. Greenh. Gas Control* **2011**, *5* (4), 686–693. https://doi.org/10.1016/J.IJGGC.2011.01.005.

(277) Lisbona, P.; Martínez, A.; Romeo, L. M. Hydrodynamical Model and Experimental Results of a Calcium Looping Cycle for CO2 Capture. *Appl. Energy* **2013**, *101*, 317–322. https://doi.org/10.1016/J.APENERGY.2011.11.067.

(278) Romano, M. C. Modeling the Carbonator of a Ca-Looping Process for CO 2 Capture from Power Plant Flue Gas. *Chem. Eng. Sci.* **2012**, *69* (1), 257–269. https://doi.org/10.1016/J.CES.2011.10.041.

(279) Hanak, D. P.; Anthony, E. J.; Manovic, V. A Review of Developments in Pilot-Plant Testing and Modelling of Calcium Looping Process for CO 2 Capture from Power Generation Systems. *Energy Environ. Sci.* **2015**, *8* (8), 2199–2249. https://doi.org/10.1039/C5EE01228G.

(280) Ortiz, C.; Valverde, J. M.; Chacartegui, R.; Perez-Maqueda, L. A. Carbonation of Limestone Derived CaO for Thermochemical Energy Storage: From Kinetics to Process Integration in Concentrating Solar Plants. *ACS Sustain. Chem. Eng.* **2018**, *6* (5), 6404–6417. https://doi.org/10.1021/acssuschemeng.8b00199.

(281) Romano, M. C. Modeling the Carbonator of a Ca-Looping Process for CO2 Capture from Power Plant Flue Gas. *Chem. Eng. Sci.* **2012**, *69* (1), 257–269. https://doi.org/10.1016/j.ces.2011.10.041.

(282) Kyaw, K.; Kubota, M.; Watanabe, F.; Matsuda, H.; Hasatani, M. Study of Carbonation of CaO for High Temperature Thermal Energy Storage. *J. Chem. Eng. Japan* **1998**, *31* (2), 281–284. https://doi.org/10.1252/jcej.31.281.

(283) Ortiz, C.; Chacartegui, R.; Valverde, J. M.; Alovisio, A.; Becerra, J. A. Power Cycles Integration in Concentrated Solar Power Plants with Energy Storage Based on Calcium Looping. *Energy Convers. Manag.* **2017**, *149*, 815–829. https://doi.org/10.1016/j.enconman.2017.03.029.

(284) Chuachuensuk, A.; Paengjuntuek, W.; Kheawhom, S.; Arpornwichanop, A. A Systematic Model-Based Analysis of a Downer Regenerator in Fluid Catalytic Cracking Processes. *Comput. Chem. Eng.* **2013**, *49*, 136–145.

https://doi.org/10.1016/j.compchemeng.2012.10.003.

(285) Wang, W.; Ramkumar, S.; Li, S.; Wong, D.; Iyer, M.; Sakadjian, B. B.; Statnick, R. M.; Fan, L.-S. Subpilot Demonstration of the Carbonation−Calcination Reaction (CCR) Process: High-Temperature CO 2 and Sulfur Capture from Coal-Fired Power Plants. *Ind. Eng. Chem. Res.* **2010**, *49* (11), 5094–5101. https://doi.org/10.1021/ie901509k.

(286) Hanak, D. P.; Anthony, E. J.; Manovic, V. A Review of Developments in Pilot-Plant Testing and Modelling of Calcium Looping Process for CO2 Capture from Power Generation Systems. *Energy and Environmental Science*. 2015. https://doi.org/10.1039/c5ee01228g.

(287) Plou, J.; Martínez, I.; Grasa, G. S.; Murillo, R. Experimental Carbonation of CaO in an Entrained Flow Reactor. *React. Chem. Eng.* **2019**, *4* (5), 899–908. https://doi.org/10.1039/C9RE00015A.

(288) Ma, Y.; Zhu, J.-X. Experimental Study of Heat Transfer in a Co-Current Downflow Fluidized Bed (Downer). *Chem. Eng. Sci.* **1999**, *54* (1), 41–50. https://doi.org/10.1016/S0009-2509(98)00233-4.

(289) Li, Z.; van Sint Annaland, M.; Kuipers, J. A. M.; Deen, N. G. Effect of Superficial Gas Velocity on the Particle Temperature Distribution in a Fluidized Bed with Heat Production. *Chem. Eng. Sci.* **2016**, *140*. https://doi.org/10.1016/j.ces.2015.10.020.

(290) Zhang, D.; Koksal, M. Heat Transfer in a Pulsed Bubbling Fluidized Bed. *Powder Technol.* **2006**, *168* (1). https://doi.org/10.1016/j.powtec.2006.06.017.

(291) Turrado, S.; Arias, B.; Fernández, J. R.; Abanades, J. C. Carbonation of Fine CaO Particles in a Drop Tube Reactor. *Ind. Eng. Chem. Res.* **2018**, *57* (40), 13372–13380. https://doi.org/10.1021/acs.iecr.8b02918.

(292) Chang, M.-H.; Chen, W.-C.; Huang, C.-M.; Liu, W.-H.; Chou, Y.-C.; Chang, W.-C.; Chen,

W.; Cheng, J.-Y.; Huang, K.-E.; Hsu, H.-W. Design and Experimental Testing of a 1.9MWth Calcium Looping Pilot Plant. *Energy Procedia* **2014**, *63*, 2100–2108. https://doi.org/10.1016/j.egypro.2014.11.226.

(293) Kremer, J.; Galloy, A.; Ströhle, J.; Epple, B. Continuous CO 2 Capture in a 1-MW Th Carbonate Looping Pilot Plant. *Chem. Eng. Technol.* **2013**, *36* (9), 1518–1524. https://doi.org/10.1002/ceat.201300084.

(294) Arias, B.; Diego, M. E.; Abanades, J. C.; Lorenzo, M.; Diaz, L.; Martínez, D.; Alvarez, J.; Sánchez-Biezma, A. Demonstration of Steady State CO2 Capture in a 1.7MWth Calcium Looping Pilot. *Int. J. Greenh. Gas Control* **2013**, *18*, 237–245. https://doi.org/10.1016/j.ijggc.2013.07.014.

(295) Champagne, S.; Lu, D. Y.; Symonds, R. T.; Macchi, A.; Anthony, E. J. The Effect of Steam Addition to the Calciner in a Calcium Looping Pilot Plant. *Powder Technol.* **2015**, *290*, 114–123. https://doi.org/10.1016/j.powtec.2015.07.039.

(296) Duelli (Varela), G.; Charitos, A.; Armbrust, N.; Dieter, H.; Scheffknecht, G. Analysis of the Calcium Looping System Behavior by Implementing Simple Reactor and Attrition Models at a 10 KW Th Dual Fluidized Bed Facility under Continuous Operation. *Fuel* **2016**, *169*, 79–86. https://doi.org/10.1016/j.fuel.2015.11.070.

(297) Chang, M.-H.; Huang, C.-M.; Liu, W.-H.; Chen, W.-C.; Cheng, J.-Y.; Chen, W.; Wen, T.-W.; Ouyang, S.; Shen, C.-H.; Hsu, H.-W. Design and Experimental Investigation of Calcium Looping Process for 3-KW Th and 1.9-MW Th Facilities. *Chem. Eng. Technol.* **2013**, *36* (9), 1525–1532. https://doi.org/10.1002/ceat.201300081.

(298) Erans, M.; Jeremias, M.; Zheng, L.; Yao, J. G.; Blamey, J.; Manovic, V.; Fennell, P. S.; Anthony, E. J. Pilot Testing of Enhanced Sorbents for Calcium Looping with Cement Production. *Appl. Energy* **2018**, *225*, 392–401.

https://doi.org/10.1016/j.apenergy.2018.05.039.

(299) Symonds, R. T.; Champagne, S.; Ridha, F. N.; Lu, D. Y. CO2 Capture Performance of CaO–Based Pellets in a 0.1 MWth Pilot-Scale Calcium Looping System. *Powder Technol.* **2016**, *290*, 124–131. https://doi.org/10.1016/j.powtec.2015.08.044.

(300) Hilz, J.; Helbig, M.; Haaf, M.; Daikeler, A.; Ströhle, J.; Epple, B. Investigation of the Fuel Influence on the Carbonate Looping Process in 1 MWth Scale. *Fuel Process. Technol.* **2018**, *169*, 170–177. https://doi.org/10.1016/j.fuproc.2017.09.016.

(301) Cotton, A.; Patchigolla, K.; Oakey, J. E. Engineering Scale-up Challenges, and Effects of SO2 on the Calcium Looping Cycle for Post Combustion CO2 Capture. *Energy Procedia* **2014**, *63*, 6404–6412. https://doi.org/10.1016/j.egypro.2014.11.675.

(302) Cotton, A.; Patchigolla, K.; Oakey, J. E. Hydrodynamic Characteristics of a Pilot-Scale Cold Model of a CO2 Capture Fluidised Bed Reactor. *Powder Technol.* **2013**, *235*, 1060–1069. https://doi.org/10.1016/j.powtec.2012.10.011.

(303) SOLPART | High temperature Solar-Heated Reactors for Industrials Production of Reactive Particulates https://www.solpart-project.eu/ (accessed Oct 25, 2022).

(304) SOCRATCES | SOlar Calcium-looping integRAtion for Thermo-Chemical Energy Storge https://socratces.eu/ (accessed Oct 25, 2022).

(305) Sakellariou, K. G.; Criado, Y. A.; Tsongidis, N. I.; Karagiannakis, G.; Konstandopoulos, A. G. Multi-Cyclic Evaluation of Composite CaO-Based Structured Bodies for Thermochemical Heat Storage via the CaO/Ca(OH)2 Reaction Scheme. *Sol. Energy* **2017**, *146*, 65–78. https://doi.org/10.1016/j.solener.2017.02.013.

(306) Jesús Arcenegui Troya, J.; Enrique Sánchez-Jiménez, P.; Perejón, A.; Moreno, V.; Manuel Valverde, J.; Allan Pérez-Maqueda, L. Kinetics and Cyclability of Limestone (CaCO3) in

Presence of Steam during Calcination in the CaL Scheme for Thermochemical Energy Storage. *Chem. Eng. J.* **2021**, *417* (February), 129194. https://doi.org/10.1016/j.cej.2021.129194.

(307) Tesio, U.; Guelpa, E.; Verda, V. Integration of Thermochemical Energy Storage in Concentrated Solar Power. Part 1: Energy and Economic Analysis/Optimization. *Energy Convers. Manag. X* **2020**, *6* (February), 100039. https://doi.org/10.1016/j.ecmx.2020.100039.

(308) Hanak, D. P.; Manovic, V. Economic Feasibility of Calcium Looping under Uncertainty. *Appl. Energy* **2017**, *208*. https://doi.org/10.1016/j.apenergy.2017.09.078.

(309) Mantripragada, H. C.; Rubin, E. S. Calcium Looping Cycle for CO2 Capture: Performance, Cost And Feasibility Analysis. *Energy Procedia* **2014**, *63*, 2199–2206. https://doi.org/10.1016/j.egypro.2014.11.239.

(310) Romano, M. C.; Spinelli, M.; Campanari, S.; Consonni, S.; Cinti, G.; Marchi, M.; Borgarello, E. The Calcium Looping Process for Low CO2 Emission Cement and Power. *Energy Procedia* **2013**, *37*, 7091–7099. https://doi.org/10.1016/j.egypro.2013.06.645.

(311) Cormos, C.-C. Economic Evaluations of Coal-Based Combustion and Gasification Power Plants with Post-Combustion CO 2 Capture Using Calcium Looping Cycle. *Energy* **2014**, *78*, 665–673. https://doi.org/10.1016/j.energy.2014.10.054.

(312) De Lena, E.; Spinelli, M.; Gatti, M.; Scaccabarozzi, R.; Campanari, S.; Consonni, S.; Cinti, G.; Romano, M. C. Techno-Economic Analysis of Calcium Looping Processes for Low CO2 Emission Cement Plants. *Int. J. Greenh. Gas Control* **2019**, *82*, 244–260. https://doi.org/10.1016/j.ijggc.2019.01.005.

(313) Michalski, S.; Hanak, D. P.; Manovic, V. Techno-Economic Feasibility Assessment of Calcium Looping Combustion Using Commercial Technology Appraisal Tools. *J. Clean. Prod.* **2019**, *219*, 540–551. https://doi.org/10.1016/j.jclepro.2019.02.049.

(314) Bayon, A.; Bader, R.; Jafarian, M.; Fedunik-Hofman, L.; Sun, Y.; Hinkley, J.; Miller, S.; Lipiński, W. Techno-Economic Assessment of Solid–Gas Thermochemical Energy Storage Systems for Solar Thermal Power Applications. *Energy* **2018**, *149*, 473–484. https://doi.org/10.1016/j.energy.2017.11.084.

(315) Muto, A.; Hansen, T. Demonstration of High-Temperature Calcium-Based Thermochemical Energy Storage System for Use with Concentrating Solar Power Facilities. *Doe Osti.Gov* **2019**.

(316) Muto, A.; McCabe, K.; Real, D. High-Temperature Calcium-Based Thermochemical Energy Storage System for Use with CSP Facilities. In *AIP Conference Proceedings*; 2018; Vol. 2033, p 100006. https://doi.org/10.1063/1.5067127.

(317) Colelli, G.; Chacartegui, R.; Ortiz, C.; Carro, A.; Arena, A. P.; Verda, V. Life Cycle and Environmental Assessment of Calcium Looping (CaL) in Solar Thermochemical Energy Storage. *Energy Convers. Manag.* **2022**, *257* (December 2021), 115428. https://doi.org/10.1016/j.enconman.2022.115428.

(318) Corona, B.; Cerrajero, E.; López, D.; San Miguel, G. Full Environmental Life Cycle Cost Analysis of Concentrating Solar Power Technology: Contribution of Externalities to Overall Energy Costs. *Sol. Energy* **2016**, *135*, 758–768. https://doi.org/10.1016/j.solener.2016.06.059.

(319) Lamnatou, C.; Chemisana, D. Concentrating Solar Systems: Life Cycle Assessment (LCA) and Environmental Issues. *Renew. Sustain. Energy Rev.* **2017**, *78*, 916–932. https://doi.org/10.1016/j.rser.2017.04.065.

(320) Gasa, G.; Lopez-roman, A.; Prieto, C.; Cabeza, L. F. Life Cycle Assessment (Lca) of a Concentrating Solar Power (Csp) Plant in Tower Configuration with and without Thermal Energy Storage (Tes). *Sustain.* **2021**, *13* (7). https://doi.org/10.3390/su13073672.

(321) Cavallaro, F.; Marino, D.; Streimikiene, D. Environmental Assessment of a Solar Tower Using the Life Cycle Assessment (LCA). In *Smart Innovation, Systems and Technologies*; 2019; Vol. 101, pp 621–628. https://doi.org/10.1007/978-3-319-92102-0_67.